POLITECNICO DI MILANO

SCHOOL OF INDUSTRIAL ENGINEERING AND INFORMATION
MASTER OF SCIENCE IN MECHANICAL ENGINEERING

Effect of Linear Final Electromagnetic Stirrer Operational Parameters on Continuous Cast High Carbon Steel Billet Quality

Supervisor: Prof. Carlo Mapelli

Graduation Thesis:
Abdullayev Elvin
Matricola: 872943
Ayaz Bilalov
Matricola: 872945

Academic Year 2019 - 2020

ACKNOWLEDGEMENT

We would like to take this opportunity to express my gratitude to everyone who supported me throughout this MSc project.

We would like to sincerely thank Prof. Mapelli Carlo for his valuable guidance, support and encouragement as supervisor which helped us greatly in the successful completion of this thesis work.

We would like to thank Davide Mombelli and Prof. Silvia Barella for her valuable guidance and encouragement as co-supervisor which helped us in the successful completion of this thesis work.

We wish to thank Ing. Ludovica Rovatti for providing the necessary support and arrangement towards the successful completion of this thesis.

We would like to thank our friends and relatives for their support and encouragement towards the successful completion of MSc program.

Last but not the least, We would like to thank our parents who during these years have comforted me morally and encouraged us to achieve our goals.

Contents

List of Tables

List of Figures

ABSTRACT

Metallographic studies have been made of the “White band” (zone of negative segregation), porosity, central segregation of non-metallic elements, primary dendrite arm spacing (PDAS) and columnar dendrites inclination angle (CDIA) formed by combined electromagnetic stirring of 140mm square continuous cast steel billets. Three F-EMS locations have been studied in terms of effects mentioned above, especially porosity reduction and segregation distribution comparing to a billet sample without final electromagnetic stirrer. The application of electromagnetic stirring (EMS) technique promotes the formation of an equiaxed crystal zone in the strand. It causes the refinement of the solidification structure the reduction in the content of inclusions and improvement in the quality of the surface, sub surface and the inner structure of the cast product. Various experiments are performed by changing the surface current given to the coils of final electromagnetic stirrer in 3 different locations after straightener of continuous casting machine. Nine high carbon steel billets casted by combined (M+S+F-EMS) electromagnetic stirring are taken, and macro/micro-etching was performed on them to reveal the macro and microstructure. The images of macro and micro etched samples are analysed using respectively an image and compositional analysis. Comparison in terms of porosity analysis, homogeneity of segregation in the center has been done on the billets produced with and without electromagnetic stirring. As a result best configuration has been selected in terms of F-EMS parameters, position, current and speed.

1. INTRODUCTION TO CONTINUOUS CASTING

1.1 Historical Background

In recent years with the stress on the production of clean steels, there are higher requirements for the microstructure and the composition homogenization of the cast product. Continuous casting process is not a very old manufacturing process. As early as 1856, the continuous strip casting process was introduced by Bessemer. The production of nonferrous metals using continuous casting was common during the 1930s and 1940s. The continuous casting of steel did not gain widespread use until the 1960s. Earlier attempts suffered due to some technical difficulties such as "breakouts", where sticking of solidifying steel shell to the mould, tears, and allows molten steel to pour out over the bottom of the machine. To overcome this problem in 1934 Junghans used vertically oscillating the mould, utilizing the concept of "negative strip" where the mould travels downward faster than the steel shell during some portion of the oscillation cycle to dislodge any sticking. Many other developments and innovations have transformed the continuous casting process into the sophisticated process currently.

In 1980s, continuous casting grew into the biggest casting method, exceeding the conventional ingot steel casting route. In the ingot casting route, individual moulds are filled with molten steel to produce steel ingots. The continuous casting method has a lot of benefits compared to the older ingot casting methods. The major advantages are improvement of steel quality, better yield, and savings of energy and manpower. Today, about 95% of the world's steel production is made by continuous casting and a great number of steel qualities are cast in very wide variety of dimensions.[1]

Figure 1.1 shows the schematic representation of the various types of continuous casting processes.

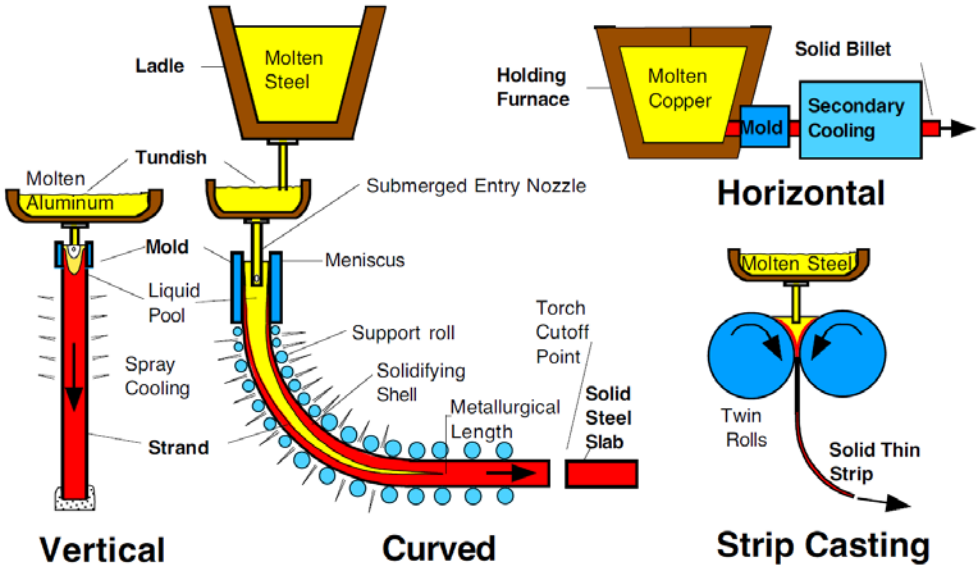

Figure 1.1 Various continuous casting processes **[2]**

1.2 Continuously Cast Sections

Casted sections semis are classified into slab, bloom or billets casters.

• Slab: Slab casters are the cast sections whose cross-sectional area is greater than the bloom casters. Usually greater than two times the bloom casters.
• Bloom casters: Conventional cast sections which may be square or rectangular in shape above 150 mm square in area.
• Billet casters: Billets are the smaller square sections, such as below 200 mm square.

Below figure 1-2 represents the different continuously cast sections

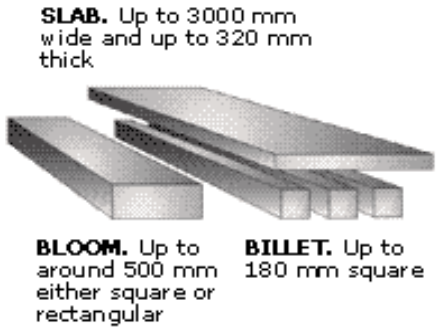

Figure 1.2 Various continuously cast sections

Vertical caster machines are turned to curved machines within years. The main disadvantages of the vertical casters were:

- The excessive height to achieve higher production rates.
- The extra costs in buildings and crane height
- The mechanism for turning the slab to a horizontal position after cutting was complex and expensive.
- Other main disadvantage is that the duty on the roller support system due to the greater ferro static forces caused by the machine heights.

The main advantages of the continuous casting process over the ingot casting as follows:

- Improved yield
- Reduced energy consumption
- Savings in manpower
- Improved product quality and consistency of quality
- Lower emissions harmful to the environment and plant operators
- Reduced stock levels and shorter deliver times
- Reduction in capital costs for new steel plants

The largest slabs currently continuously cast are 2725 mm * 254 mm. In 1951 a continuous casting plant was installed at Barrow Steel, Great Britain to develop the casting of billets ranging from 50 mm to 100 mm square and small slabs 150 mm * 50 mm with the conjunction of Irving Rossi with the Junghans / Rossi principle of casting with a reciprocating mould. An important early development of this machine was to bend the cast billet by a pneumatically powered tilting frame enabling the billet to be discharged horizontally prior to torch cutting which enabled the higher productivity with less machine height. In 1954 a breakthrough came in the form of 'negative strip'. This involved accelerating the mould on the downward stroke of its cycle so that the speed of mould exceeds that of exit velocity of the product for part of the oscillation cycle.

1.3 Overview of Continuous Casting

Continuous casting is process of transforming molten metal into solid. This is the most efficient way to solidify large volumes of metal into simple shapes and they are used for subsequent processing.

Continuous casting is determined from other solidification processes by its steady state nature. The molten metal solidifies against the mould walls and it is simultaneously withdrawn from the bottom of the mould at a rate which maintains the solid/liquid interface at a constant position with time. This process works best when all of its aspects operate in this steady-state manner. [3]

1.4 Basic Principles of Continuous Casting Process

Continuous casting is the process whereby molten metal is solidified into a "Semi-finished" billet, bloom, slab or beam blank.

In the continuous casting process, illustrated in Figure 1.2, molten metal is poured from the ladle into the tundish and through a submerged entry nozzle into a mould cavity. The mould is water-cooled so that enough heat is extracted from the molten metal to solidify a shell of enough thickness. The shell is withdrawn from the bottom of the mould at a "casting speed" that matches the inflow of metal, so that the process ideally operates at steady state. Below the mould, water is sprayed to further extract heat from the strand surface, and the strand eventually becomes fully solid when it reaches the "metallurgical length".

Solidification starts in the mould and continues through the different zones of cooling while the strand is continuously withdrawn at the casting speed. Finally, the solidified strand is straightened, cut, and then discharged for intermediate storage or hot charged for finished rolling. [4]

The continuous casting process is used to overcome a few ingot-related difficulties such as piping, mould spatter, entrapped slag and structure variation along the length of the product. It is used to produce blooms, billets, slabs and tubing directly from the molten metal. In this process, molten metal flows into a refractory-lined intermediate pouring vessel, where impurities are skimmed off [5].

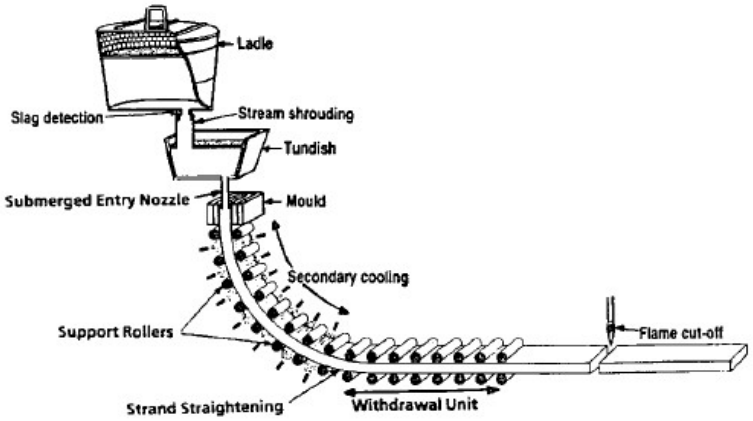

Figure 1.3 Continuous casting process **[9]**

The main sections of a Continuous casting machine are as follows

- A Tundish is above the mould which supplies liquid steel to the mould at a regulated rate.
- A water-cooled copper mould is the primary cooling zone, through which the liquid steel is fed from the tundish. It generates a solidified outer shell sufficiently strong enough to maintain the strand shape as it passes into the secondary cooling zone.
- A secondary cooling zone in association with a containment section positioned below the mould, through which the strand, the major portion of which is still in liquid state, passes and is sprayed with water or air mist for further solidification of the strand.
- Except in case of straight vertical casting machines, in all other type of casting machines, an unbending and straightening section are used.
- A severing unit like cutting torch or mechanical shears are used to cut the solidified strand into pieces for removal and further processing.[6]

1.5 Solidification of Continuous Casting Material

Solidification in continuous casting technology is initiated in a water-cooled open-ended copper mould. The steel shell which forms in the mould contains a liquid steel core which gradually solidifies as the strand moves through the caster guided by many roll pairs. High carbon steel tends to solidify over a wide temperature range during casting due to large solidification range *i.e.* difference between the liquidus and the solidus temperatures.

The solidification process initiated at meniscus level in the mould is completed in secondary cooling zones using a combination of water spray and radiation cooling. This relates to handling of very high heat flux in the mould, nurturing of the initial thin and fragile solid shell for avoidance of breakout during descent of the strand down the mould, designing of casting parameters in tune with the solidification dynamics of the steel grade for minimisation or elimination of surface and internal defects in the cast product. Safe caster operation, i.e., without metal breakout and achievement of acceptable product quality require understanding of both process engineering and metallurgy of solidification. [7]

Early in continuous casting, solidification occurs in the form of partial freezing of the meniscus curvature originating from the mould liquid contact point. To minimise shell sticking and tearing, friction between the strand surface and mould wall must be kept below a critical level depending upon the shell strength. Minimisation of the friction and continuous release of the shell from the mould have been achieved through the introduction of mould oscillation aided by lubrication.

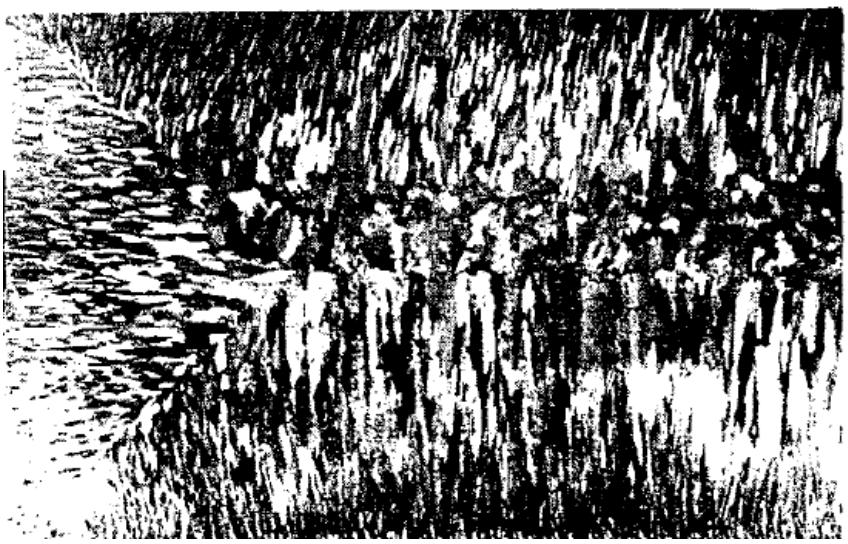

Figure 1.4 Solidification structure of a continuously cast slab

Solidification front causes unstable dendritic growth and a large percentage of the thickness of the solidified strand consists of inter-dendritic growth. The crystal structure of dendrites can be described as following a 'fir tree' pattern. Branches take the form of primary, secondary or tertiary dendrite arms.
During the solidification of blooms and billets the solidification is two dimensional and for high liquid steel temperature the unstable growth of the dendrites can cause bridging ahead of the feed point of solidification. This behaviour is termed the 'mini ingot theory'.
Figure 1.5 explains the various steps along the solidification process.
In the upper part of the strand (step 1) there is uniform columnar growth whilst lower down the strand (step 2) columnar growth becomes unstable because of the uncontrolled convection currents and thermal gradients in the liquid pool. In some regions the columnar growth produces solidification bridges (step 3) which isolate small pockets of liquid steel. The solidification of these pockets is very similar to ingot solidification, hence the term 'mini ingot'. The trapped liquid solidifies with segregation at the final point of solidification together with a shrinkage cavity (step 4). The actual final macrostructure is shown in step 5.

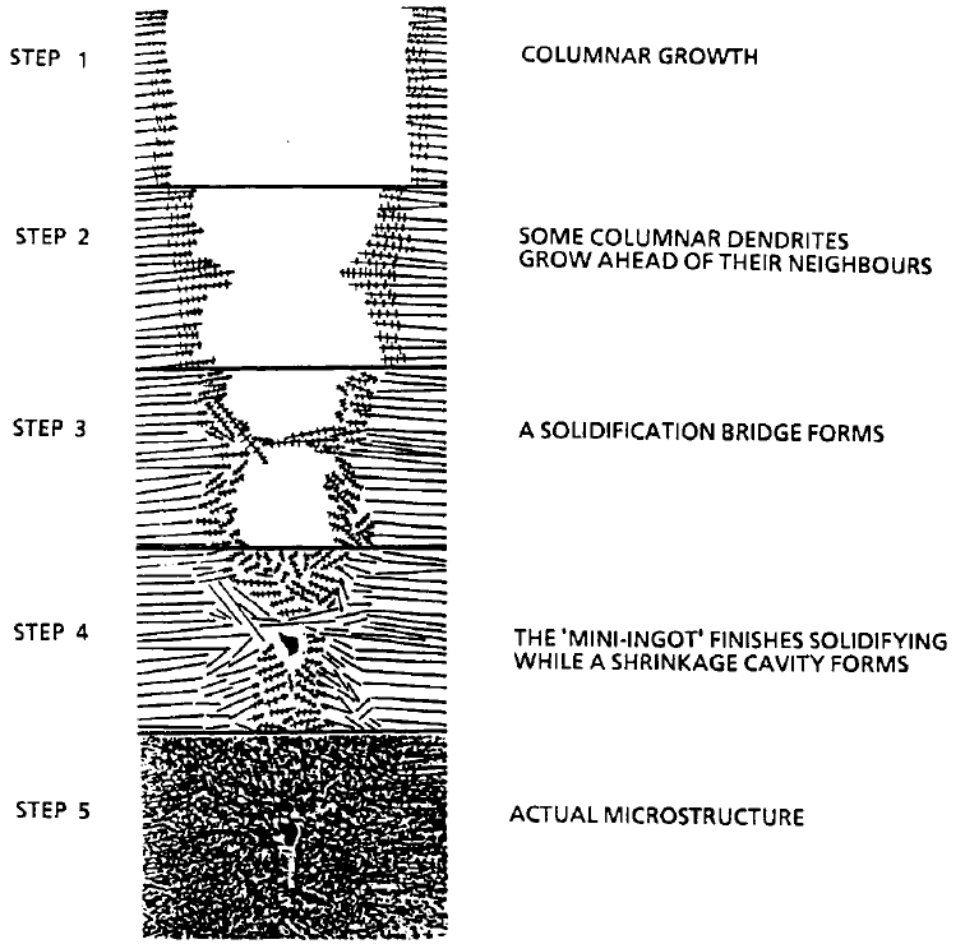

Figure 1.5 Various stages of solidification in billets explaining the mini ingot theory **[8]**

1.6 Solidification Microstructures

Depending upon the cooling conditions a chill zone is first formed at the region in contact with mold followed by columnar and then equiaxed zone at the core (**Figure 1.6**). A large equiaxed zone is desired to reduce inter-columnar segregation, axial segregation and central looseness. [18]

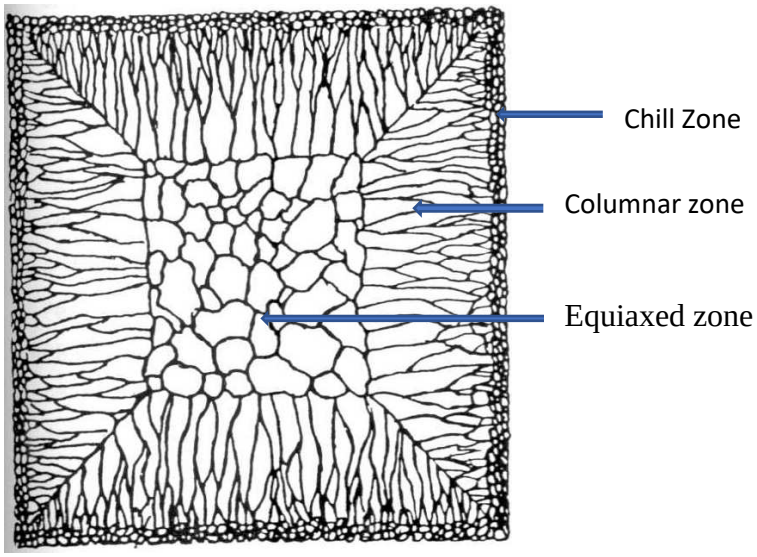

Figure 1.6 Solidification microstructure of the billet [1]

Dendrite means 'tree-like' and it has stem, branches, sub-branches (known as primary, secondary and tertiary arms). According to Flemings, dendrite may be said to form when secondary arms appear. Dendrite arm spacing is an important parameter in the morphology of cast structure.

Chill Zone

This consists of equiaxed crystal and randomly oriented dendrites (Fig.1.6). As soon as the molten metal meets mold wall, there is rapid chilling of the outer layer.

Columnar Zone

When the under cooling is low i.e. the temperature of the liquid is above the nucleation temperature, further nucleation almost ceases, and growth starts from the existing crystal at solid liquid interface. With increasing solidification, a second zone, consisting of columnar crystals, develops. This columnar zone is produced by growth of crystals in preferred crystallographic directions, <100> in the case of body centered cubic ferrite and face-centered cubic austenite. Such growth preferentially takes place along the heat flow direction which gives rise to the columnar zone. Since, the number of crystals becomes fewer as we move inwards, the grain size also increases. Dendrites located near the outer chill zone have more random orientation than these further inward in the columnar zone. Columnar zone also contains some equiaxed crystals.

Equiaxed Zone

In this zone, the equiaxed crystals as well as the dendrites are oriented at random. Nearly all the solidification microstructures which can be exhibited by a pure metal or an alloy can be divided into two groups, single phase primary crystals and polyphase structures. The most important growth form is the tree like primary crystal, i.e. the dendrites and the polyphase structures are called eutectics.

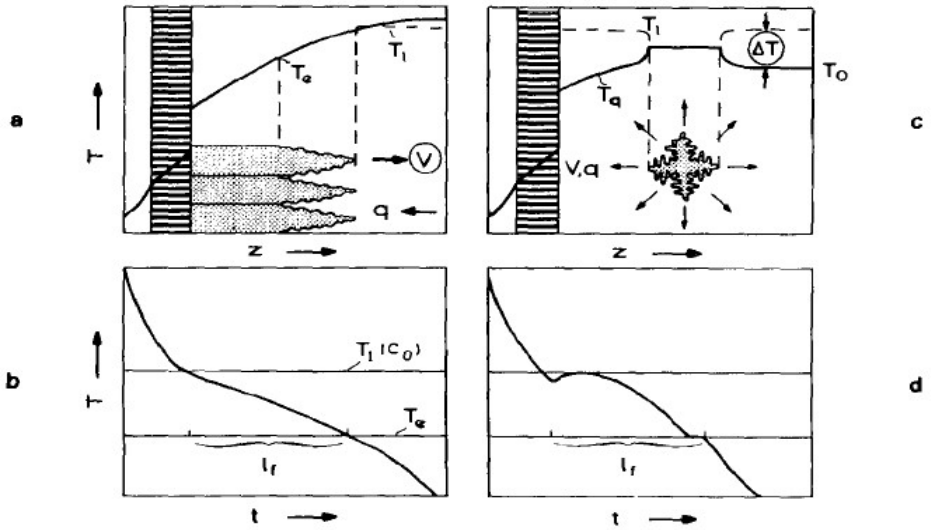

Figure 1.7 Thermal fields and cooling curves of alloy dendrites **[9]**

As per Figure 1.8, the case of directional (columnar) growth is illustrated in diagram (a) and that of equiaxed growth in diagram (c). If a thermocouple is placed at a fixed position in the melt and overgrown by dendrites, different cooling curves will be recorded for directional growth (b) and equiaxed growth (d). This difference is essentially due to nucleation in the case of equiaxed solidification. [19]

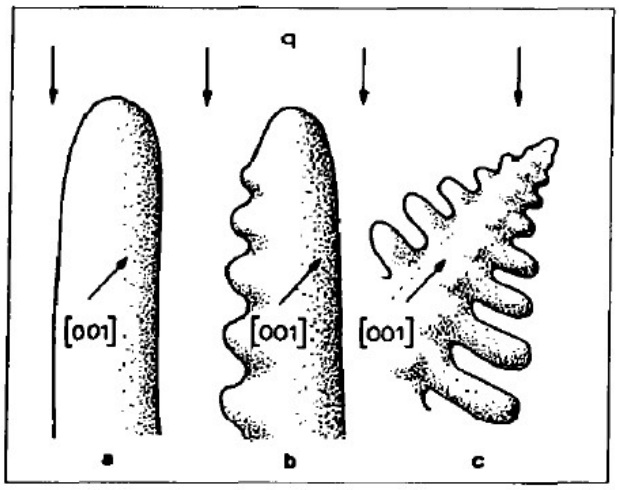

Figure 1.8 Cells, dendrite cells and dendrites.[12]

During directional growth in a positive temperature gradient, cells can exist as a stable growth form (a). However, intercellular instability lead to a dendritic cell formation (b). The asymmetry of the form may be caused by asymmetry of the thermal field. Dendrites will be particularly common in conventional castings and are

characterised by growth of the trunks and branches along preferred crystal orientations such as [0 0 1] in cubic crystals (c). In the case of equiaxed dendritic growth of alloys, the problem of coupled heat and mass- transport must be solved. In the case of directional growth of alloy dendrites, the situation is somewhat simpler because, due to the imposed temperature gradient, the latent heat is transported through the solid while solute is rejected ahead of the tips. In this case, only mass diffusion need to be considered. This permits an approximate solution of the problem of alloy dendrite growth in the columnar zone.

Increasing the cooling rate is known to reduce both the primary dendrite arm spacing (PDAS) and the secondary dendrite arm spacing (SDAS). Also, it has been shown that secondary arm spacing increases with time spent in the liquid-solid region. The equations of the PDAS and SDAS were based on experimental data for low alloy steels. The below Table 1.1 results indicated that the cooling rate and carbon content basically govern the calculation of PDAS, especially for low carbon steel, However, the carbon content governs the selection of mathematical expression to predict SDAS for low alloy steels. [21]

The primary arm spacing λ_1, was calculated as a function of cooling rate C_R and nominal steel carbon content Co (weight percentage) from the following equation:

Expression Developed to Estimate the PDAS	
Equation	Equation Parameters
$\lambda_1 = K(C_R)^m(C_0)^n \quad (\mu m)$ (1)	K=278.748 m=-0.206277638 $0 \le C_0 \le 0.15$ n= -0.316225+2.0325C_0 $0.15 \le C_0 \le 1.0$ n=-0.0189-0.491666C_0

Table 1.1 Expression to Estimate the PDAS as per cooling rate

Expression Developed to Estimate the SDAS	
Equation	Equation Parameters
$0 \le C_0 \le 0.53$ $\lambda_2 = A_1(C_R)^{-n} \quad (\mu m)$ (2)	A_1=148 N=0.38
$0.53 \le C_0 \le 1.5$ $\lambda_2 = A_2(t_f)^d \quad (\mu m)$ (3)	A_2=21.52764-9.4C_0 d=0.4+0.08C_0

Table 1.2 Expression to Estimate the SDAS as per cooling rate

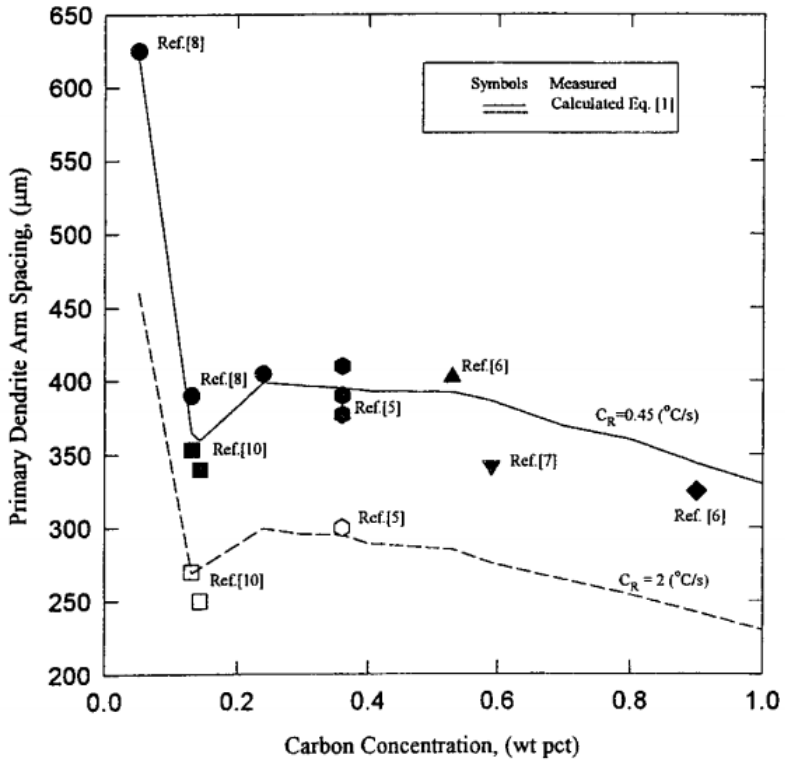

Figure 1.9 Comparison between measured PDAS and calculated PDAS by using equation (1) from Table 1.1 as a function of carbon concentration with two different cooling rates.[16]

Dendrites make up the bulk of the microstructure of most alloys, but several important eutectic alloys are also used in practice. Eutectic morphologies are characterized by the simultaneous growth of two (or more) phases from the liquids. Due to their excellent casting behaviour, which is often like that of a pure metal, and the advantageous composite properties exhibited by the solid, casting alloys are often of near- eutectic composition.

1.7 Heat Transfer in Continuous Casting

By its nature, continuous casting is primarily a heat-extraction process. The conversion of molten metal into a solid semi-finished shape involves the removal of the following forms of heat.[13]

- Superheat from the liquid entering the mould from the tundish.
- The latent heat of fusion at the solidification front as liquid is transformed solid.
- The sensible heat, i.e., cooling below the solidus temperature from the solid shell.

These heats are extracted by a combination of the following heat-transfer mechanisms:

- Convection in the liquid pool.
- Heat conduction down temperature gradients in the solid shell from the solidification front to the colder outside surface of the cast.

- External heat transfer by radiation, conduction and convection to surroundings.

Heat transfer is the major phenomenon occurring in continuous casting, it is also the limiting factor in the operation of a casting machine. The distance from the meniscus to the cut-off stand should be greater than the metallurgical length, which is dependent on the rate of heat conduction through the solid shell and of heat extraction from the outside surface, in order to avoid cutting into a liquid core. Thus, the casting speed must be limited to allow enough time for the heat of solidification to be extracted from the strand. Heat transfer not only limits maximum productivity but also influences cast quality with respect to the formation of surface and internal cracks.

During Heat transfer, metals expand and contract during periods of heating or cooling. These sudden changes in the temperature gradient through the solid shell, resulting from abrupt changes in surface heat extraction, causes differential thermal expansion and the generation of tensile strains.
Depending on the magnitude of the strain relative to the strain-to-fracture of the metal and the proximity of the strain to the solidification front, cracks may form in the solid shell. The rate of heat extraction also influences the ability of the shell to withstand the bulging force due to the ferro-static pressure owing to the effect of temperature on the mechanical properties of the metal. Therefore, heat transfer analysis of the continuous casting process should not be overlooked in the design and operation of a continuous casting machine.

1.8 Categories of Surface Defects

From the standpoint of quality, surface cracks normally pose more of a problem than internal cracks because, being exposed to air, the crack surfaces oxidize and do not reweld during rolling. Below figure shows the various types of surface defects which can occur on the as-cast semis for both slabs and blooms/billets. [16][17]

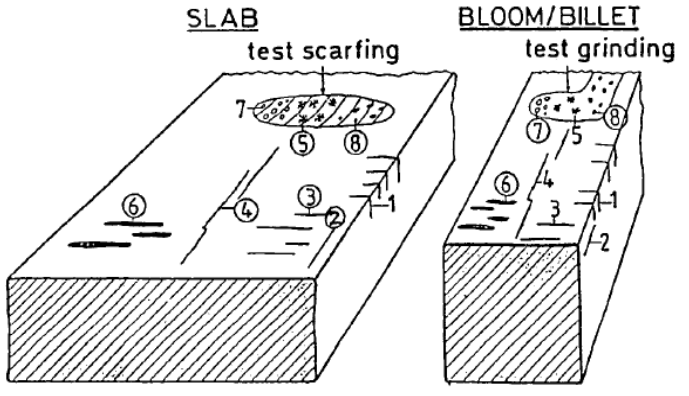

Figure 1.10 Different type of Surface defects [1]

1.8.1 Longitudinal Cracks

They are formed in the direction of extraction of the steel. The presence of this defect causes rejection of the Continuous Cast product.
The factors which influences Longitudinal cracks are as follows:

- chemical composition e.g. a carbon level of between 0.08% and 0.14% (the peritectic range) causes non-uniform heat transfer
- mould powder slag layer not uniform
- poor mould level control
- high mould wear and poor mould surface
- uneven oscillation movement
- insufficient strand support below mould, including misalignment
- non-uniform cooling often related to mould powder and mould Oscillation

Remedy- increasing the perimeter of the moulds

1.8.2 Pin Holes

Cause- evolution of gases resulting from casting powder decomposition during casting
Remedy- proper mixing of molten metal and lubrication of mould

1.8.3 Transverse Cracks

These cracks usually appear due to the tensions on the longitudinal direction of strand. Normally these cracks are ground within the permissible prescribed limits provided they are not deep.
Cause- the thermal stresses due to the uneven solidification
Remedy- set proper secondary cooling and minimizing the localized temperature fluctuations
The factors which influences Transverse cracks are as follows:

- mould powder
- a sensitive chemical composition
- mould taper too large
- poor oscillation conditions
- a low surface temperature at straightening
- non-uniform cooling
- abrupt speed changes

1.8.4 Star Cracks

These cracks are very fine and caused by fragile nature of the strand at high temperatures. They are visible only on scale free surface. The surface is usually ground locally to remove the defect. Intense local cooling and presence of copper at the austenitic grain boundary cause star cracks.

Cause- intense local cooling, which induce local tensions
The factors which influences Star cracks are as follows:

- copper from mould plates
- uneven cooling of surface

Remedy- correlation between the spray flow and the casting speed (automatic flow control)

1.8.5 Corner Cracks

These are cracks present in the edge of the cast steel product. They appear due to high temperature variations in the liquid steel, higher aluminium content in the steel, higher sulphur level in the steel, non-uniform edge temperature, excess friction in the edges during casting because of non-uniform distribution of casting powder, and lower superheat of the steel.
Sticking marks and deep oscillation marks can also be considered as surface defects.

Surface Cracks			
Type	**Cause**	**Influencing Factors**	**Corrective Action**
Longitudinal, midface cracks	Tensile strain generated in the mould and upper spray zones	Crack frequency increased by: - carbon levels of 0.12 pct - increasing S and decreasing Mn/S - varying or increasing casting speed - casting with high pouring temperatures - casting wide slabs - mold conditions - improper water cooling, loss of taper, irregular mold oscillation, improper mold powder, worn molds. - Overcooling in upper spray zones. - Insufficient support in below mold. - Poor alignment between and sub-mold support system	Adjust mould conditions to ensure uniform cooling. Reduce cooling in upper spray zones and check sub-mould support system.

Longitudinal, corner cracks	Nonuniform cooling in corner region In slabs off-corner cracks caused by bulging of narrow face in mould	Cracking associated with: Reversal of mold taper owing to distortion or wear. Large corner gaps in plate molds High tundish temperature High casting speed Incorrect foot roller setting Steel containing 0.17-0.25 pct C, S>0.035 pct, P>0.035 pct Long molds and steel with 0.15 to 0.23 pct C give rise to worse cracking	Plate mould walls with chromium. Reface the mould. Check alignment and lubrication for uniformity. Check mould support conditions.
Transverse, midface and corner cracks	Large surface temperature gradients in spray zone and straightening within favourable range of temperature between 700°C and 900°C	Strongly influenced by steel composition Al, V, Nb, Mn >1 pct being the most important elements	Reduce spray cooling and make as uniform as possible to minimize cooling/reheating and maintain surface temperature above 900°C through to straightener
Star cracks	Scraping of copper from mould	Secondary cooling	Plate mould walls with chromium. Adjust machine alignment

Table 1.3 General Information about surface cracks

1.9 Categorisation of Internal Defects

Internal Defects are following:

- Intracrystalline Cracks:

Cause- internal stresses due to different rates of cooling of outer and deeper layers
Remedy- minimized by proper mixing of the molten metal, lowering the Sulphur level

- Internal Blow Holes:

Cause- insufficient de-oxidation of steel, Moisture present in the casting powder
Remedy- Enough de-oxidation of steel by using dry materials and additives

- Shrinkage Porosity:

Cause- metal changes phase from the molten state to the solid state, it always shrinks in size
Remedy- Proper mixing of molten metal

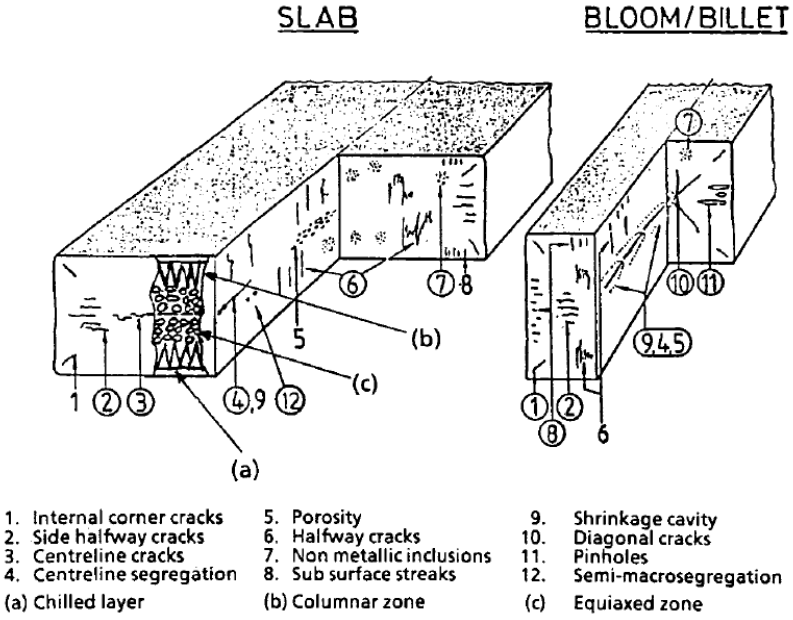

Figure 1.11 Internal defects **[1]**

The main internal defects in continuously cast semis are:

1. **Intercolumnar Segregation/Cracks:**

- high superheat
- bad machine condition at the point of formation
- secondary cooling too low
- too high surface reheating causing thermal stresses

2. **Centre Segregation (including semi macro segregation) and centreline cracks:**
   - bad machine condition at area of final solidification
   - secondary cooling water too low

3. **Triple Point Cracks:**
   - cooling slab narrow face too high
   - cooling slab narrow face too low
   - bad machine condition in the area of formation

Triple-point cracks, such as shown in **Figure 1.11**, arise during the casting of slabs. Viewed in a transverse section, they are oriented normal to the narrow face within the V-shaped region of the slab where the three solidification fronts meet. The zone of cracking, according to Mori, lies between 3 and 10 cm from the surface. Ozeki and Duke report that the cracks may vary in length from 0.6 cm to several inches and in width from a thin dark line to an open crack. They have also found the susceptibility of steel to triple point cracking to be dependent on chemistry increasing with decreasing manganese levels below 0.9 pct Mn. Steels with low manganese contents are particularly prone to crack formation when Mn/S is less than 30. There is general agreement that the cracks are caused by bulging of the wide face of the slab owing to insufficient containment of the solid shell. While this situation can arise if a set of rolls is too widely gapped, it may also result from rolls that are too narrowly gapped. In the latter case, bulging may occur at the next roll station. Bulging of the wide face provides the tensile strain for triple-point cracking because it leads to concavity of the narrow face owing to the relative high strength of the colder corners. The tensile strain is then greatest close to the solidification front where the steel is the least ductile. Prevention of this type of crack clearly can be achieved by maintenance of the proper gap between rolls throughout the metallurgical length of the slab.

4. **Inclusions:**
   - dirty steel
   - re-oxidation of steel
   - insufficient pouring tube depth

5. **Midway cracks**

Many publications exist in the literature which discuss the factors that contribute to midway crack formation. It is generally agreed that excessive secondary cooling and a high casting temperature are operating factors responsible for midway cracks. In addition, the chemistry of the steel exerts an important influence; sulphur and phosphorus affect the crack susceptibility of steel.

Excessive spray cooling is a major factor in the formation of midway cracks because it leads to subsequent reheating of the strand surface which provides the driving force for cracking. Reheating causes the surface to expand and this imposes a tensile strain

in the interior region of the solid shell which, as seen earlier, is weak and nonductile above about 1340°C.

From this analysis, midway crack formation can be prevented either by minimizing the tensile strain, *i. e.* the surface reheating, or by increasing the strength and ductility of the steel in the high temperature zone. Minimization of the tensile strain can be achieved by paying close attention to the design of the spray system to ensure that the rate of cooling does not decrease abruptly between mould and sprays, sprays and radiation cooling or between successive spray nozzles.

6. Centreline Cracks

Centreline or core cracks appear in the central region of a cast section and form toward the end of solidification. Looking first at slabs, the cracks can be found in all grades of steel independent of composition and superheat. The formation of centreline cracks is strongly influenced by machine and operating variables such as spray water intensity, roll alignment low in the strand and casting speed. Cracking can be reduced by re-gapping rolls, reducing speed and/or increasing spray cooling. From this it can be deduced that the strain causing the cracks is generated by bulging of the wide face owing to inadequate containment. The strain is normal to the bulging face and acts on regions of low ductility near the solidus at the centreline. Increasing spray cooling has a beneficial effect because it results in a cooler shell that can more effectively withstand the ferro static pressure. Reduction of the casting speed has a similar influence; and because the metallurgical length is reduced proportionately, the centreline temperature is lowered below the range of high temperature low ductility before bulging occurs. That steel composition has little effect on crack formation is an indication that the strains are larger than the ductility of most steel grades above 1340°C. Since bulging is the driving force for centreline cracks in slabs, maintenance of the correct roll gaps is vital for crack minimization. Ozeki and Duke have described two systems-load cells mounted in each roll station in the machine and a "gapping sled " which can be attached to the starter bar - to facilitate the checking of roll gaps. In the casting of billets, bulging plays a lesser role in the formation of centreline cracks; and Van Drunen have suggested that the sudden drop in centreline temperature at the completion of solidification generates the cracking strains. The abrupt decrease in centreline temperature is a natural phenomenon, occurring in any casting, and arises when the final trace of latent heat has been extracted from the centre region. The drop-in centreline temperature is considerably more rapid than the decrease in surface temperature with the result that the centre region contracts. The centre is constrained from contraction, however, by the surrounding colder steel and thus is put into tension. It has been suggested that severe secondary cooling may contribute to the formation of these cracks. This may be possible if, due to the arrangement of the sprays, considerable reheating of the surface below the secondary cooling zone coincides with the bottom of the liquid pool. Then the tensile stresses imposed on the central region by reheating will magnify the tensile stresses developing from rapid centreline cooling. In the extreme, this situation could lead to severe centreline cracks.

Formation of centreline cracks could be suppressed by applying water sprays at the point of complete solidification, since then the surface temperature could be made to drop at an equivalent rate to the centreline, thereby lowering the central tensile stresses.

7. Diagonal Cracks

This type of crack, normally seen in billets, is associated with rhomboidity. Diagonal cracks usually run between obtuse corners of the rhomboid section. Rhombicity is a greater problem with smaller sizes of billets and high pouring temperatures. It can be corrected by installing corner rolls at the top end of the roll apron as well as by maintaining symmetrical cooling in the sprays. Clearly, diagonal cracks result from distortion of the billet which can arise if two adjacent faces are cooled more rapidly than the other faces in the mould or secondary cooling zone. The contraction of the steel in the vicinity of the colder faces generates a tensile strain, oriented diagonally between these faces. If sufficiently large, the strain causes distortion and cracks to form at right angles to the strain axis; that is between the obtuse corners. The cracks form initially in the high temperature zone of low ductility but may grow outward toward the corners depending on the magnitude of the strain. To minimize diagonal crack formation, care must be taken to achieve equal cooling on each of the four faces. This requires good alignment between the mould and roller cages and avoidance of plugged or bent spray nozzles in the secondary cooling zone.

Internal Cracks			
Type	**Cause**	**Influencing Factors**	**Corrective Action**
Midway cracks	Surface reheating in or below spray chamber	High casting temperature, S and P> 0.02 pct increase crack formation	Adjust spray system to minimize reheating. Lower pouring temperature, minimize P and S levels Regap rolls.
Triple-point cracks	Bulging of wide face of slabs	Cracking increases with decreasing Mn below 0.9 pct Mn and with Mn/S<30	Regap rolls
Centreline cracks	In slabs, bulging of wide face	Spray water intensity, casting speed, roll alignment low in the strand. Severe secondary cooling and high	Regap rolls, reduce casting speed or increase spray cooling

	In billets, rapid cooling of centre region below pool	pouring temperature may enhance crack formation	Adjust secondary cooling near bottom of pool
Diagonal cracks	Asymmetrical cooling in mould or sprays	High pouring temperature and smaller billet sizes increase cracking	Install corner rolls at the bottom of the mould, check alignment between mould and roller apron. Look for plugged spray nozzles.
Straightening/ bending cracks	Excessive deformation near solidification front due to straightening or bending	Bending on liquid centre	Reduce tensile strain at solidification front to less than 0.3 pct. Lower casting speed
Pinch roll cracks	Excessive pinch roll pressure	Squeezing on liquid centre	Reduce pinch roll pressure

Table 1.4 General information about internal defects

1.10 Segregation in Continuous Casting of Steel

Segregation is an important feature of the solidification of steels. Solubility of dissolved elements is higher in the liquid phase than in the solid and it will tend to come out of solution ahead of the solidification front. This solute rich material may be trapped between the arms of the growing dendrites, leading to micro segregation, or may be trapped at the centreline or forced into channels within the equiaxed zone by macroscale factors related to solidification shrinkage and strand geometry. The Centreline and Off-centre 'V' type segregates arises due to these effects.

The main factors influencing segregation are:

- steel chemistry
- superheat
- casting speed
- cooling regime
- Machine geometry

1.10.1 Macro Segregation

Macro segregation has been one of the major problems during the continuous casting process of high carbon steel billets or blooms. The reason is that high carbon steel tends to solidify over a wide temperature range, so the size of the mushy zone is relatively large. However, during the continuous casting process of steels, the solidifying dendrites reject dissolved elements continuously at the solidification front, due to less solubility of solutes in the solid phase as compared to liquid phase, thereby leading to gradual enrichment of remaining liquid and forming the solute elements segregation. Generally, macro segregation refers to nonuniformity of chemical composition over a large area in the cast section, so the desired level of chemical homogeneity cannot be obtained even after prolonged heat treatment. All types of macro segregation in castings form within the solid-liquid zone.

In most cases, they are the results of slow inter-dendritic flow, driven by shrinkage, geometry, solid deformation or gravity. The F-EMS has been widely used for continuous casting billets. This reason is that it can reduce effectively macro segregation by combining with the mold electromagnetic stirring (M-EMS).

1.10.2 Micro Segregation

Micro segregation refers to freezing of solute-enriched liquid in the inter-dendritic spaces. But it does not constitute a major quality problem, since the effects of micro segregation can be removed during subsequent soaking and hot working.

Localised micro segregation causes macro segregation because of physical movement of liquid and solid phases, most important being flow of inter-dendritic liquid.

1.10.3 Centreline Segregation

Centreline Segregation is a major defect in Continuous casting. It relates to the central porosity in the most cases. In steel, centrally segregated regions are responsible for inconsistent mechanical properties in the finished products due to formation of low ductility structures. Positive centreline segregation of elements like sulphur leads to hot-shortness during hot working of continuous cast products. Centreline segregation cannot be removed by annealing because homogenization would require much larger time than are economically acceptable under production conditions.

These are the some of the techniques to reduce the degree of segregation are:

- electromagnetic stirring
- accurate prediction and control of sump position and machine geometry
- soft reduction (mechanical or thermal)
- optimised casting practice (casting speed, machine taper, superheat, cooling regime)

Electromagnetic stirring (EMS) was applied not only in the mould but in specific positions along the strand, mostly known as strand (S-EMS) and final (F-EMS)

positions. FEMS position is considered the position at which the mushy zone along the centreline becomes solid, or the position around the final solidification of the product. This is an effective technical solution to lessen the problem and is currently applied in some caster installations worldwide.

1.11 Electromagnetic Stirring (EMS)

Electromagnetic stirring technology has been used in the continuous casting of steel for many years but the effect of the application and subsequent benefits of stirring the liquid core depends very much on section size, steel grade and product application.

1.11.1 Principle of Electromagnetic Stirrer

The electromagnetic stirrer utilizes the principle of a linear motor. It differs from the conventional mechanical and decompression types as it is a non-contact stirrer in which no part touches the molten metal. As shown in the figure 1.12, a coil is installed at the bottom of the furnace generates a moving magnetic field (H) if a 3 phase AC voltage is applied to this coil(inductor). Electric power force is generated in the molten metal due to the action of magnetic field and causes induction current (I) to the flow (Fleming's Right hand rule). This current then acts with the magnet field of the inductor to induce electromagnetic force (F) in the molten metal according to the Fleming's left-hand rule. This force is known as Lorentz force.

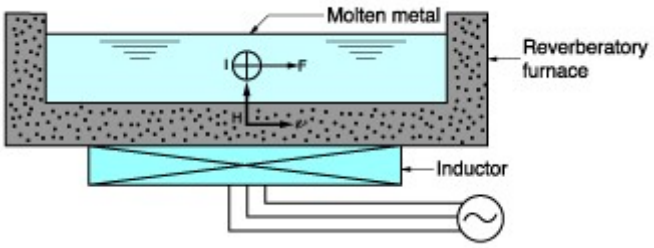

Figure 1.12 Principle of electromagnetic stirrer.[10]

Due to the Lorentz force, there is a generation of a torque that gives the liquid steel a rotational movement. The generated torque depends on the following factors.

- Intensity of supply current
- Number of windings forming a coil
- Frequency
- System geometry.

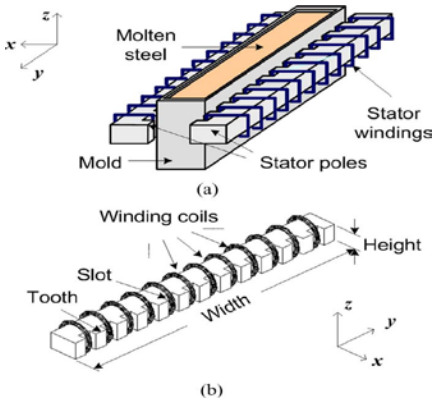

Figure 1.13 Electromagnetic stirrer (a) Conceptual diagram. (b) One side of the stator.[11]

These parameters change depending on the stirrer type. Thus, the magnetic field acts as a non-intrusive stirring device and it can, in principle, be engineered to provide any desired pattern of stirring. The stirrer design, size and position etc. depend on the continuous casting machine data, the steel grades to be produced and the casting parameters. Electromagnetic melt stirring systems create a rotating magnetic induction field with an induction of B, which induces eddy current j in a direction perpendicular to B, whose velocity is v. Induction B and current j create the electromagnetic force, which works on every unit of volume of steel and bring about a stirring motion in the liquid steel. The vector product (v x B) demonstrate a connection between the electromagnetic field and the flow of the liquid steel. The speeds of the liquid steel caused by the EMS is somewhere in the range of 0.1 m/s to 1.0 m/s.

Basically, there are two types of stirring as applied to continuous casting "rotary" stirring and "up and down" (or axial) stirring. During the last decade, many versions of these types of stirring have been proposed in many patents, some more sophisticated than others, but all or nearly all of them can be classified in either of the categories mentioned above.

1.11.2 Rotary Stirring

The original work on rotary stirring was done by a group of researchers in Austria. Billets cast in a round mould were stirred at the mould level or just below the mould. Indeed, the mould is the only area that rotary stirring might make sense; stirring substantially below the mould in a rotary fashion may create more problems than it would solve. As stated, there is some merit in rotary stirring of rounds in the mould. Solid inclusions are removed from the surface of the casting and heat transfer is enhanced by forcing the solid skin of the strand to be in better contact with the mould. There is no danger of rupturing the skin by rotary stirring in the mould. But the major advantage of rotary stirring is in the ease of equipment design. Electrical engineers are very familiar with this type of electromagnetically induced motion because it is the same as that of nearly all electric motors in use today.

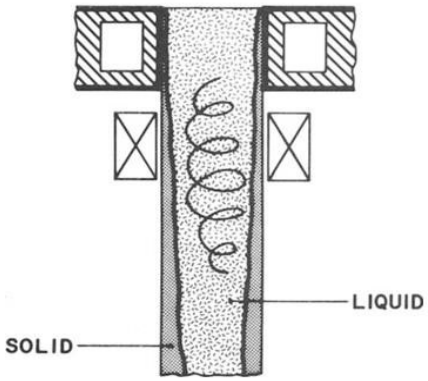

Figure 1.14 Rotary Stirring [12]

While rotary motion, presents no engineering design problem, it might not be the best type of motion from the metallurgical point of view. One of the basic problems with rotary stirring is that the liquid is subjected to centrifugal forces which would tend to segregate its light constituents (inclusions for instance) toward the centre (see Figure 1.14). This imposes an upper limit on the velocity of the liquid, which is not necessarily the same limit set by the appearance of the "picture frame" effect. Sometimes these considerations can be ignored, as when casting rounds for pierced tubing, possibly. However, another more inflexible limitation cannot be ignored. Raising the circular velocity of the liquid disproportionately increases the pressure on the solid shell, which may then rupture. This danger is particularly acute when casting a steel that contains highly segregating elements, such as P, Se, and Pb. The low-melting liquid that these constituents form occupies space between the dendrites reducing any strength the shell might have.

Another undesirable situation that arises when stirring below the mould in a rotary fashion, particularly when it is done in one level only, is the effective separation of the liquid pool into two parts, an upper (hot) part above the stirring level and a lower (cold) part below the stirring level. Besides disrupting the natural flow in the pool, this partitioning may cause bridging problems. Bridging, in turn, intensifies macro segregation as may be demonstrated by some problems reported recently when rotary stirring was applied below the mould only. Such a problem is particularly likely to develop when stirring with low velocities. Large fragments of dendrites separated from the mushy zone in the stirred region cannot be reduced in size because of the low intensity of stirring. These large fragments sink to the lower (cold) part of the pool where they have a chance to grow, form clusters, and cause bridging.

There might be another disadvantage to rotary stirring. Early data have indicated that to reduce substantially the inclusion size and content of steel by EMS, the velocity of the liquid must exceed a certain lower limit. For instance, for 4335 type steel this limit has been shown to be over 50 cm/s, which is comparable to the velocities occurring during the rimming action in large ingots where a clean skin is also produced. There is a near certainty that the previously mentioned upper limits,

for safe rotary liquid motion, conflict with the high-speed requirements for inclusion reduction. The same is true to produce the new solidification structures, namely the fibrous structure and the flow modified or thamnitic structures, which also require high velocities. Segments of the steel industry that have been aggressively pursuing new developments for quality, in general, and induction stirring may soon be pursuing these structures through high velocity stirring.

1.11.3 Intermittently Reversing Stirring

A variation of the rotary stirring mode has been suggested, originally by some Japanese investigators. The technique provides for intermittently reversing flow direction which, it is claimed, improves the size of the equiaxed zone. The above discussion for rotary stirring applies here, with a few more qualifications. Intermittent motion does waste energy, but it has merit in meeting one objective of EMS, frustrating columnar growth. Reversing flow in stirring not only might break dendrites into smaller fragments by shear in local turbulence cells, it can also frustrate the unidirectional growth of columnar dendrites, as these dendrites would attempt to grow into the flow (upstream) all the time. It is doubtful, however, that other possible benefits of EMS can be derived with this technique.

1.11.4 Axial Stirring

The axial or "up and down" version of stirring provides for moving the liquid portion of a solidifying strand in a direction parallel to the axis of the strand, this type of induced motion can be used to intensify the naturally occurring, thermally induced, convective flow patterns. In the mould area, there are reasons to reverse the natural flow. In the continuous casting of steel, the mould area constitutes a small part of liquid pool which may be as deep as 15 m (50 ft) or more (depending on the speed and size of the machine). Below the mould the flow is "down" adjacent to the solid skin and "up" at the centre of the strand.

The "up and down" version of EMS is the most appropriate from the metallurgical point of view. The velocity of the liquid is practically unlimited in this technique, which provides ample freedom for the application of desired controls. The danger of breakouts is minimized, because the electromagnetically induced forces tend to contain the liquid rather than force it against the solid shell. There are other major benefits. The hot liquid from the top is brought quickly to the bottom of the pool, which tends to reduce somewhat the thickness of the shell and to keep the temperature gradient high across the mushy zone. Both these effects enhance the heat flow, which in turn might be useful toward increasing the productivity of the casting machine. There is another way the productivity may be enhanced with this version of EMS. The contour of the solid shell can be modified to form a round bottom and the depth of the pool reduced; this would allow higher casting speeds. The extent of centreline shrinkage and segregation can be reduced as well, since the isotherms are changed and growth at the centre of the strand has an increased upward component.

Finally, even the inclusions that form during solidification, such as the notorious alumina clusters, are not allowed to be entrapped in the solid. They are swept quickly to the top of the pool where they have a chance to join the slag (that is, floating over the meniscus) and, thus, be eliminated. This type of flow is rather difficult to implement; particularly if stirring is to be applied over a considerable part along the metallurgical length, i.e., the continuous version of "up and down" stirring. It should be emphasized, however, that the difficulties in this case are in the electrical engineering side of the problem. It is relatively difficult to implement one-directional flow without major perturbations that show up either between coils or at the end of a series of coils that form a linear motor. These anomalies are reflected in cast structures as bands of either positive or negative segregation. Further, "up and down" stirring normally requires a rather large area of the strand free of support rolls, or at least modification of the rolls, so that they do not interfere with the fields of the linear motors used. Finally, the linear motors used for this type of stirring have very low efficiency (of the order of 1% or even less), primarily because of the high resistance of their electromagnetic loops (large air gaps and solid metal-skin gaps).

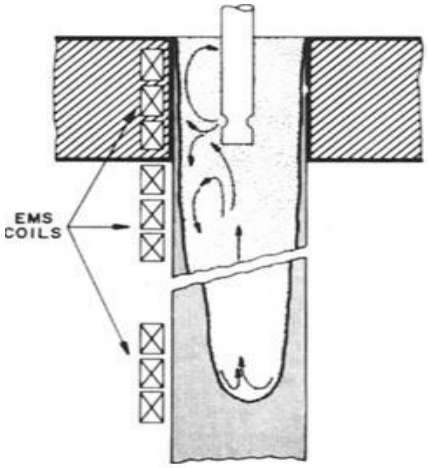

Figure 1.15 Axial Stirring [12]

1.11.5 Three Principal Types of Stirring

- In- mould stirring (sometimes termed as primary EMS)
- Stirring below the mould where there remains a large percentage of liquid steel (sometimes termed as secondary EMS or below mould stirring)
- Stirring just prior to the final solidification point (termed as final EMS)

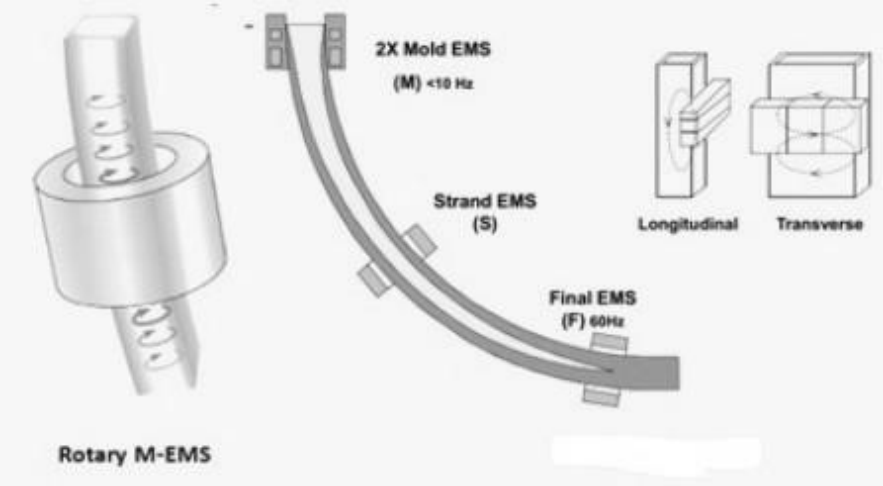

Figure 1.16 Types of EMS [14]

M-EMS

M-EMS is usually installed in the lower part of the mould for stirring of the liquid steel in the mould. It improves surface, sub surface and inner strand quality. The application of M-EMS results into reduction of pinholes, centre porosity and segregation in the cast product. It improves the solidification structure, reduces the surface roughness and increases the heat delivery rate. M-EMS is either of round or square design and it can be installed internally or externally. For providing flexible control of stirring speed in the mould meniscus, dual coil M-EMS has been developed. The dual coil M- EMS consists of two independent EMS. The upper EMS is meant for flow control in the meniscus and the lower EMS performs the stirring of main metal in the mould. The reduction in the liquid steel speed in the meniscus is achieved by rotating the upper EMS magnetic field in the opposite direction to that of the lower EMS. Such a design of dual M-EMS widens the opportunities for using the EMS technique under various conditions of continuous casting of steel.

S-EMS

S-EMS produces a stirring force that pushes the liquid steel horizontally along the cast product width and generates a butterfly type flow pattern in the liquid steel. When SEMS can be placed behind the support rollers (Figure 1.17) then it is not dependent on a minimum support roller diameter and hence in this case can be optimally placed along the strand from the metallurgical point of view. S – EMS when built into the support rollers requires a minimum roller diameter to include the iron core and windings. In this case the stirrer is placed at a distance from the meniscus and hence is less effective. S-EMS operates at low frequency to ensure good penetration of the stirrer force through the strand. As a result, the liquid steel has transverse stirring as shown in Figure 1.16. S–EMS is usually used in combination with M – EMS. S– EMS can be of either linear or rotary type stirrer. Most common is the linear stirrer, which is easy to install and protect against heat radiation and

possible breakouts. S-EMS promotes the formation of equiaxed structure. It promotes grain refinement in the cast product and reduces the shrinkage cavity, centre segregation and internal cracks. It also removes superheat effectively.

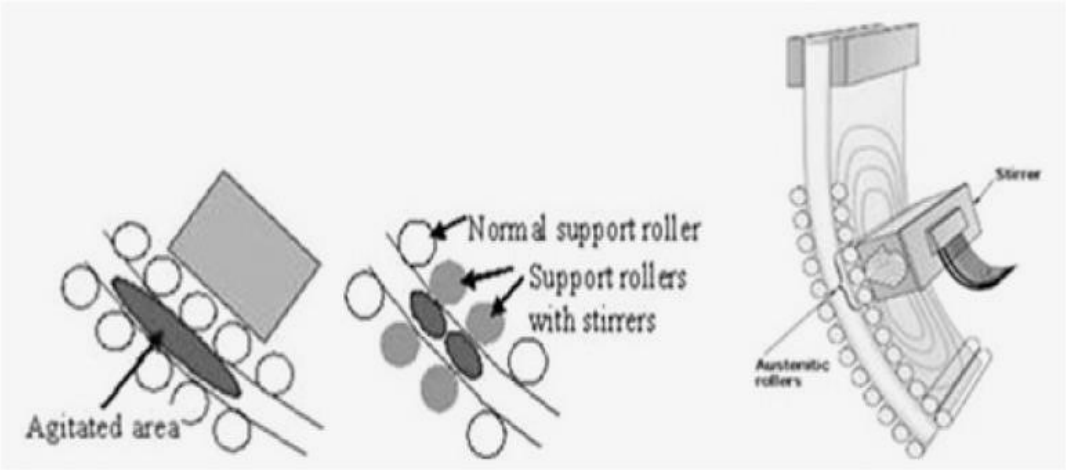

Figure 1.17 Location of Secondary EMS [14]

F- EMS

There is equally strong interest in using EMS to stir far below the mould in the final solidification zone of a continuous casting strand. However, conventional EMS systems have proven to be somewhat ineffective when applied in this region. As a potential solution, there recently has been considerable interest in applying modulated Lorentz forces to develop a broadly distributed vigorous stirring in the final zone. F-EMS is generally installed in combination with M-EMS or S-EMS to reduce and cut peaks in centre segregation. F-EMS is particularly efficient when casting high carbon or high alloy steel grades. Also with the use of F- EMS, it is found that the solidification structure of the cast product is improved and there is increase in the ratio of the equiaxed structure and the inner porosity. The shrinkage is reduced, and the ratio of central carbon segregation is decreased. Further the secondary dendrite arm spacing (SDAS) is improved, and the ratio of central equiaxed grain is considerably increased, which results in finer grains. Therefore, the quality of the cast product is enhanced with the F-EMS.

For more demanding qualities the use of EMS can be justified when the costs of the quality defects, conditioning or rejections, or the costs of casting larger sections are too large.

- Carbon steel with carbon less than 0.2 %, Rotary stirring is used.
- In some cases, In Mould stirring is preferred than the secondary stirring because in the secondary stirring we find the negative segregation. In-fact negative segregation does not have any effect on the mechanical properties but

one minor exception is that it can cause local variation in the hardenability which is not appreciated.

- Carbon content between 0.2 and 0.5%, two stage stirring is used. It is better to complement the in mould stirring with the secondary stirring or final stirring.
- For carbon content greater than 0.5% and alloy steels with a large solidification range, three stage stirring is used.

1.12 Literature Review - Advantages of EMS

Advantages of EMS in the final product depend on the application and some examples are given below

- Better hot workability, during extrusion forging of the bars the frequency of internal failures is lower
- Improved shearing ability by avoiding the structure which causes cracks
- Improved hardenability because of improved homogeneity
- Improved wire rod drawing performances with a low frequency of cup and cone breakages
- Higher and more consistent fatigue properties of bars

Any benefits from EMS for slabs can be negated from the poor geometry. So, care should be taken for the machining. Method of reducing submerged nozzle convection currents with the electromagnetic brake (EMBR) for improving cleanness. This consists of two sets of coils placed along the outer walls of the mould faces. The magnetic field reduces the liquid steel velocity and impurities float to the surface where they are trapped by the mould powder. The roll gap geometry of bloom casters and more significantly slab casters can have a major influence on the internal quality of continuous cast semis and on various types of segregation and consequently the increased levels of some elements in these segregated areas. The main types of segregation caused by deviations from the true roll gaps are as follows

- Inter columnar macro segregation
- Centreline macro segregation
- Off centreline semi macro segregation (also termed V segregation or spot segregation)

In the temperature range 1300°C up to the solidus the ductility of steel is very low. This is due to liquid phases of FeS and MnS which have segregated to the boundaries between dendrites. FeS and MnS both have melting points much lower than steel and hence these weak boundaries open at quite low tensile strains.

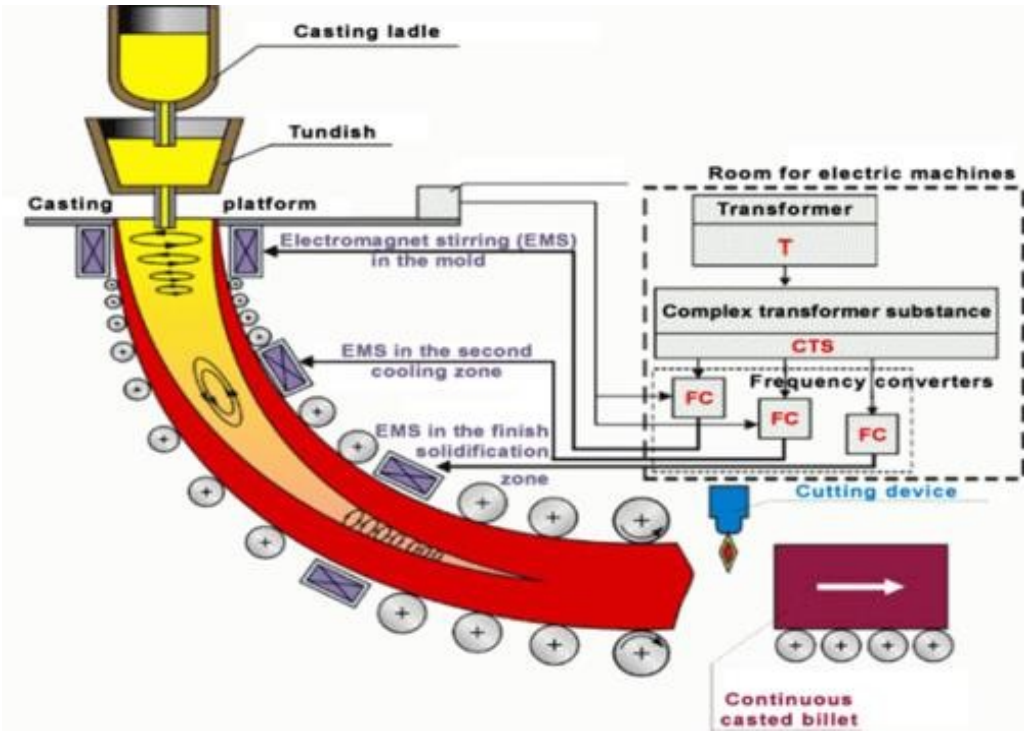

Figure 1.18 Continuous casting with all the stirrers [15]

	M-EMS	M-EMS + F-EMS	M-EMS + S-EMS + F- EMS	M-EMS+S-EMS	S-EMS	S-EMS + F- EMS
Pinhole and blowhole	+++	+++	+++	+++	–	–
Surface & subsurface cracks	+++	+++	+++	+++	–	–
Breakout reduction	++	++	++	++	+*	+*
Surface cracks (round)	++	++	++	++	–	–
Solidification structure & internal cracks	++	++	+++	++	+**	+**
Centerline segregation, centre porosity	++	+++	+++	++	++	+++
V segregation	+	+++	+++	++	+***	++

* S-EMS in high position
** Better structure only in centre part of the product, after position of S-EMS, worse structure in external part compared to application of M-EMS. Risks of negative segregation when excessive stirring applied.
*** with S-EMS in low position

Figure 1.19 Benefits using one or more EMS [14]

One of the metallurgical problems found in continuously cast products is the development of large columnar dendritic zones. The effect of columnar growth on the mechanical properties such as loss of ductility in steel has been investigated by

Weiser. Alberney, *have* shown that centreline defects in continuous casting can be significantly reduced by controlling the columnar growth regions. The control of columnar growth is crucial in producing good quality strand cast products.
Essentially, induction stirring causes a sweeping flow along the solid-liquid interface which affects the final solidification structure because it influences the local growth conditions such as the temperature gradient, the boundary layer thickness, and the structure and size of the "mushy zone". Since macro-segregation is known to result from interdendritic fluid flow, reduction in the length of the "mushy zone" should effectively reduce the extent of macro-segregation, particularly along the centreline. Past research at the Republic Steel Research Centre has shown that electromagnetic stirring is an effective means of improving continuously cast steel solidification structures by preventing columnar growth.
The size of columnar zones and associated inter-dendritic segregation and shrinkage porosity are greatly reduced by the use of in-strand or in-mould electromagnetic stirring. The latter technique effectively increases the size of the equiaxed solidification zone and greatly reduces the amount of centreline shrinkage. The relative size of columnar and equiaxed zones in a cast cross section are also affected by superheating of liquid steel. High superheating in unstirred billets increases the size of the columnar zone because the nucleation of equiaxed dendrites is retarded. Electromagnetic stirring reduces the effects of high superheats but does not completely compensate for the increased size of columnar zones developed by high superheat temperatures.

Superheat was one of the most fundamental factors recognized from the early years of continuous casting especially for medium and high carbon steels. In an early report, pilot plant tests were performed casting 150 x 150 mm x mm billets of high carbon steels. It was proven that at low superheats or even sub-liquidus casting temperatures, the centreline segregation was minimized. The electromagnetic stirring at the mould (M-EMS) exhibited some benefits, and the application of EMS at the strand (S) and final (F) stages of solidification started being installed in some casters worldwide. It was found that the combination of EMS, that is, (S+F)-EMS for blooms and (M+S+F)-EMS for billets, is the most effective method for reducing macro-segregation among various EMS conditions, causing them to solidify more rapidly during the final stages of solidification, providing more finely distributed porosities and segregation spots along the central region. The optimum liquid pool thickness was found to decrease as the carbon content increased, which may be attributed to longer solidification times in the solid fraction range from fs= 0.3 to 0.7. The effect of superheat on the solidification structure was analysed, verifying the empirical fact that increasing superheat the columnar dendritic growth increases against the equiaxed one. They concluded that convection effects influenced micro-segregation behaviour of the studied high carbon ($C \leq 0.7\%$), and high manganese steels.

The effect of final electromagnetic stirring parameters with current intensity increasing from 300 A to 400 A and frequency increasing from 4 Hz to 12 Hz, on the electromagnetic forces and carbon concentration distribution in the central cross section of 70 steel square billet has been studied.[37] The optimal F-EMS parameter

to make uniform the central cross-sectional carbon concentration and minimize the center carbon segregation of 70 steel billets has been obtained with a current intensity of 280 A and frequency of 12 Hz. Under this stirring parameter, the carbon segregation indexes for all sampling points are in the range of 0.92–1.05, which is attributed to the fact that its stirring intensity is more suitable for decreasing the strand center temperature and increasing the solidification rate of billet. Therefore, the rejected solute element has limited time to transport after electromagnetic stirring which promotes the reduction of center segregation.

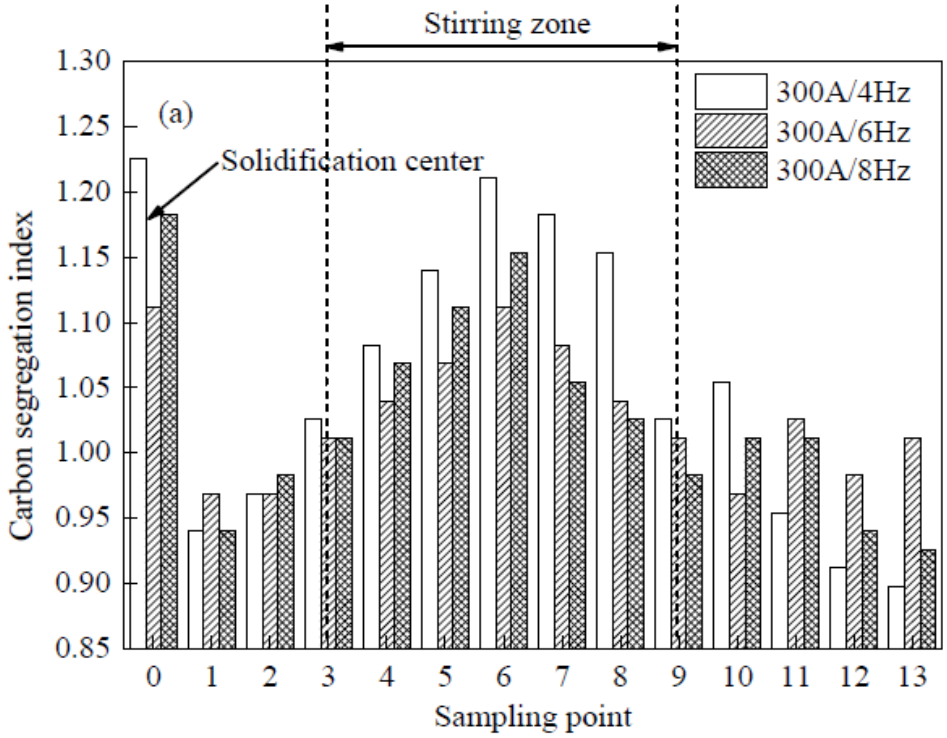

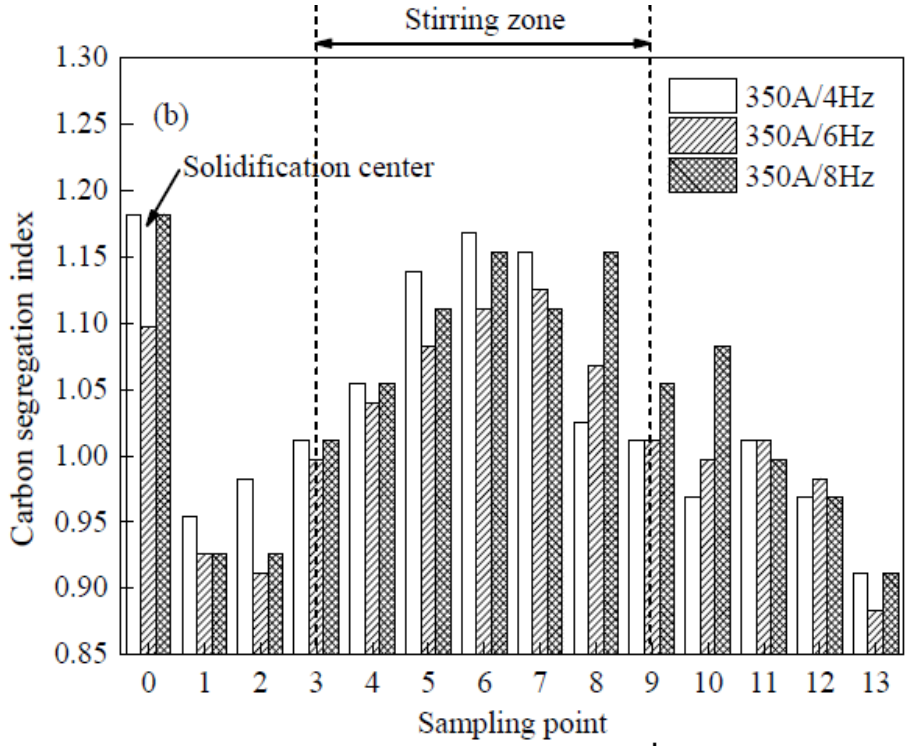

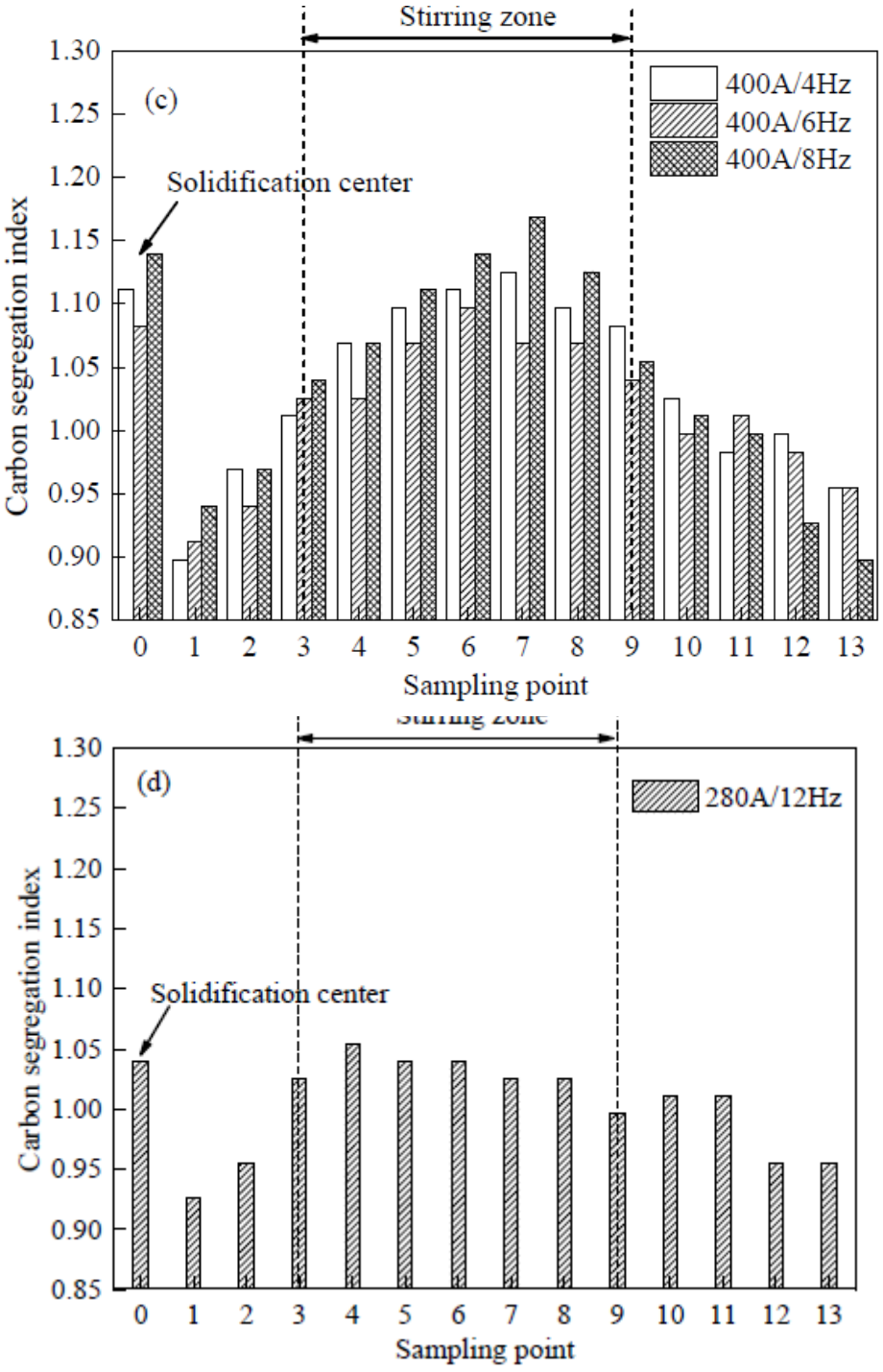

Figure 1.20 The Carbon segregation index in the middle of the billet cross-section along the radial center line and diagonal with different stirring parameters: (a) 300 A, 4–8 Hz; (b) 350 A, 4–8 Hz; (c) 400 A, 4–8 Hz [37]

It is well known that porosities and shrinkage cavity occur in the central part of continuous casting blooms and billets. Although there are good results in carbon segregation levels at a stirring current and frequency of 280 A and 12 Hz, respectively,

further investigations have shown that the F-EMS has a significant impact on the other internal qualities of a square billet. Figure 1.21 shows the macroscopic structure of a longitudinal section at a current intensity of 280 A and frequency of 12 Hz compared to a current of 300 A and frequency of 4 Hz. As seen in Figure 1.21a, at the billet centreline, where the last remaining portion of the liquid pool solidifies, a large area of shrinkage porosities has been formed. The central shrinkage porosity of the billet with current of 280 A and frequency of 12 Hz is less pronounced and more uniform in distribution, as shown in Figure 1.21 b. Moreover, there exists a serious segregation defect such as center black spot in the etched macrograph with current of 300 A and frequency of 4 Hz. However, the segregation defect of the billet apparently subsides with a current of 280 A and frequency of 12 Hz, which illustrates that the current of 280 A and frequency of 12 Hz is the optimal F-EMS parameter to improve the segregation.

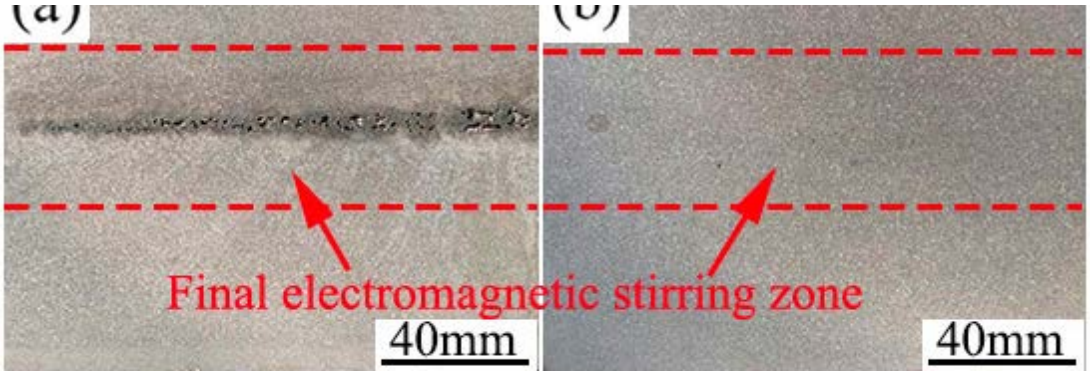

Figure 1.21 The macroscopic structure of longitudinal section with current intensity of 300 A and frequency of 4 Hz (a), and current intensity of 280 A and frequency of 12 Hz (b), respectively.

The effect of F-EMS parameters on centre segregation was investigated in 140 mm × 140 mm billet continuous casting process. In the model, the initial growth of equiaxed grains which could move freely with liquid was treated as slurry, while the coherent equiaxed zone was regarded as porous media. The results show that the stirring velocity is not the main factor influencing centre segregation improvement, which is more affected by current intensity and stirring pool width. Because solute transport is controlled by solidification rate as stirring pool width, centre segregation declines continuously with current intensity increasing. As liquid pool width decreases and less latent heat needs to dissipate in the later solidification, the centre segregation could be improved more obviously by F-EMS. Due to centre liquid solute enrichment and liquid phase accumulation in the stirring zone, centre segregation turns to rise reversely with higher current intensity and becomes more serious with stirring pool width further decreasing, it forms positive segregation and solute can be concentrate with weak stirring, leading to centre segregation deterioration. With the optimized current intensity, centre segregation improvement is better with respect to F-EMS. [33]

Some F-EMS stirring techniques are more effective than others in terms of structure morphological transformation from original dendritic to globulitic and in its refining. Macrostructure of casts without the use of stirring is different from the one with the use of stirring. The structure can be obtained with conventional stirring is largely globule-shaped with some presence of dendrites and dendrite fragments. The structure obtained with modulated stirring consists of entirely globule-shaped crystals and structure appears to be more refined.

Grain size can be varied by applying different stirring setting. With F-EMS conventional stirring, the grain diameter would be reduced in both cast mid radius and in central area with comparison with the unstirred structure. A further grain diameter reduction was achieved with counter-rotating modulated and unmodulated stirring. However, the smallest grain diameter in of the casts was obtained with unidirectional modulated stirring, in comparison with the grain diameter in the cast without stirring.

In general, the microstructure of samples using F-EMS consists of globules and elongated grains in the structure obtained with stirring, and fine intergranular eutectic network containing different compounds. The coarse dendritic structure of the ingots cast without stirring can be transformed into mainly globular one with some rosette shaped as a result of the conventional stirring application. The structure obtained with unidirectional modulated stirring consists of a mixture of fine round-shape globules and large elongated grains. This structure also appears to be more refined in comparison with that obtained with the conventional stirring. [34]
The globule mean area and length in the microstructure of the combined mid-radius and centre area of the cast obtained with conventional stirring is when compared with the structure of the other casts. The globule mean area in the structure can be reduced, but not in case of structure obtained without stirring. The structure obtained with unidirectional modulated stirring in the casts, the globule mean area in these casts is reduced in comparison with conventional stirring. A similar trend is determined in reduction of the globule length. Concurrent with globule size reduction, their density has increased. [35]
The effect of the M-EMS on the solidification structures was obtained under fixed superheat, casting speed, secondary cooling intensity, and M-EMS frequency. The ratio of the central equiaxed grain zone was found to increase with decreasing superheat, increasing casting speed, decreasing secondary cooling intensity, and increasing M-EMS current. But the equiaxed zone is limited for M-EMS. Since it has more responsibility towards columnar zone. The grain size obviously decreased with decreasing superheat and increasing M-EMS current but was less sensitive to the casting speed and secondary cooling intensity.[36]

1.13 White Band Segregation

The increasing use of electromagnetic stirring (EMS) over recent years has brought with it increased interest in the problem known as white bands. The white band is a zone of negative segregation (appearing white on Sulphur prints) often found in Strand EMS stirred products and corresponding to the position of the solidification

front during stirring [11]. The visual appearance of segregation has not only given rise to the name but is probably also the white band's most undesirable feature. The extent of negative segregation at the white band is less than the positive segregation at the center line, but it's continued presence after hot working can result in a deterrent to customer acceptance, mostly on cosmetic grounds. Kor [21] has suggested an explanation, in which the white band is the

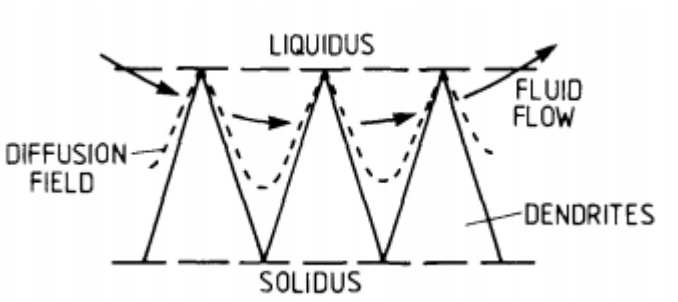

Figure 1.22 Schematic illustration of the solute washing mechanism for white band formation.

result of changes in growth rate at the start and end of strand stirring. White band is due to the solute washing mechanism which was firstly found by Bridge and Rogers [32]. This proposes that the turbulent flows caused by EMS penetrate the dendrite mesh and sweep out enriched interdendritic liquid (Figure 1.22). However, in order to maintain this action it is necessary to assume that the removed solute is very rapidly dispersed throughout the remaining liquid. This being so, it is difficult then to explain the observed solute enrichment at the end of stirring.

2 EXPERIMENTAL ANALYSIS OF BILLETS

2.1 Plant Description

The billet caster of “Acciaierie di Calvisano” has recently been revamped, aiming at casting medium and high carbon steels in submerged mode. The continuous casting machine has a 5 m bending radius and square sections range from 110 to 160 mm. Both design and installation of three stirrers per strand -namely Mould, Strand and Final Stirrer- allowed “Acciaierie di Calvisano” to keep a casting speed as high as 3 m/min also for the new steel grades and achieve significant improvements in terms of surface quality and solidification structure, too. Carbon macro-segregation, central porosity and sub-cortical defects -such as inclusions and cracks- have been significantly reduced. The casting machine has the equipment and updates as per below:

- hydraulic oscillating benches equipped with oscillation monitoring system;
- 900 mm moulds with foot rolls;
- Installation of mould and strand stirrers;
- Measurement and control system of powder thickness in the mould;
- Automatic system for powder feeding in the mould;
- Revamping of secondary cooling;
- New system for polycentric straightening (multi-radius);
- Hydris to check H2 level;
- Thermo-camera for the continuous monitoring of billet temperature before the straightening machine.
- Level 2 for process control.

Machine main technical characteristics are the following:

- Two ladle bogies on tracks;
- Two lifting tundish cars, on tracks;
- Submerged casting with 3QC sliding gate and SEN and open casting with gauged refractory nozzle;
- strands: 4;
- ladle size: 80 ton;
- radius: 5 m; machine length: 23 m;
- oxycutting station;

Number of billets manufactured, speed and productivity are summarized in the following table:

Square section [mm]	Casting speed [m/min]	Nominal productivity [t/h]
120	3,5	93
130	3,2	101
140	2.3	110
160	2.4	115

Table 2.1 Sizes manufactured, casting speed and productivity.

The main target of this intervention aimed at widening the quality range of producible steels through the inclusion of high, medium and low carbon wire-drawing steels, welding steels whose quality has to satisfy customers' needs in terms of absence of defects in conformity with ASTM E381 rule, size of austenitic grain from 6 to thinnest -according to ASTM E112 rule, method Mc Quaid-Ehn and inclusion levels K4<35 according to ASTM E45 rule.

The intervention became necessary mostly because of the limited characteristics of the bending radius, namely 5 m of the continuous casting machine and its high casting speeds.

2.2 Mould and Strand Electromagnetic Stirrers

Final linear electromagnetic stirrer installation was performed at final stage to find the best configuration of current, F-EMS position as per and casting speed through the evaluation of all the results of metallurgic tests. Below **Figure 2.1** show equipment schematic view.

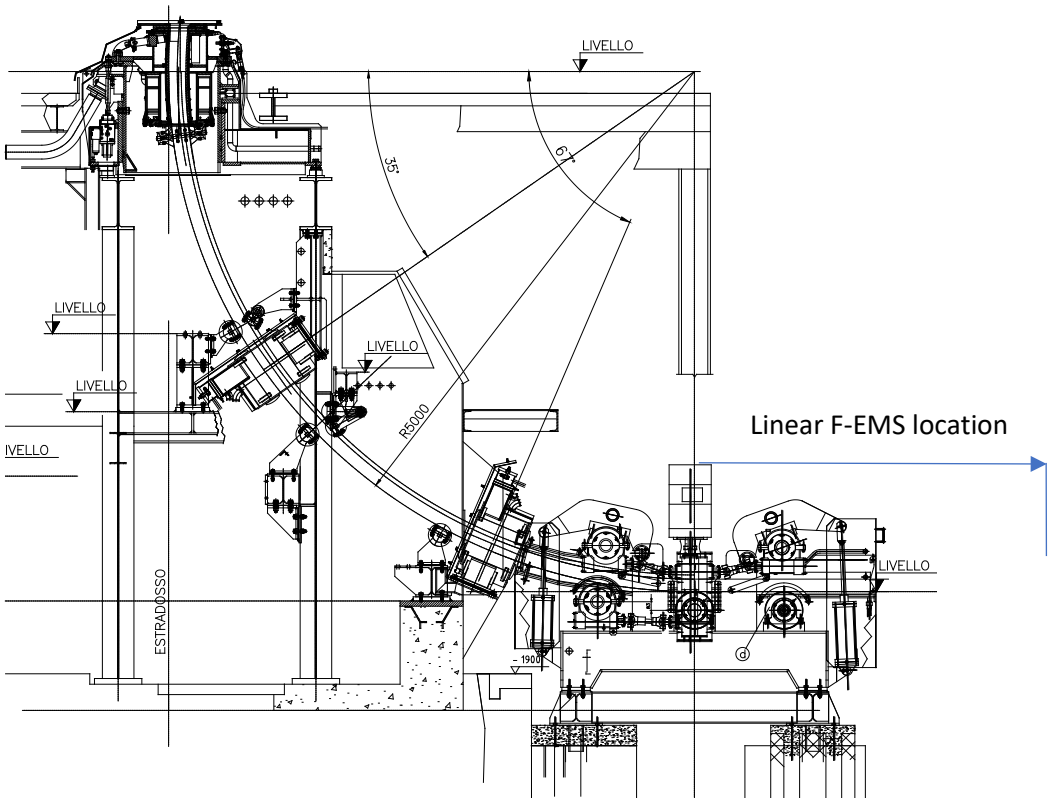

Figure 2.1 Positions for the installation of Linear EMS

The initial stirrer configuration was M-EMS and S-EMS in mold and strand levels.. It was decided to install final L-EMS with variation of distance by 2m, 2.75m and 3m as per above **Figure 2.1**. It envisaged the installation of the stirrer in a low position and after the horizontal straightener. Billets were fabricated as for the different stirring configurations of 600A, 700A, 800A at constant EMS positions and frequency 25 hz. After experimental analysis final configuration was decided. A series of 10 billet samples are produced with linear F-EMS and compared to the one without linear F-EMS.

2.3 Experiment Procedure

The objective of this experiment is to analyse the quality of continuous cast high carbon steel billets through the transverse (140mm x 140mm) and longitudinal sections (140mm x 200mm) produced by applying mould, strand electromagnetic stirring at constant parameters and the final linear electromagnetic stirring at changing casting speed and EMS positions. The quality of the billets can be examined by analysing the extent of defects in the macro and microstructure which are revealed by macro and micro etching, respectively. After the etching, photographs of the macro-etched billets are taken and analysed further in various aspects of quality determining factors using image analysis software Image-J, in the next step selected billets, according to the casting parameters of L-EMS position and current intensity, are interacted with scanning electron microscope (SEM) that produced images of sample

billets and provided information about the surface topography and composition of the sample. The results of the image analysis are documented and discussed in detail in the next chapter.

2.4 Casting parameters

There are 11 billets under the analysis out of which 10 are casted using all the three stirrers M-EMS, S-EMS and F-EMS. One billet is casted only with two stirrers M-EMS, S-EMS. The F-EMS used is a linear type one. The variation in the casting parameters of billets are as follows:

Sample No	EMS set	EMS position*	Casting speed	C	Mn	Si	P	S	Cu	Cr	Ni	Mo	Sn	Al
3491L1	600 A-25hz	2	2.3	0.82	0.75	0.23	0.012	0.003	0.07	0.26	0.06	0.01	0.005	0.030
3490L1	700 A-25hz	2	2.3	0.81	0.71	0.27	0.014	0.004	0.12	0.26	0.07	0.01	0.007	0.027
3492L1	800 A-25hz	2	2.3	0.81	0.72	0.24	0.009	0.004	0.09	0.26	0.08	0.02	0.006	0.025
3493L1	600 A-25hz	2.75	2.3	0.80	0.71	0.24	0.010	0.002	0.07	0.26	0.06	0.01	0.005	0.027
3494L1	700 A-25hz	2.75	2.3	0.83	0.74	0.24	0.009	0.002	0.09	0.26	0.07	0.02	0.006	0.028
3495L1	800 A-25hz	2.75	2.3	0.81	0.72	0.18	0.010	0.003	0.07	0.26	0.05	0.01	0.005	0.025
3496L1	600 A-25hz	3.5	2.3	0.82	0.74	0.20	0.009	0.002	0.08	0.26	0.06	0.02	0.005	0.028
3497L1	700 A-25hz	3.5	2.3	0.82	0.74	0.21	0.009	0.002	0.08	0.26	0.07	0.02	0.005	0.031
3498L1	800 A-25hz	3.5	2.3	0.80	0.74	0.21	0.008	0.003	0.09	0.25	0.06	0.01	0.005	0.026
3499L1	800 A-25hz	3.5	2.5	0.80	0.74	0.21	0.008	0.003	0.09	0.25	0.06	0.01	0.005	0.026
***Distance from RD**														

Table 2.2 Casting parameters of billets

2.5 Macro-etching

Macro-etching, also known as deep etching, is used in metallography primarily to reveal the macro structure of the specimen sample by etching it with a suitable acid or reagent. Macro-etching of transverse or longitudinally oriented samples, i.e., oriented with respect to the hot-working axis, enables the metallurgist to evaluate [9] the quality of a relatively large area quickly and efficiently.

Macro-etching has been applied on the billet samples to acquire degree of uniformity of metals and alloys by revealing:

• Structural details (inclination angle of columnar dendrites, white bands due to stirring, primary dendrite arm spacing and etc.) resulting from solidification,

• Chemical uniformity (distribution of carbon, manganese, chromium, silicon) in qualitative terms

• Physical discontinuities due to solidification (porosity, crack formation) working etc

The first three features are best revealed by hot-acid etching and the remaining four are best revealed by room temperature etchants.

The present study involves the following activities:

- collection of CC high carbon billet samples and corresponding casting data
- evaluation of segregation pattern by macrostructural examination of samples
- measurement of dendrite arm spacing at various locations of the billet sections
- determination of the degree of segregation of carbon, Sulphur, phosphorus and manganese qualitatively using Scanning Electron Microscope
- correlation among the degree of segregation

Transverse sections were obtained by cutting the billet samples through the cross section, perpendicular to their geometrical axis and longitudinal sections were obtained by slicing the billet samples along their geometrical axis with minimum amount of material loss. After cutting, all samples were subjected to fine grinding and polishing to obtain a smooth surface finish. Dirt and oil from the surfaces were removed by acetone.

Thanks to the new continuous caster, stirrers working parameters need to be optimized as for amperage and L-EMS distance in order to find their best efficiency. Therefore, such optimization required according to the continuous casting parameters of high alloy carbon steel as per below table.

2.6 Hot-etching

In the first step, the billets are macro-etched with the 1:1 hydrochloric acid and water, a typical reagent to etch iron and steel alloys.

The etchant is prepared by pouring 1 part of HCl into the beaker and then 1 part of H2O is added, heated to a temperature of 70 – 80 °C. Then the billet is immersed in the etchant solution and is left for 15-60 minutes allowing the billet to react with the etchant. Here since our billet is large and the etchant cannot be at 70°C-80°C for long time, to ensure the etching process to take place the billet is also heated to about 80°C so that the required temperature for the etching will be available for the time duration of reaction. After the etching of sample, characteristics such as inclusions, cracks, porosity, dendrites are revealed. The images obtained after the hot acid etching of cross-section billets contributed to acquire parameters like Primary Dendrite Arm Spacing (PDAS), Columnar Dendrite Inclination Angle (CDIA) using image analysis software Image-J. While the analysis of Porosity, Strand stirrer segregation diameter and Linear Final Stirrer Segregation diameter are done after the second macro-etching.

2.7 Cold Etching

The etchant used for second phase of macro-etching is 50g $(NH_4)_2S_2O_8$ (ammonium bisulfide) mixed in 500 ml H_2O at room temperature. The billet is swabbed with the etchant until desired etch is obtained.

Second macro-etching is performed both on cross-section billets and longitudinal section billets. This cold etching is performed to observe pores clearly, segregation due to strand stirrer and linear final stirrer. The images of transverse and longitudinal sections and analysed using Image-J software and porosity, strand stirrer segregation, linear EMS segregation are evaluated.

Cold solution of ammonium bisulfite with water is applied on the billets in order to see the pores clearly on the transverse and longitudinal sections of billets.

- The solution is poured on billet surface and left for some minutes and then swab with a clean velvet
- Rinse the surface with ethanol and swab again
- The procedure should be repeated three or four times until the macrostructure appears well.

In addition, the pictures have been taken while the acid is on the surface, in order to see the white band segregation diameter caused by strand stirrer and the segregation lines along the center due to final linear stirrer on the longitudinal sections to measure segregation diameters.

2.8 White Band Segregation

In order to understand the effects of Linear Final EMS on white bands, strand stirrer segregation diameter and L-EMS segregation diameter values are calculated. The distances between the two bands in longitudinal section, white band diameters due to

S-EMS and L-EMS as shown in the Figure 2.2 are measured with the help of Image-J software using the images of cold etched longitudinal sections. Because the bands appear not exactly linear, 4 measurements are made along the billet axis and their mean value is used to make the comparison between all the billets under analysis. Also, the thickness of the band is measured using Image-J by taking 9 measurements along the band and they are plotted showing the mean value and interval around the mean value. As per below figure S-EMS white band diameter and thickness are indicated as yellow and red marking, respectively. Blue marker shows the linear F-EMS white band diameter.

a) b)

Figure 2.2 Billet sample a) transverse and b) longitudinal sections

2.9 Porosity Area Fraction in Different Positions

As for the different stirring configurations, the central area of the macros was analyzed to evaluate the effect of linear stirrers on the distribution of central porosity. In particular, 9 points were analyzed by using image-J software. The porosity areas are calculated in each position and the obtained results are documented and discussed in the next chapter. They were located within a 50 mm square area in the center of samples.

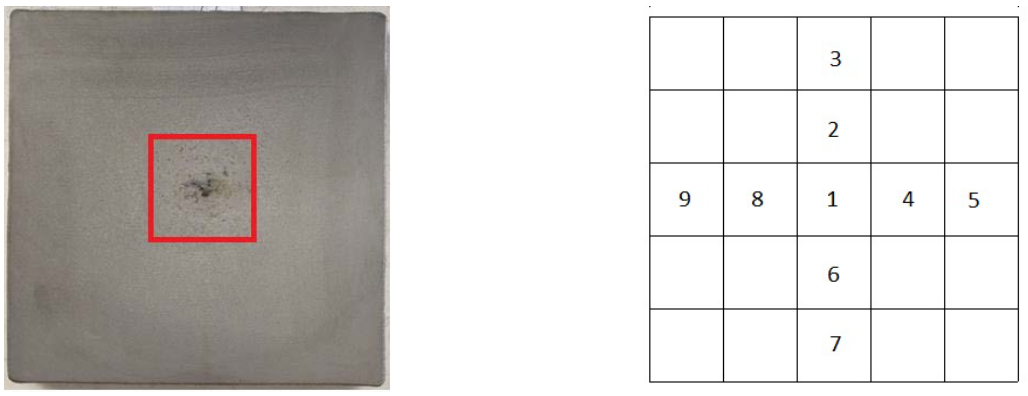

a) b)

Figure 2.3 Scaling method to evaluate central porosity

2.10 Porosity analysis of Longitudinal Section

In the longitudinal sections, porosity is present mainly at the center due to shrinkage of solidified metal. An area of 140 mm x 200mm in the center of both the longitudinal sections of each billet is considered and porosity area index is calculated as follows:

$$\textbf{Porosity area index} = \frac{\textbf{Porosity area calculated}}{\textbf{Length of billet under analysis}}$$

- Porosity area is obtained from Image-J software
- Area of billet under analysis = 200mm x 140mm

2.11 Columnar Dendrite Arm Spacing

The primary dendrite arm of the columnar crystal was off its original growing direction as shown in **Figure 2.4** due to the rotating molten steel flow under the action of the EM force due to M-EMS and S-EMS; the deflection angle of the columnar crystal is largest at the middle width of the billet and smallest at the corner of the billet. The deflection angle was the result of solute depletion in the upstream direction and higher solute concentration in the downstream direction due to convective flow around the tip of the columnar crystals. When frequency remains constant, increase in the current intensity to M-EMS causes increase in the angle of inclination. Also, there will be an increase in the angle with increase in frequency of M-EMS and the current being constant. The change of L-EMS parameters doesn't have any effect on the inclination angle of columnar dendrites.

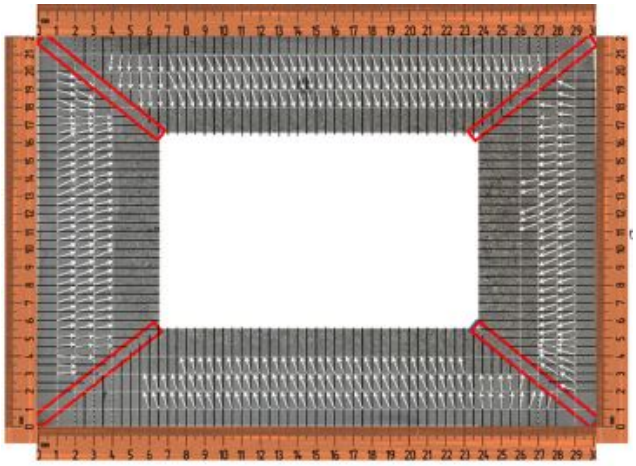

Figure 2.4 The measurement of columnar dendrite inclination angle [23]

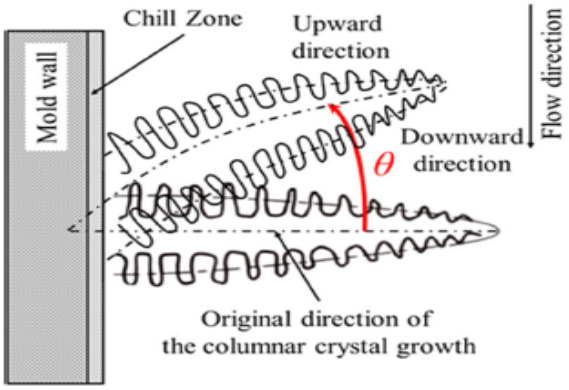

Figure 2.5 Inclination angle of columnar dendrite [23]

The deflection angle of columnar dendrites is measured in a cross-sectional plane of the billets in the side regions on all four sides such as intrados, extrados, right and left. The method used to measure the inclination angle is as per **Figure 2.5** 4 measurements are acquired by 90-θ, and their mean and interval are taken into account.

2.12 Primary Dendrite Arm Spacing (PDAS)

Optimum properties of castings can be achieved through control of the as-cast dendritic structure. Dendrites grow initially in the form of rods. However, growth perturbations or minor changes in the liquid around the growing dendrite occur. These temperature and compositional perturbations in the liquid cause bumps to form on the side of the rods, which grow outward into the liquid forming the secondary arms. In a like manner, tertiary arms can form on the secondary arms and so forth. 20 adjacent primary dendrites have been taken randomly from 4 positions of billets and the distance with millimetres between them is measured in order to get average. All the values from 4 positions are collected in a sample for each billet and the statistical parameters are evaluated.

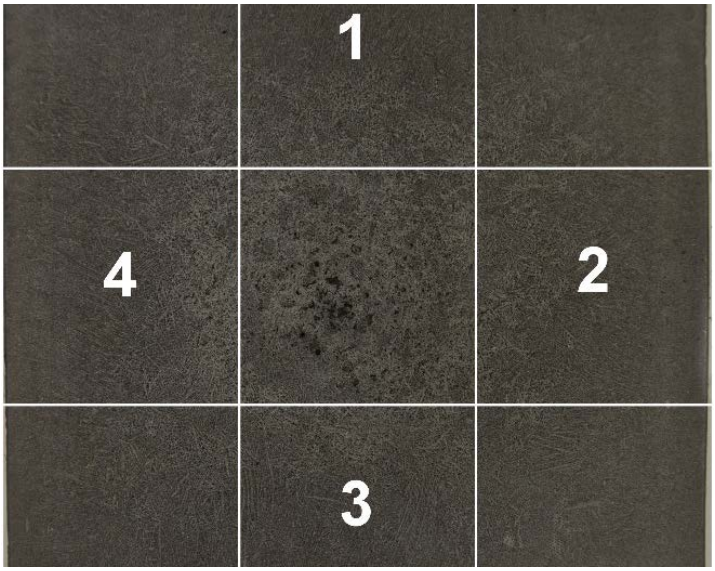

Figure 2.6 PDAS measurement locations

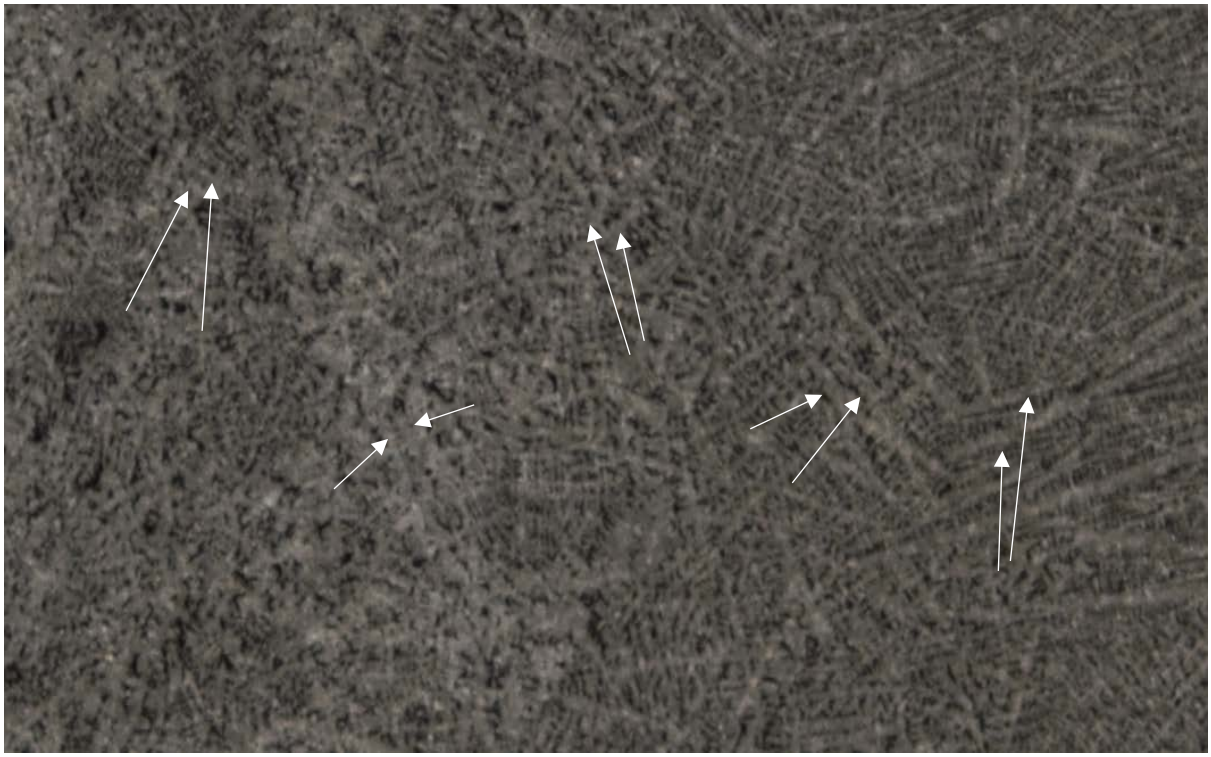

Figure 2.7 Adjacent dendrites shown with marking close to the center

2.13 Micro Etching

Metallography is the study of the microstructure of metals and alloys by means of microscopy.

- Sectioning
- Mounting (which is necessary when the sample cannot be held properly due to its shape and/or size, while polishing)
- Grinding
- Polishing
- Etching

Before micro etching, the transverse sections of billet samples have been cut through the center in which piece is marked from 1 to 5, intrados to the center respectively, to evaluate the degree of C, Si, Cr, Mn segregation qualitatively using Scanning Electron Microscope over region of strand stirrer white band segregation and final linear stirrer central white band segregation. Scanning Electron Microscope has been used for only billet samples 3490L1, 3491L1, 3492L1, 3494L1, 3494L4, 3498L1 at magnifications of 50x (see Appendix A for 1000x magnification).

The etchant used for the high carbon steel billets' transverse sections is 5% Nital solution (95% ethanol, 5% HNO_3). After applying the etchant of nital to the surface of the billet for 10-15 seconds, it is washed with ethanol and dried immediately to avoid overetching of the billet.

3 RESULTS & DISCUSSION

Strand EMS and final linear EMS white band segregation circle diameters, inclusion pits, PDAS, inclination angle of columnar dendrites, chilled, columnar and equiaxed zones on the transverse section of billets are analyzed after the hot etching of the transverse sections of the billets. On the other hand, cold etching of both transverse and longitudinal sections gave the results about the porosity area and its distribution and strand EMS and final linear EMS white band segregation circle average diameter along the longitudinal sections of billets. As shown in Figure 3.1 inclusion pits present around the center which can occur due to the oxidation of the pouring stream, generally between the tundish and mold that produces large oxide inclusions. All the billet samples have white band segregation circle due to the strand stirrer which is visible from the transverse side.

Figure below shows the morphology and macrostructure of the central zone on the cross section of different samples. The results show that for the slices obtained from the trials, equiaxed grains and columnar ones are both observed on the cross sections of solidified casting. The macrostructures of both samples produced with or without F-EMS are composed of inclined columnar dendrites due to mold and strand EMS, then columnar to equiaxed transition occurred. Equiaxed grains are found in the central area. All the samples have white band segregation circle due to the strand stirring. With applied current and frequency from 600 A to 800 A at 25 Hz by final linear EMS in the final stage of solidification, as shown in the Figure 3.1a the white band segregation circle of final linear EMS is visible compared to the one in Figure 3.1b. Macrostructure is refined in terms of porosity shrinkage, and black inclusion pits doesn't seem in the white band region because of the reduced carbon segregation, distributed around the center homogenously. The sample in Figure 3.1b, inclusion pits and shrinkage cavity is concentrated in the center.

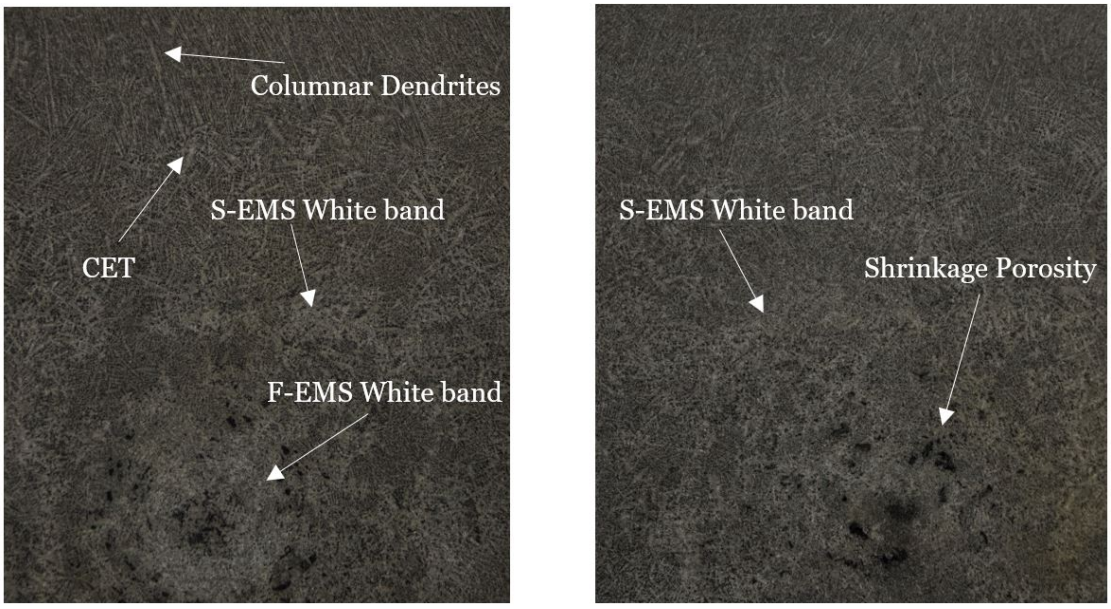

a) Sample with final EMS b) Sample without final EMS

Figure 3.1 Macrostructure in central zone on transverse section of billets.

3.1. Porosity Analysis

Pores presenting on the billets are clearly visible to measure in the images taken after cold macro-etching. The hot etching of the billets also shows the pores but often there is a chance for the Image-J software to consider inclusion pits as pores because both pores and inclusion pits appear dark in color. So, the porosity area is calculated using the images of macrostructure after the cold etching of billets.

3.1.1. Central Porosity in Transverse Sections of Billets

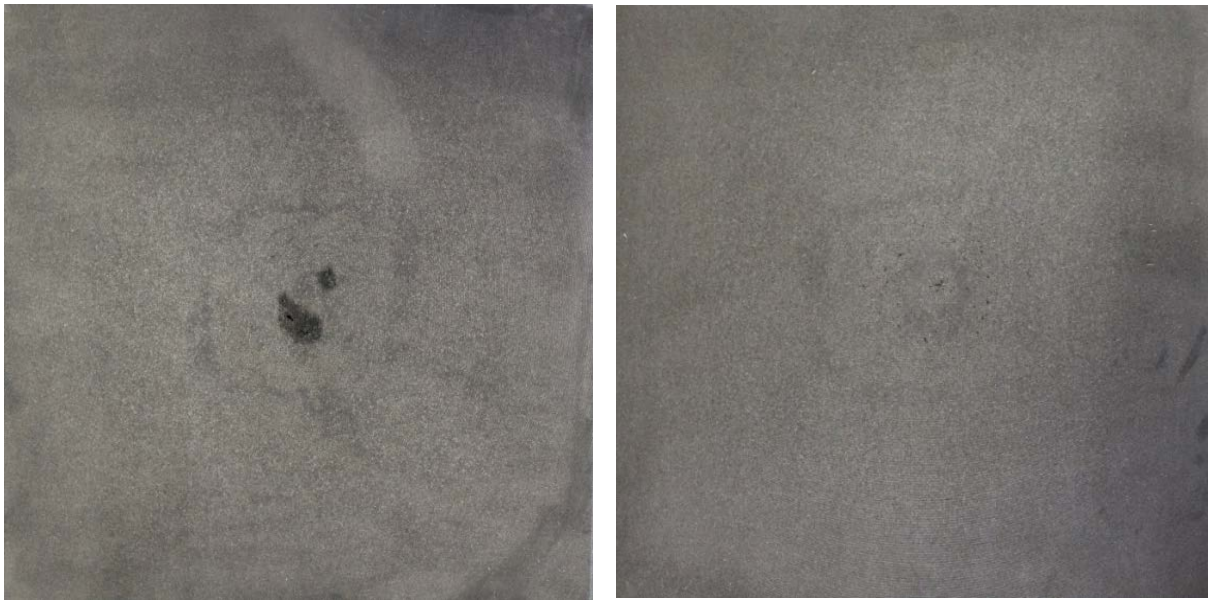

a) b)

Figure 3.2 Images of billets after cold etching showing the pores (a) casted without final EMS (b) casted with final linear EMS

It is observed from the figure above that there is finer porosity with higher dispersion at the center of the billet casted without final linear EMS. All the billets casted with the final linear EMS shows similar results in which the porosity in all billets is quite less compared to the billet produced without final EMS. The molten metal pool solidifying last at the center of the strand gets homogeneous in temperature with stirring effect and shrinkage porosity reduces by applying final electromagnetic stirrer.

Central porosity in center of the transverse sections of billets within the 50 mm^2 area is analysed in 9 different points. Final linear EMS samples are compared in terms of porosity in order to choose the best among them. 3494L4 porosity is indicated with red dot as per below figures.

Position 1

Referring to below **Figure 3.3**, we can say that porosity index is the highest for the billet 3498L1. It is observed that when the current given to the coils is less and the position of the final linear EMS is close to the straightener, the porosity areas are of less magnitude and when the position is far from the straightener, the porosity areas are of higher magnitude. If we consider also the longitudinal sections' porosity index which is clarified in the next step we can choose best configuration of current 600A with 2.3 m/min casting speed and 2.75m EMS position (Sample No. 3493L1), and in 700A current with 2.3 m/min casting speed and 2m EMS position (3490L1). It is also appropriate configuration with billet cross sectional porosity index. When the casting speed for the last billet (3499L1) is increased, porosity is extremely low but there could be change in the decrease of equiaxed crystal ratio which could be examined further.

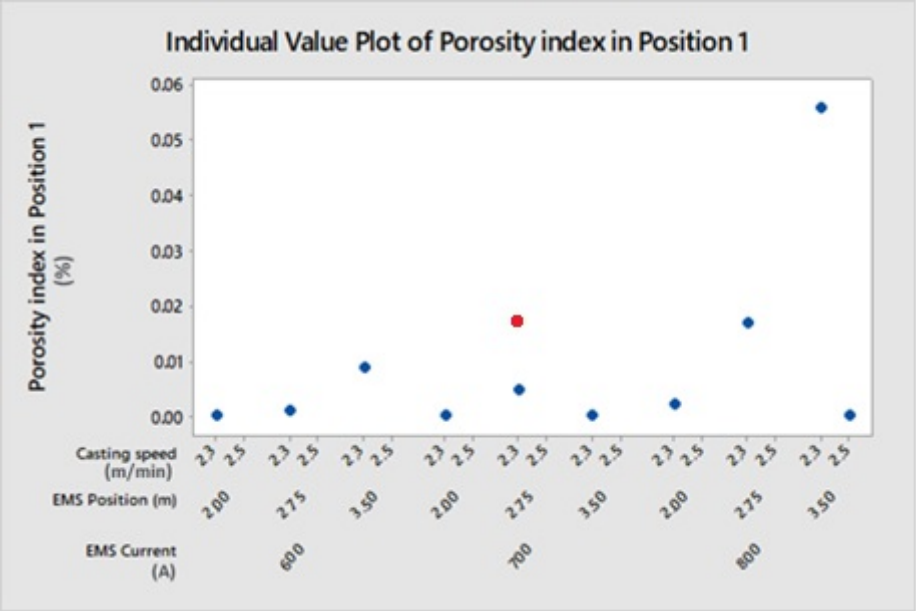

Figure 3.3 Porosity index in Position 1

In the below **Figure 3.4** for position 2 the porosity index of the billets is almost zero except 3492L1 is 0.0045 due to one pore.

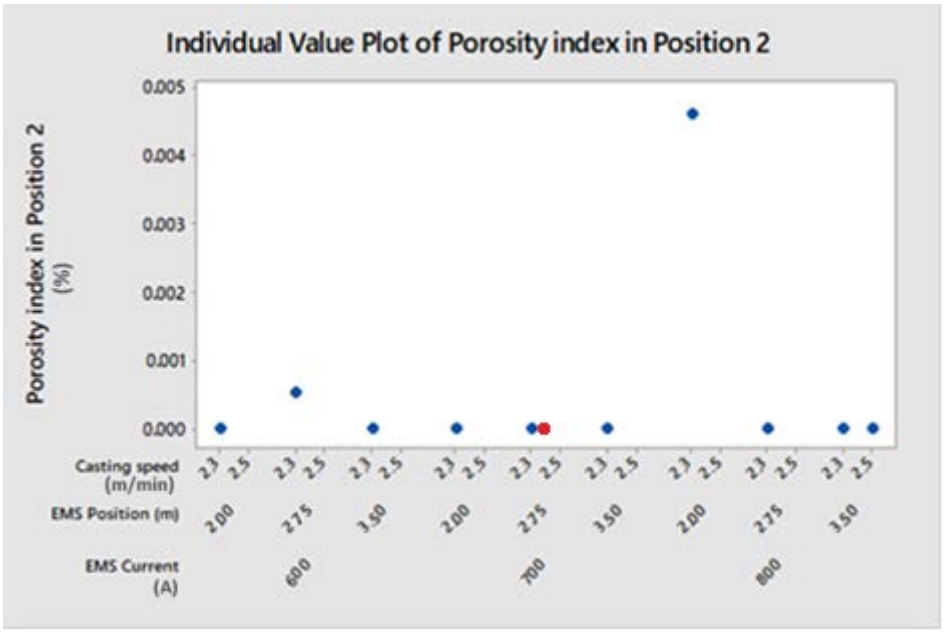

Figure 3.4 Porosity index of Position 2

All the billets have zero porosity index towards intrados as shown in **Figure 3.5.**

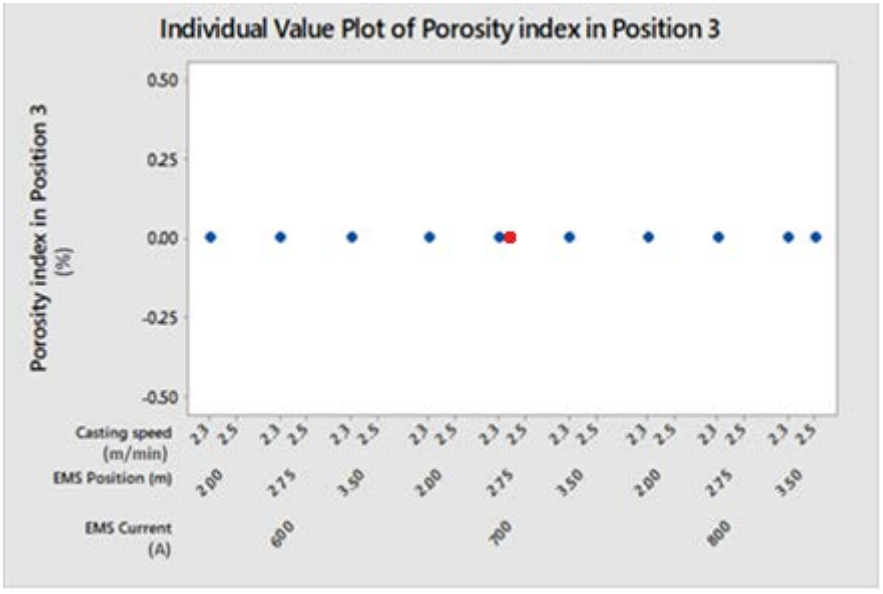

Figure 3.5 Porosity index in Position 3

In position 4, Billet 3490L1 has one pore with 0.0016 index and the remaining billets have zero porosity.

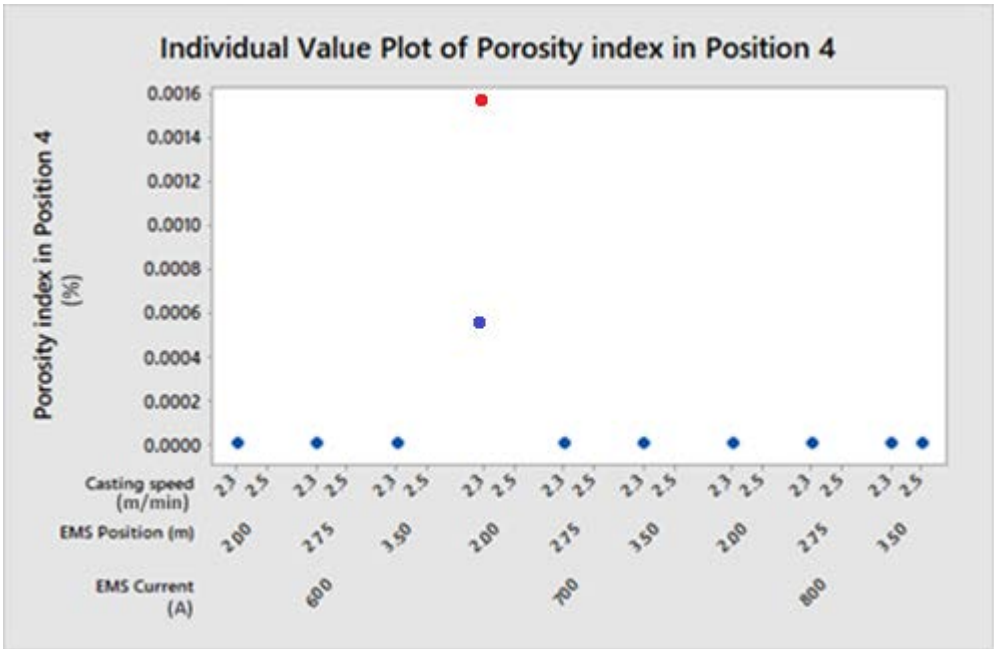

Figure 3.6 Porosity index in Position 4

All the billets have got zero porosity index as we can see from the below Figures 3.7 and Figure 3.8, 3.9 towards extrados.

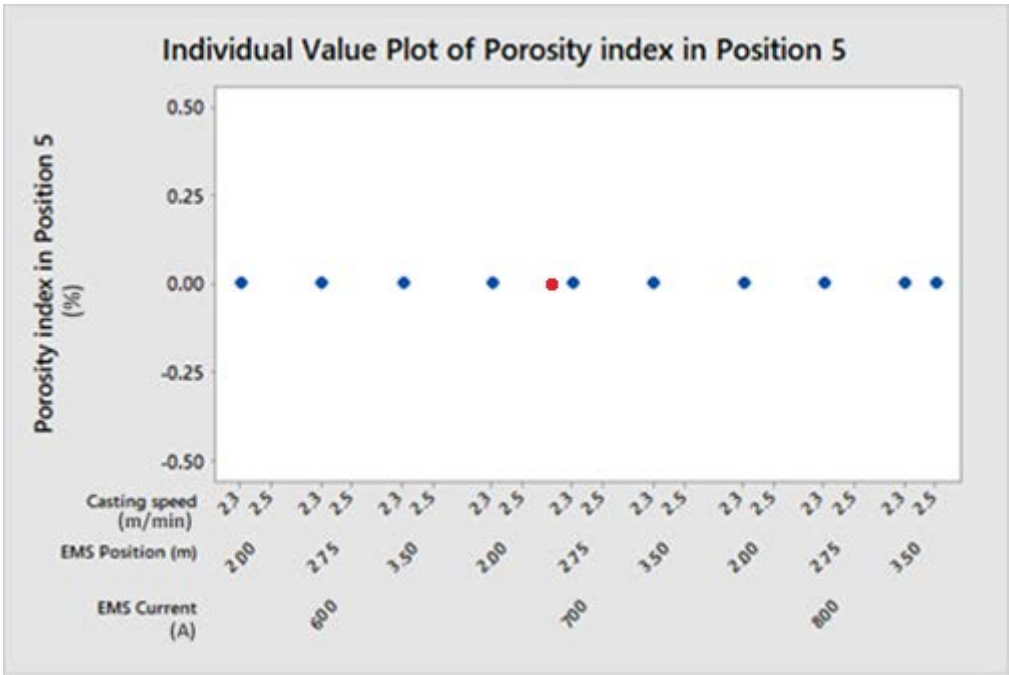

Figure 3.7 Porosity index in Position 5

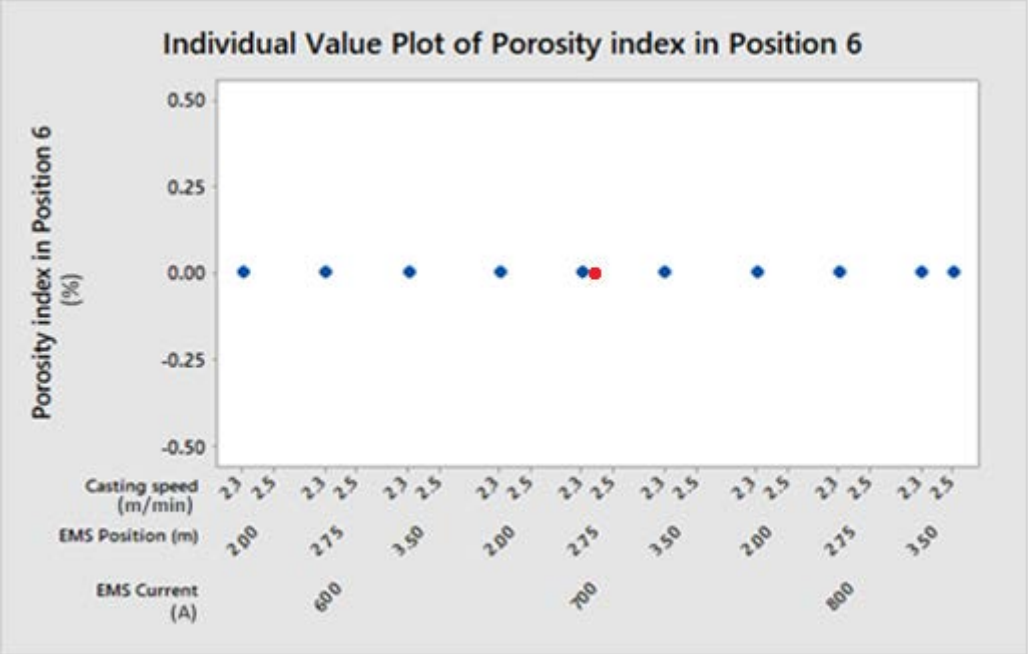

Figure 3.8 Porosity index of Position 6

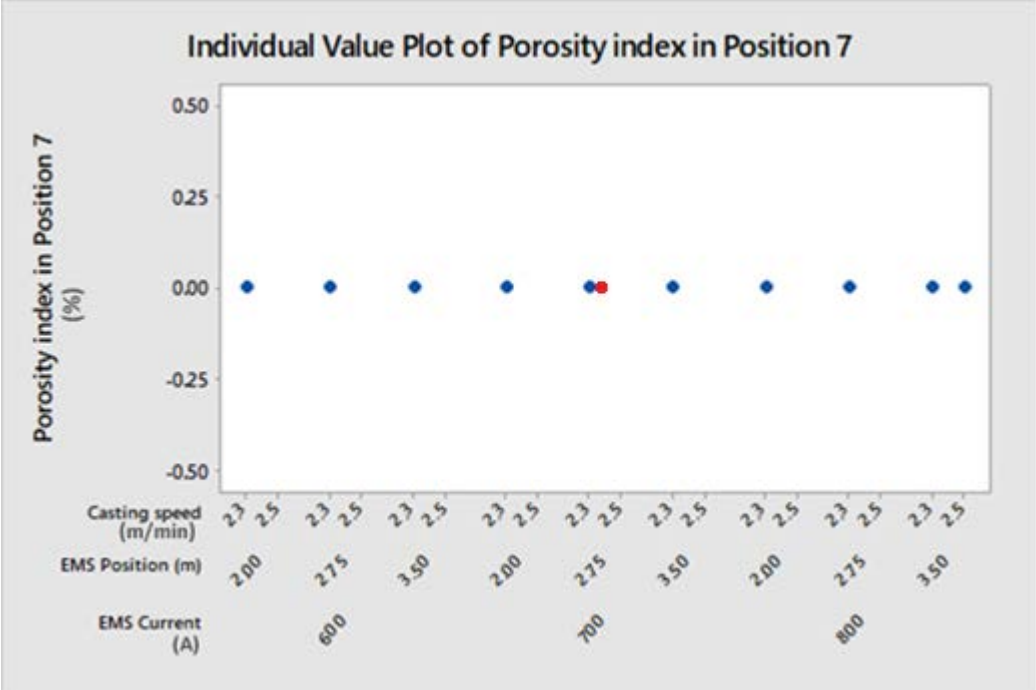

Figure 3.9 Porosity index of Position 7

Porosity defect is higher for the billet 3492L1 in position 8. But for all the remaining billets have zero porosity.

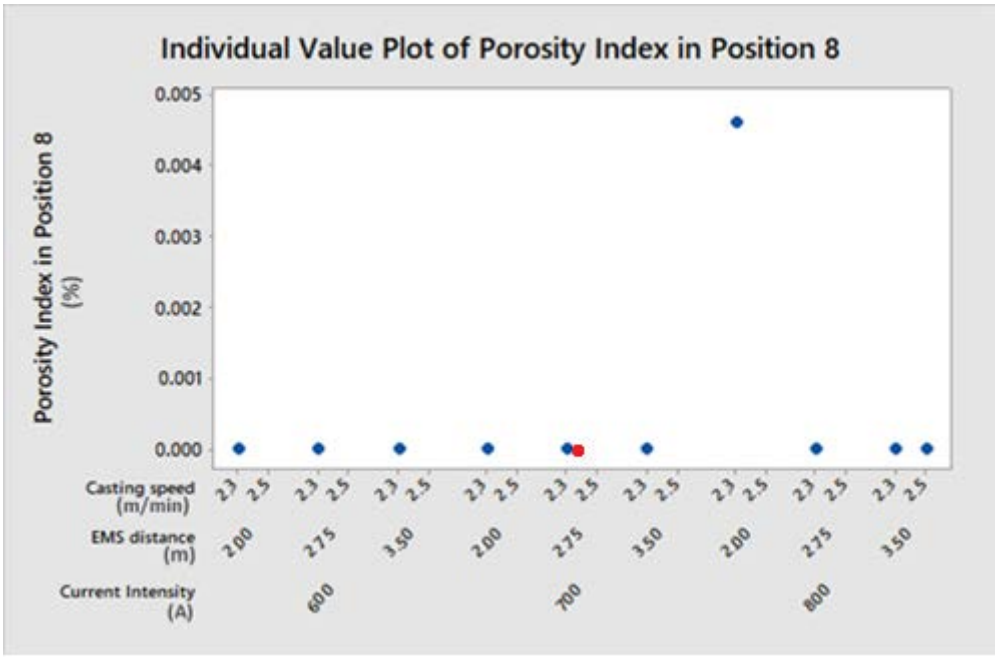

Figure 3.10 Porosity index of Position 8

In position 9, most porous billet is 3495L1 and all the remaining billets have got zero porosity index which is shown on below Figure 3.11.

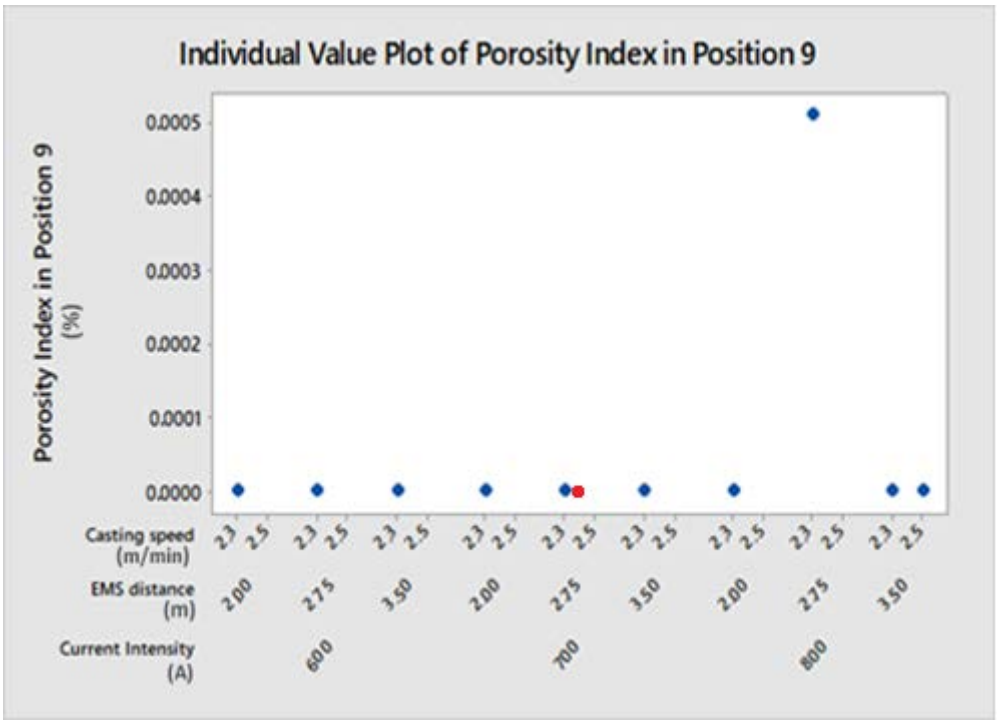

Figure 3.11 Porosity index of Position 9

Total Porosity Index is the area fraction of all pores to total area of billet transverse section. As shown in the Figure 3.12, most of the billets have the the least porosity index close to zero, but in the next step the optimal parameters of final linear EMS is clarified by measuring the least porosity in longitudinal sections in order to validate the results from transverse sections of billets.

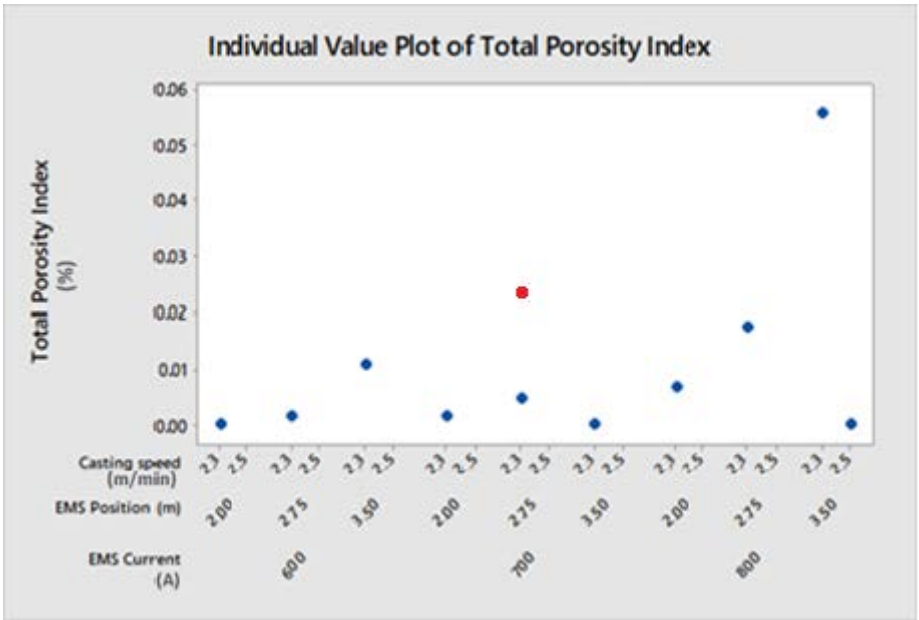

Figure 3.12 Total Porosity index

3.1.2. Porosity Analysis of Longitudinal Sections

The 70 mm x 200 mm billet's longitudinal sections have been analyzed in terms of porosity area density after applying cold etchant. Porosity in a longitudinal section of billets is compared according to the casting speed, EMS distance and current Intensity. Casting speed is the same in all the billets, but only 3499L1 was produced with 2.5 m/min casting speed. Porosity index is calculated area fraction of pores to longitudinal section length.

Porosity index is the least in current 600A with 2.3 m/min casting speed and 2.75 m final linear EMS distance (Billet 3493L1), and in 700A current with 2.3 m/min casting speed and 2 m of L-EMS position (Billet 3490L1). When the speed increases in 800 A current at constant final EMS position of 3.5 m, the porosity index increases.

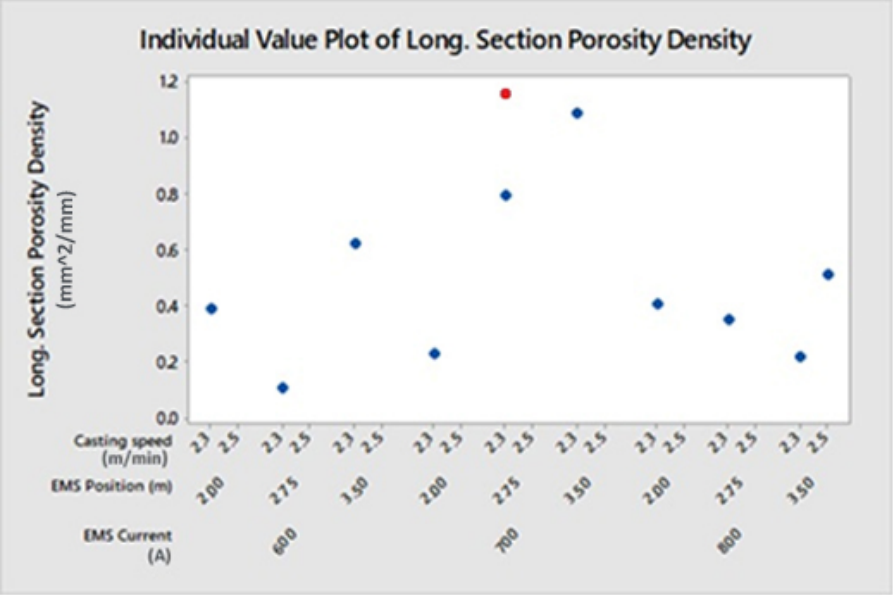

Figure 3.13 Porosity density in longitudinal sections. Porosity density in mm2/200 mm (length of the longitudinal section)

Considering the least porosity configuration of longitudinal section, the optimal configuration is chosen at final linear EMS parameters of current 600A with 2.3 m/min casting speed and 2.75 m EMS position (3493L1) as shown in **Figure 3.13**. This configuration validates the least porosity index of transverse sections of billet samples.

(a) (b)

Figure 3.14 Central porosity in longitudinal section without final EMS (b) with final linear EMS

The billet without final EMS as shown in Figure 3.14 (a) after cold etching has the highest central porosity index of 1.19 mm^2 / 200 mm length of longitudinal section as shown in Figure 3.13 red rot. It is validated that the final linear EMS has significant effect to decrease central shrinkage and porosity.

As you see from Figure 3.15, porosity area frequency is lowest in 3493L1 among all billets, so it means we can choose best configuration of current 600A with 2.3 m/min casting speed and 2.75m EMS position for billet 3493L1. Other billets have higher area porosity frequency comparing to 3493L1. However maximum porosity area frequency was observed in billet 3494L4 which was fabricated without F-EMS. At this stage we can say that the billet without F-EMS have more porosity area frequency of bigger porosity shrinkage as per below Figure 3.15. Billet 3496L1 and 3497L1 appears to have also bigger pores, that was assumed to be due to the further F-EMS distance of 3.5 m in which initial solidification occurred and F-EMS at 3.5 m can lose its stirring effect. In this case more current intensity or higher frequency electromagnetic force should be applied.

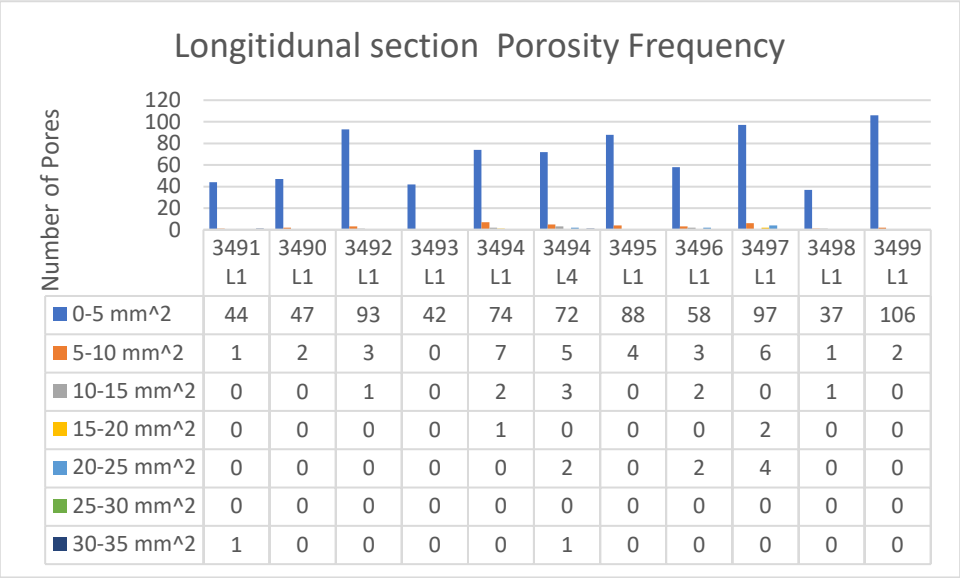

	3491 L1	3490 L1	3492 L1	3493 L1	3494 L1	3494 L4	3495 L1	3496 L1	3497 L1	3498 L1	3499 L1
0-5 mm^2	44	47	93	42	74	72	88	58	97	37	106
5-10 mm^2	1	2	3	0	7	5	4	3	6	1	2
10-15 mm^2	0	0	1	0	2	3	0	2	0	1	0
15-20 mm^2	0	0	0	0	1	0	0	0	2	0	0
20-25 mm^2	0	0	0	0	0	2	0	2	4	0	0
25-30 mm^2	0	0	0	0	0	0	0	0	0	0	0
30-35 mm^2	1	0	0	0	0	1	0	0	0	0	0

Figure 3.15 Longitudinal porosity Area Frequency

3.2. Strand Stirrer Segregation Diameter

Diameter of the white band segregation caused by strand stirrer is constant in all billets, because the strand stirrer position doesn't change. In addition, at 800 A current intensity and 3.5 m EMS position, by increasing the casting speed from 2.3 m/min to 2.5 m/min, the diameter of the white band segregation has been increased to the maximum value of 53 mm as expressed in Figure 3.16.

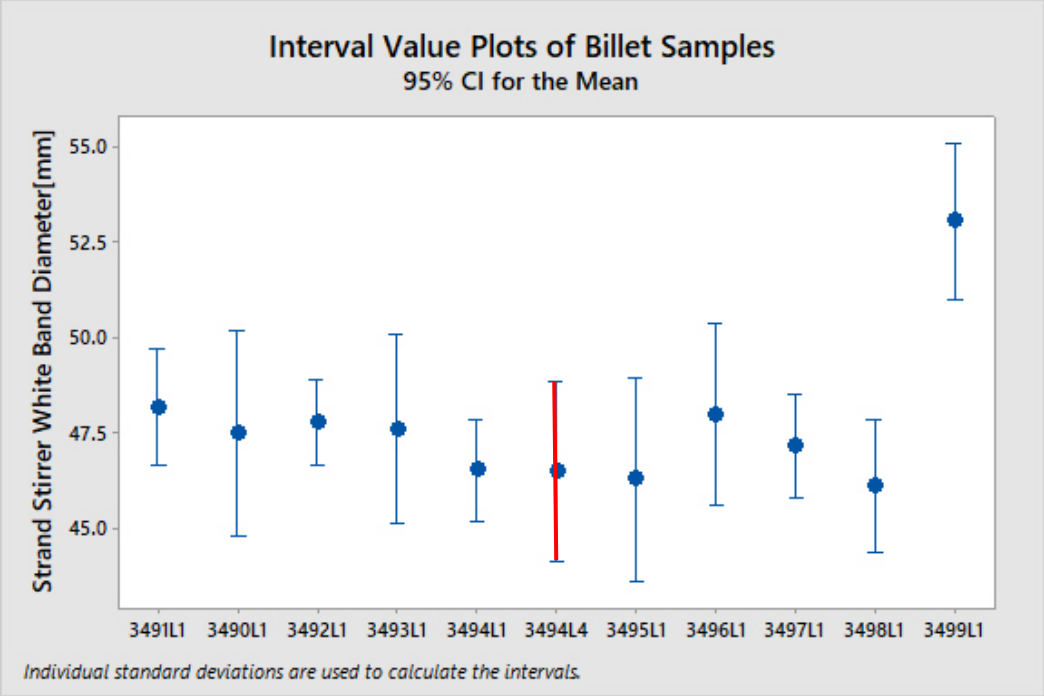

Figure 3.16 Diameter of Strand stirrer segregation relation with process parameters.

Variable	N	N*	Mean	SE Mean	StDev	Minimum	Q1	Median	Q3	Maximum
3490L1	4	0	47.493	0.852	1.705	46.000	46.072	47.145	49.260	49.680
3491L1	4	0	48.170	0.486	0.972	47.130	47.245	48.170	49.095	49.210
3492L1	4	0	47.760	0.351	0.702	46.970	47.082	47.760	48.437	48.550
3493L1	4	0	47.587	0.782	1.565	46.120	46.177	47.645	48.940	48.940
3494L1	4	0	46.513	0.422	0.845	45.380	45.665	46.630	47.243	47.410
3494L4	4	0	46.483	0.737	1.474	45.080	45.328	46.145	47.975	48.560
3495L1	4	0	46.270	0.843	1.687	44.000	44.547	46.540	47.722	48.000
3496L1	4	0	47.970	0.750	1.499	46.000	46.500	48.120	49.290	49.640
3497L1	4	0	47.155	0.425	0.850	46.120	46.350	47.155	47.960	48.190
3498L1	4	0	46.092	0.546	1.092	44.940	45.082	46.010	47.185	47.410
3499L1	4	0	53.050	0.645	1.291	51.480	51.817	53.055	54.277	54.610

Table 3.1 Statistical description of white band diameter of strand stirrer

Diameter of the F-EMS white band doesn't have relative changing trend with casting parameters, so the values of inner white band diameter changes randomly as shown in Figure 3.17. In addition, at 800 A Current and 3.5 L-EMS position, an increase of casting speed to 2.5 m/min didn't make any change in the inner diameter of segregation caused by linear stirrer. 3494L4 is not included in Figure 3.17, because it doesn't have F-EMS resulting no white band in the center.

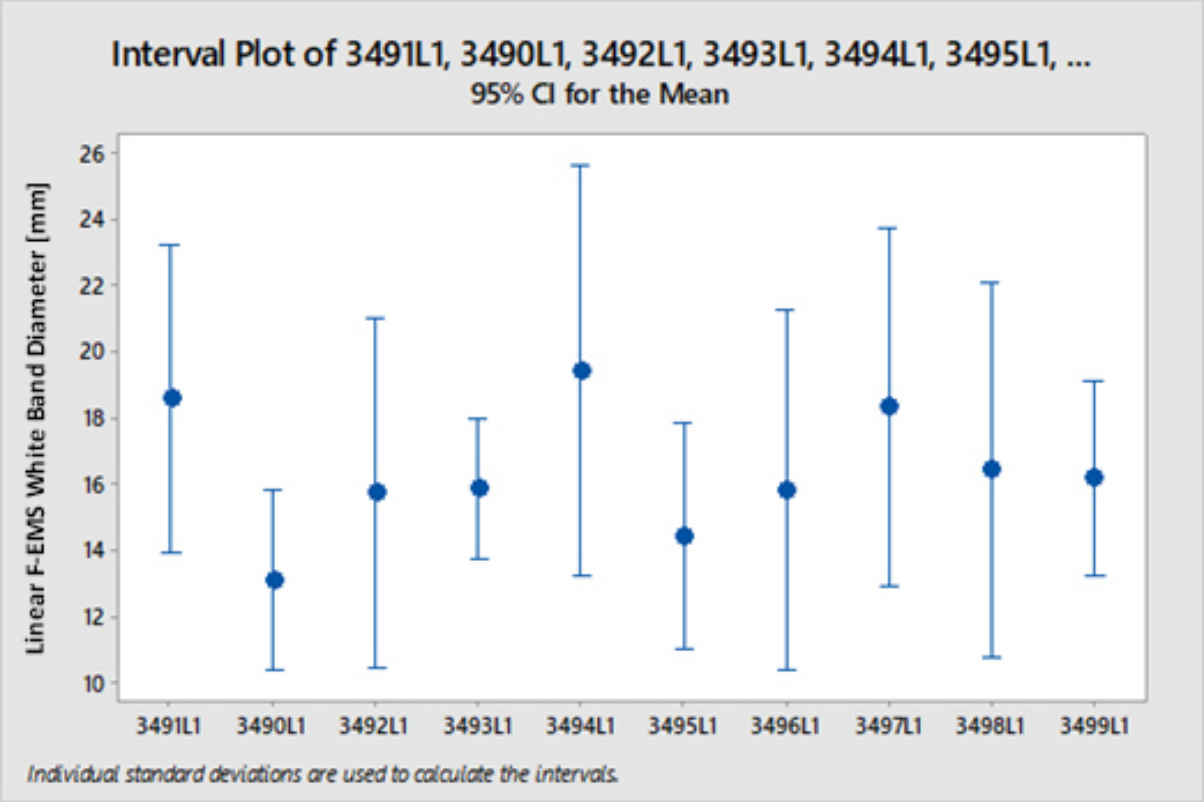

Figure 3.17 Linear F-EMS white band diameter relation with the process parameter.

Variable	N	Mean	SE Mean	StDev	Minimum	Q1	Median	Q3	Maximum
3490L1	4	12.95	1.26	2.52	10.84	11.07	12.19	15.59	16.57
3491L1	4	19.27	1.96	3.91	13.95	15.15	20.25	22.41	22.64
3492L1	4	17.18	1.62	3.24	14.63	14.70	16.25	20.61	21.61
3493L1	4	16.318	0.790	1.580	14.900	14.925	16.320	17.708	17.730
3494L1	4	20.68	2.40	4.80	15.78	16.34	20.16	25.54	26.61
3495L1	4	13.66	1.25	2.50	10.79	11.18	13.93	15.88	16.00
3496L1	4	16.61	2.31	4.62	10.77	12.15	16.84	20.86	22.00
3497L1	4	19.47	2.01	4.03	15.15	15.63	19.48	23.29	23.75
3498L1	4	17.75	1.98	3.95	13.46	14.30	17.27	21.68	23.00
3499L1	4	15.93	1.33	2.66	13.51	13.68	15.42	18.68	19.36

Table 3.2 Statistical description of white band diameter of linear F-EMS

Regardless of final linear EMS parameters, the thickness of strand white bands of all samples has mutual values in their interval as per Figure 3.18.

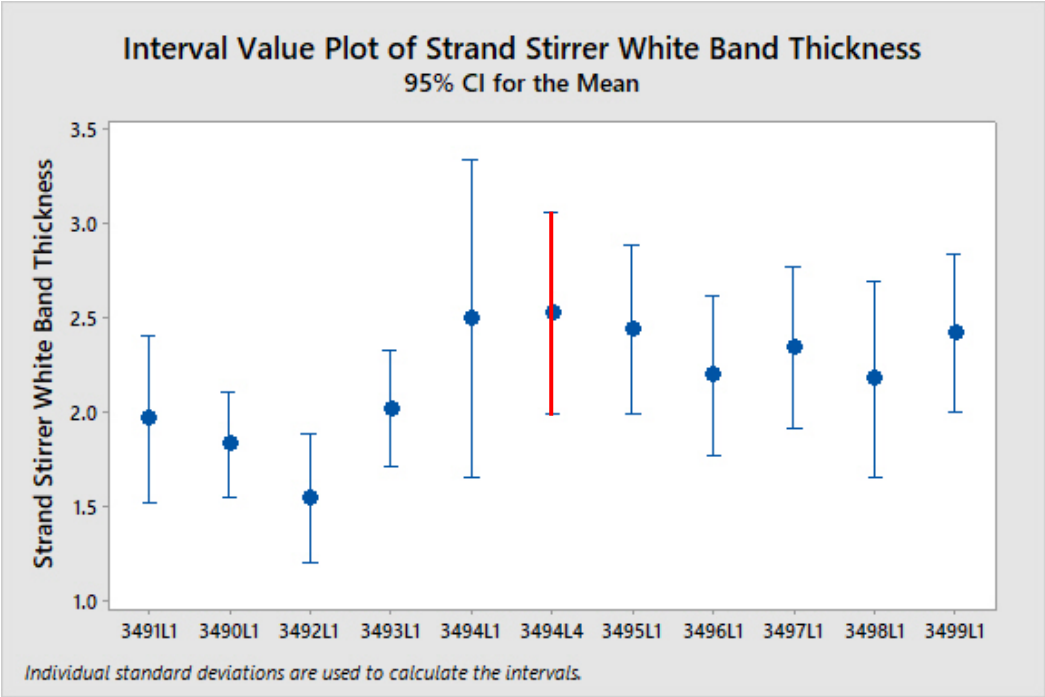

Figure 3.18 Inner thickness of strand stirrer white band relation with process parameters

Variable	N	Mean	SE Mean	StDev	Minimum	Q1	Median	Q3	Maximum
3490L1	9	1.833	0.121	0.364	1.400	1.450	2.000	2.150	2.300
3491L1	9	1.961	0.196	0.583	1.300	1.350	2.000	2.600	3.000
3492L1	9	1.544	0.149	0.448	0.900	1.150	1.600	1.900	2.300
3493L1	9	2.022	0.133	0.399	1.500	1.600	2.100	2.350	2.600
3494L1	9	2.500	0.365	1.095	1.100	1.550	2.300	3.500	4.300
3494L4	9	2.530	0.234	0.701	1.800	1.800	2.480	3.265	3.600
3495L1	9	2.444	0.194	0.581	1.100	2.200	2.600	2.850	3.000
3496L1	9	2.200	0.184	0.552	1.400	1.750	2.300	2.650	3.000
3497L1	9	2.344	0.186	0.559	1.500	1.950	2.300	2.900	3.200
3498L1	9	2.178	0.225	0.676	1.600	1.600	2.000	2.800	3.400
3499L1	9	2.422	0.181	0.543	1.600	2.000	2.300	2.950	3.200

Table 3.3 Statistical description of white band thickness of linear F-EMS

PDAS is shown in Figure 3.19, in terms of interval value plot. As per Table 3.6 PDAS is not significantly changing through the billet samples which are produced with F-EMS, on the other hand the high value of PDAS is observed in the billet 3494L4 without F-

EMS which means using F-EMS stirring during solidification, PDAS has been decreased significantly improving the ratio of central equiaxed grain which is considerably increased resulting in finer grains. Therefore, the quality of the cast product is enhanced with the F-EMS.

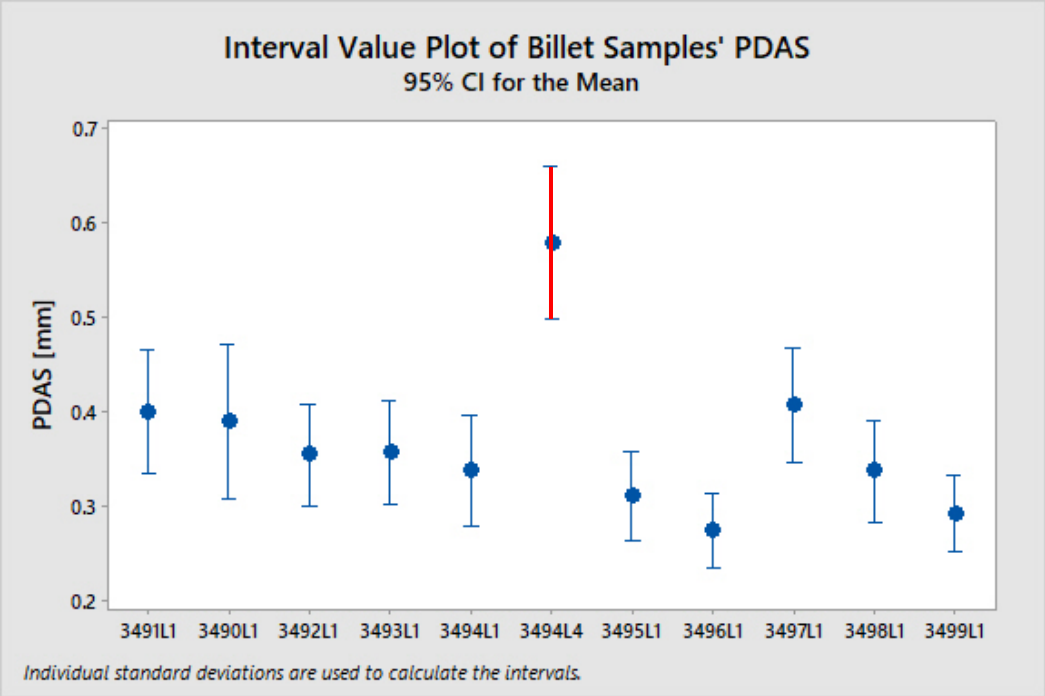

Figure 3.19 Interval Value Plot for PDAS of billet samples

Variable	N	Mean	SE Mean	StDev	Minimum	Q1	Median	Q3	Maximum
3491L1	40	0.4000	0.0324	0.2051	0.1000	0.3000	0.3500	0.5000	1.0000
3490L1	40	0.3900	0.0406	0.2570	0.1000	0.2000	0.3000	0.5000	1.1000
3492L1	40	0.3550	0.0265	0.1679	0.1000	0.2000	0.3500	0.5000	0.7000
3493L1	40	0.3575	0.0272	0.1723	0.1000	0.2000	0.3000	0.5000	0.6000
3494L1	40	0.3375	0.0290	0.1835	0.1000	0.2000	0.3000	0.5000	0.7000
3494L4	40	0.5800	0.0401	0.2534	0.2000	0.3250	0.6000	0.7750	1.1000
3495L1	40	0.3115	0.0232	0.1204	0.1000	0.2100	0.3300	0.3900	0.6300
3496L1	40	0.2753	0.0195	0.1169	0.1200	0.1900	0.2400	0.3475	0.6100
3497L1	40	0.4075	0.0298	0.1886	0.1000	0.3000	0.4000	0.5000	0.9000
3498L1	40	0.3375	0.0265	0.1675	0.1000	0.2000	0.3000	0.4000	0.8000
3499L1	40	0.2925	0.0201	0.1269	0.1000	0.2000	0.3000	0.4000	0.6000

Table 3.4 Statistical description of PDAS.

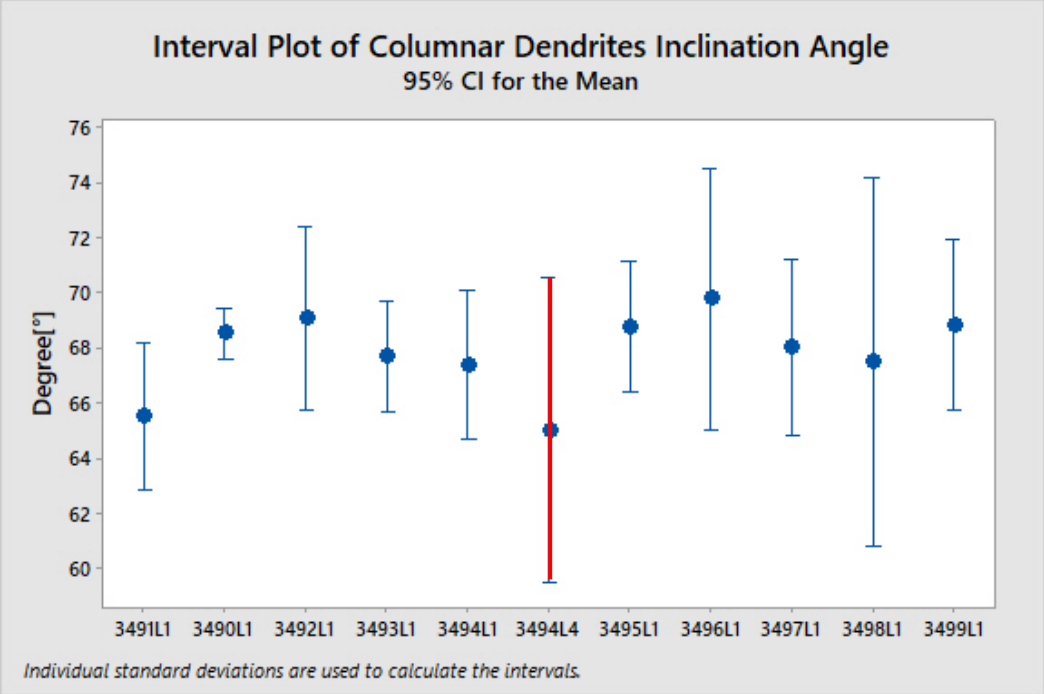

Figure 3.20 Inclination angle of primary dendrites

From the Figure 3.20 we can see that the columnar dendrites' inclination angle values for all the billets are in same range, but the lowest value of inclination angle is observed in 3494L4 billet without F-EMS which means lower inclination. The addition of F-EMS gives extra electromagnetic force to incline the columnar dendrites.

3.3. Micro Etching Results

Qualitative analysis of the non-metallic elements' distribution from the negative segregation side of strand EMS white band until the center is analysed by SEM after micro-etching. Billets 3490L1 (700 A, 2 m F-EMS position), 3491L(600 A, 2 m F-EMS position), 3492L1(800 A, 2 m F-EMS position), 3494L1(700 A, 2.75 m F-EMS position), 3498L1 (800 A, 3.5 m F-EMS position), 3494L4 (produced without F-EMS) are analysed with SEM

3491L1 - It is observed as shown in the Figure 3.21, the degree of positive segregation near white band (Area 2-3) of S-EMS, negative (Area 3-4) and positive (Area 5<) segregation of linear F-EMS increases qualitatively according to carbon content, on the other hand results clearly show solute depletion within the white band.

Figure 3.21 Micro etched billet sample 3491L1

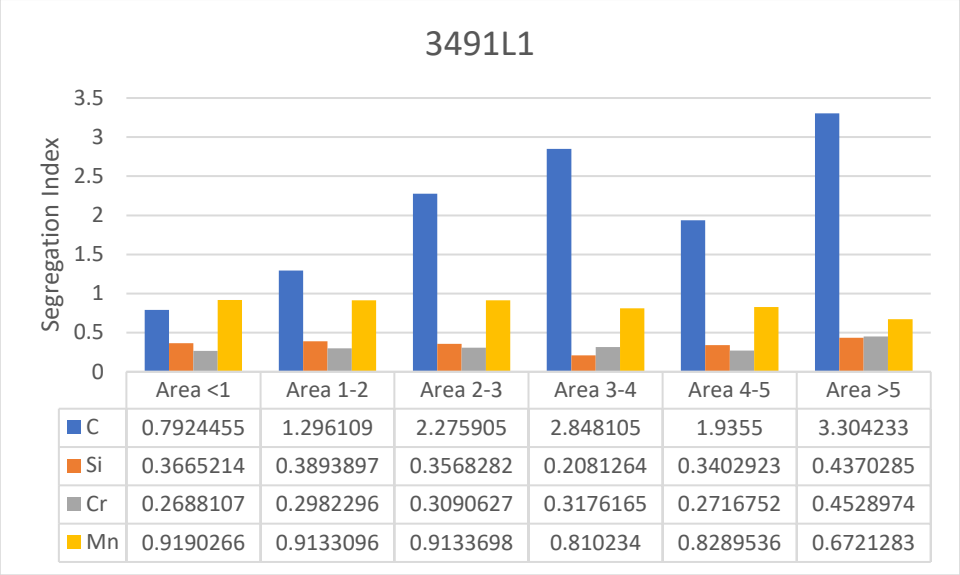

	Area <1	Area 1-2	Area 2-3	Area 3-4	Area 4-5	Area >5
C	0.7924455	1.296109	2.275905	2.848105	1.9355	3.304233
Si	0.3665214	0.3893897	0.3568282	0.2081264	0.3402923	0.4370285
Cr	0.2688107	0.2982296	0.3090627	0.3176165	0.2716752	0.4528974
Mn	0.9190266	0.9133096	0.9133698	0.810234	0.8289536	0.6721283

Figure 3.22 Qualitative representation of the C, Si, Cr, Mn in marked areas.

As per above Figure 3.22 we can observe that along the center carbon content is lower except the area >5 carbon shows. At 600 A, 2 m F-EMS position produced billet (3491L1) shows the less carbon segregation without homogenous distribution. On the other hand, Mn is 0.91 % showing higher values in less carbon segregated areas until line 3.

Billet 3490L1

White band segregation due to the S-EMS and final L-EMS are in the region of 1-2 and 3-4 respectively. Negative segregation of the white band of S-EMS is near to the line 1 towards the intrados side in the region of <1, positive segregation of white band of S-EMS is situated towards the centre in the region of 2-3. Accordingly, 2-3 region will be the negative segregation and 4-5 region will be the positive segregation of white band due to final L-EMS.

Figure 3.23 Micro etched billet sample 3490L1

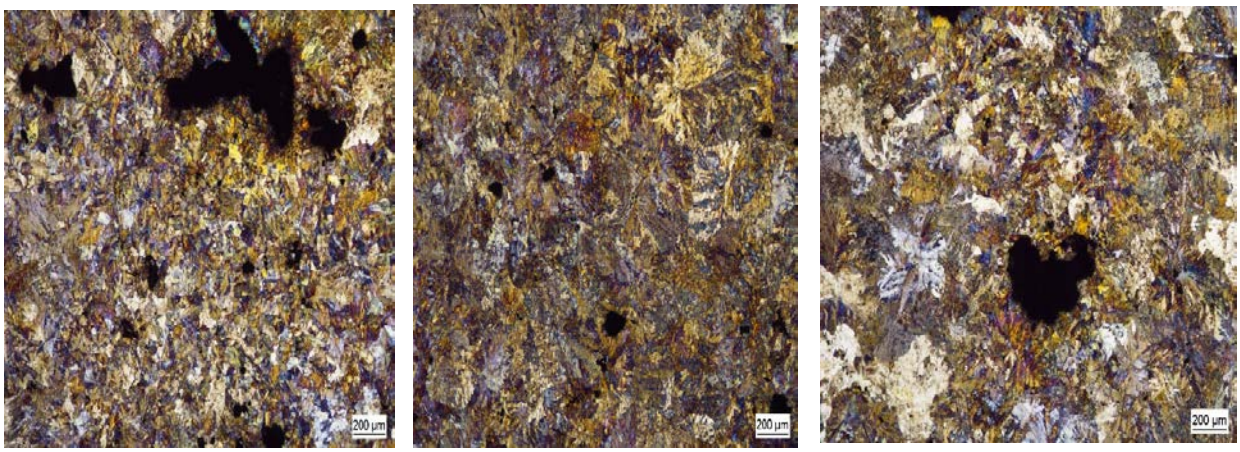

Area 1-2 Area 2-3 Area 4-5

Figure 3.24 SEM analysis of billet

Magnified pictures show microstructural formation in areas 1-2, 2-3, 4-5 as shown in Figure 3.24. They coincide with strand stirrer white band, positive segregation and linear final stirrer white band regions. White band regions composed of coarser and equiaxed grains, on the other hand positive segregation region seem not so stirred and coarser.

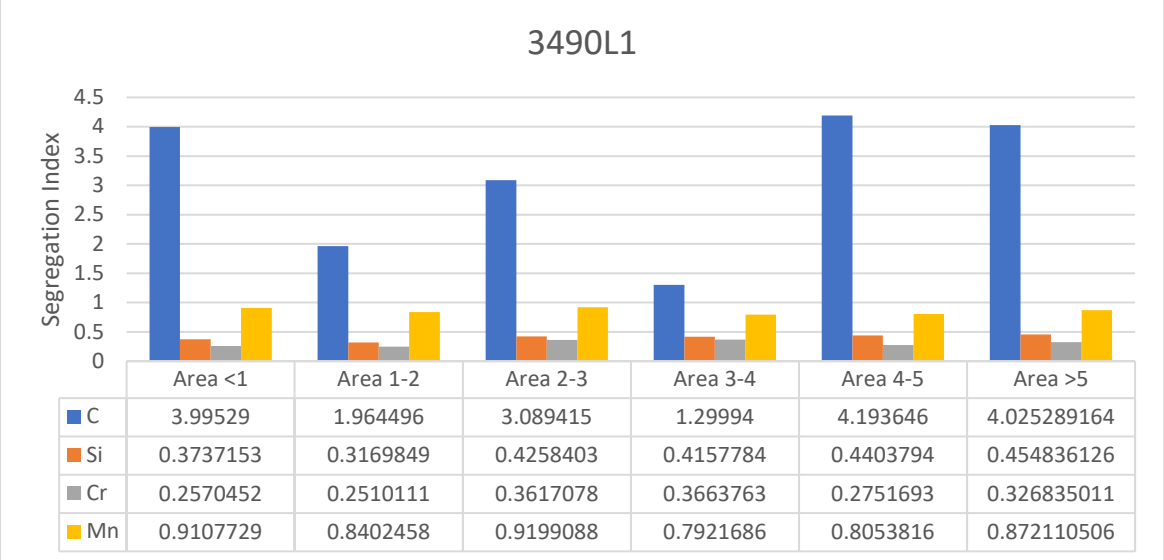

	Area <1	Area 1-2	Area 2-3	Area 3-4	Area 4-5	Area >5
C	3.99529	1.964496	3.089415	1.29994	4.193646	4.025289164
Si	0.3737153	0.3169849	0.4258403	0.4157784	0.4403794	0.454836126
Cr	0.2570452	0.2510111	0.3617078	0.3663763	0.2751693	0.326835011
Mn	0.9107729	0.8402458	0.9199088	0.7921686	0.8053816	0.872110506

Figure 3.25 Qualitative representation of the C, Si, Cr, Mn in marked areas.

It is observed as shown in the Figure 3.25 that the degree of white band negative and positive segregation of both S-EMS and L-EMS increases qualitatively according to carbon and manganese content, on the other hand results clearly show solute depletion within the white band. Mn shows the same trend of decrease as C in white band regions area 1-2 and 2-3 with 0.84 % and 0.79 % respectively. On the other hand, carbon content is high in the center it can be due to the higher width of melt pool in

the central region at shortest distance of 2 m F-EMS position in which doesn't have the proper force to stir high thickness melt pool.

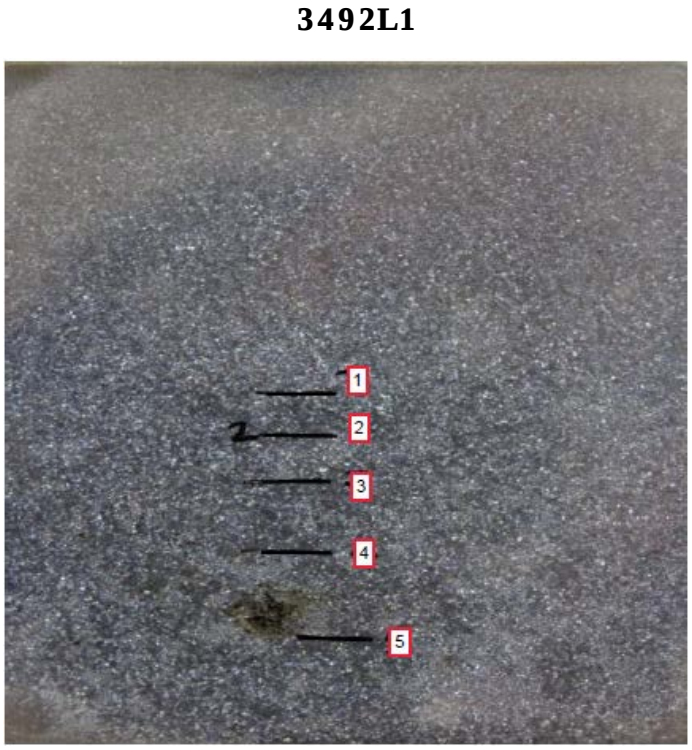

Figure 3.26 Micro etched billet sample 3492L1

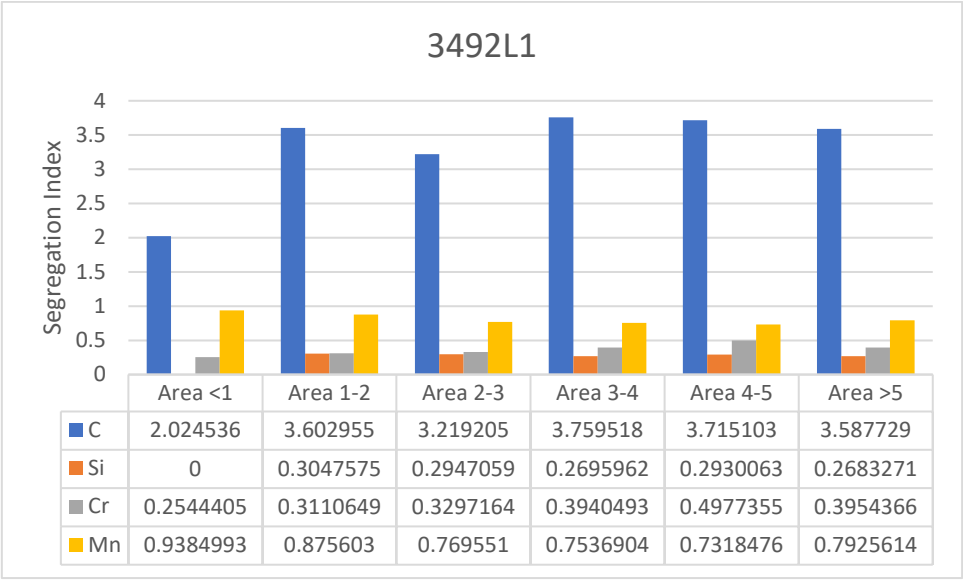

	Area <1	Area 1-2	Area 2-3	Area 3-4	Area 4-5	Area >5
C	2.024536	3.602955	3.219205	3.759518	3.715103	3.587729
Si	0	0.3047575	0.2947059	0.2695962	0.2930063	0.2683271
Cr	0.2544405	0.3110649	0.3297164	0.3940493	0.4977355	0.3954366
Mn	0.9384993	0.875603	0.769551	0.7536904	0.7318476	0.7925614

Figure 3.27 Qualitative representation of the C, Si, Cr, Mn in marked areas.

The area towards the intrados near the mark line 1 has the least solute content qualitatively due to the strand stirrer, but final linear stirrer doesn't have any significant effect in any depletion of carbon content along the centre of billet.

As the current increased to 800 A at 2 m F-EMS position the C distributed homogenously beyond the negative segregation of S-EMS white band to the center. However, Mn concentration is 0.93% in area <1 with lower carbon level, it shows lower values along the center. Mn low concentration starting from line can be due to the increase of current intensity to 800 A, because melt pool diameter becomes wider in 2 m of F-EMS position, and increase of current may have better effect in stirring of central part in terms of homogenous distribution of C and Mn.

3494L1 and L4- As per Figure 3.28 there is not any decrease of solute due to final linear stirrer and strand stirrer, all the regions around the center have the solute enrichment as described qualitatively.

3494L4 has qualitatively high weight percentage of carbon in all areas, and maximum in the center in area 4-5 and >5 compared to other samples. Mn and Cr reached the maximum value of 1.12% and 0.51 respectively in area 2-3 and <1.

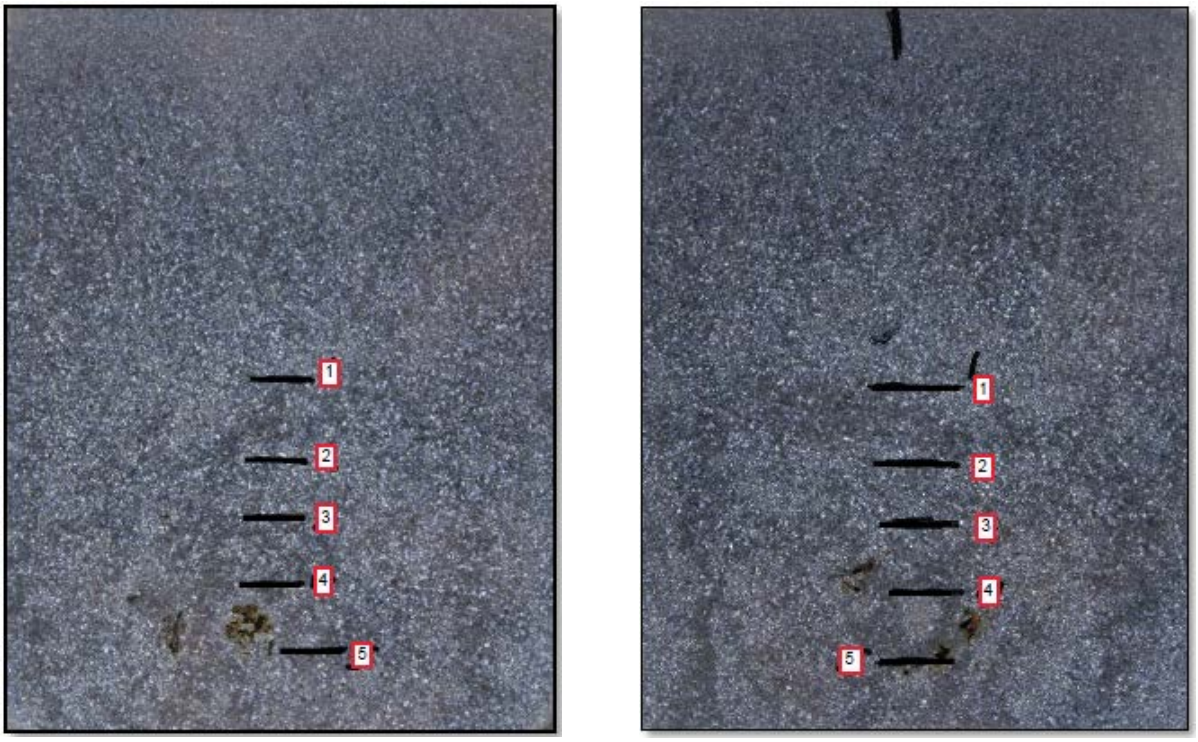

Figure 3.28 Micro etched billet sample a) 3494L1 and b) 3494L4.

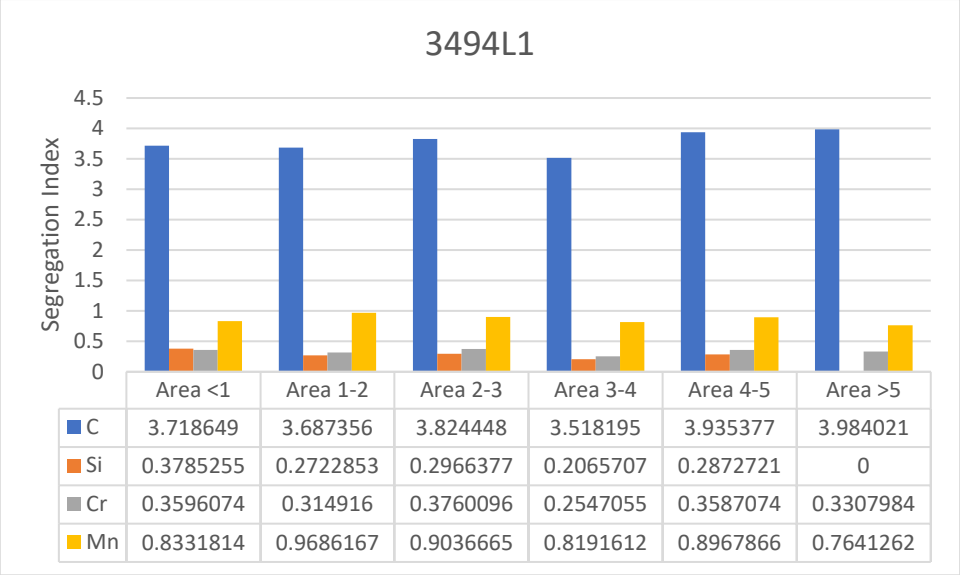

	Area <1	Area 1-2	Area 2-3	Area 3-4	Area 4-5	Area >5
C	3.718649	3.687356	3.824448	3.518195	3.935377	3.984021
Si	0.3785255	0.2722853	0.2966377	0.2065707	0.2872721	0
Cr	0.3596074	0.314916	0.3760096	0.2547055	0.3587074	0.3307984
Mn	0.8331814	0.9686167	0.9036665	0.8191612	0.8967866	0.7641262

Figure 3.29 Qualitative representation of the C, Si, Cr, Mn in marked area

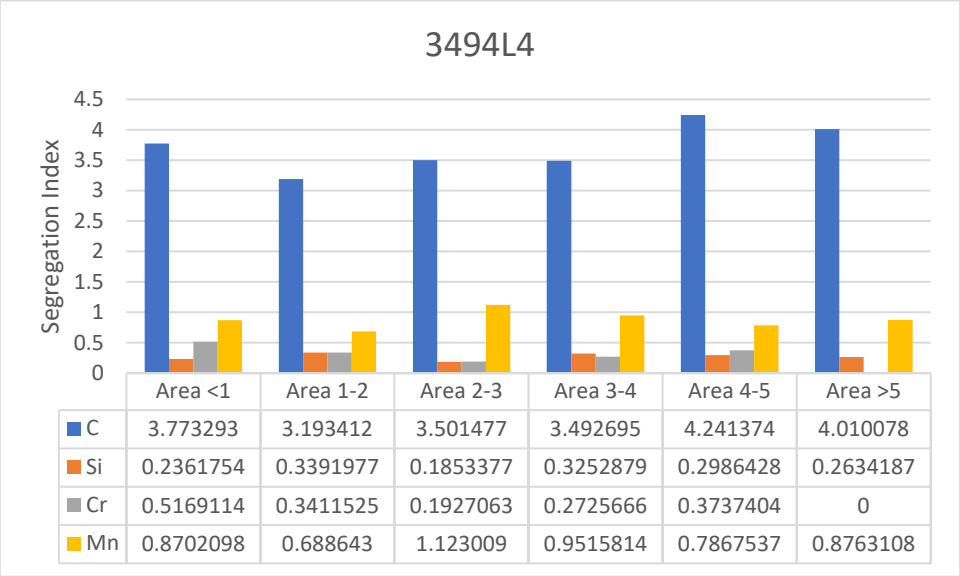

	Area <1	Area 1-2	Area 2-3	Area 3-4	Area 4-5	Area >5
C	3.773293	3.193412	3.501477	3.492695	4.241374	4.010078
Si	0.2361754	0.3391977	0.1853377	0.3252879	0.2986428	0.2634187
Cr	0.5169114	0.3411525	0.1927063	0.2725666	0.3737404	0
Mn	0.8702098	0.688643	1.123009	0.9515814	0.7867537	0.8763108

Figure 3.30 Qualitative representation of the C, Si, Cr, Mn in marked areas**.**

However, billet 3494L1 at 700 A current intensity, 2.75 m F-EMS position compared to 3490L1 produced at the same current and 2 m F-EMS position has homogenous distribution of carbon segregation, it shows higher carbon segregation qualitatively even in the white band regions. As the distance of F-EMS increased from 2 m to 2.75 m, the stirrer doesn't have enough intensity to have proper effect.

3494L1 and 3494L4 have the same compositional elements in which it can be easily seen that without F-EMS how the weight percentage of carbon segregation increases in the center area 4-5 and >5 as per Figure 3.30**.**

Mn has a non-homogenous trend along the center and appears to be maximum with 1.12 % in area 2-3 of billet 3494L4. On the other hand, 3494L1 has less segregation of **Mn** after line 2 and appears to be between maximum value of 0.9 % which is coincides to the negative segregation region of white band due to F-EMS and minimum value of 0.76% in the center area >5. The stirrer is placed in 2.75 m after straightener of machine, the melt pool diameter decreases due to initial solidification around the center starting from area 1-2 of Figure 3.29, so stirrer is more effective to decrease Mn to 0.76% segregation in area >5 of billet 3494L1.

3498L1 – In this billet sample also there is not significant decrease of solute content, but it is observed that in the area of 1-2 and 5-6 shows white band segregation of S-EMS and final L-EMS, respectively.

Figure 3.31 Micro etched billet sample 3498L1

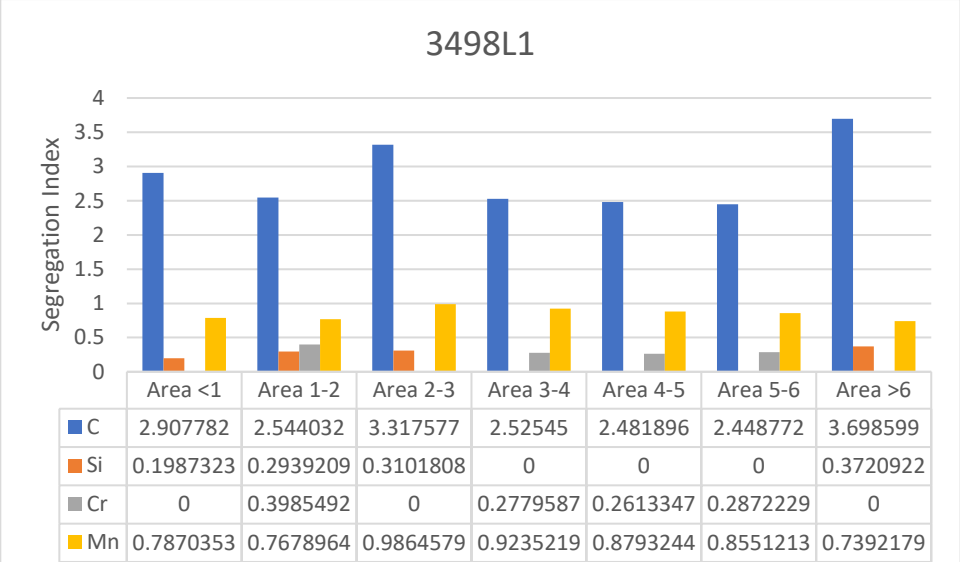

	Area <1	Area 1-2	Area 2-3	Area 3-4	Area 4-5	Area 5-6	Area >6
C	2.907782	2.544032	3.317577	2.52545	2.481896	2.448772	3.698599
Si	0.1987323	0.2939209	0.3101808	0	0	0	0.3720922
Cr	0	0.3985492	0	0.2779587	0.2613347	0.2872229	0
Mn	0.7870353	0.7678964	0.9864579	0.9235219	0.8793244	0.8551213	0.7392179

Figure 3.32 Qualitative representation of the C, Si, Cr, Mn in marked areas**.**

Billet 3498L1 doesn't have Si and Cr in several regions as per Figure 3.32. C is distributed more homogenously.
It is observed that as the F-EMS is situated in 3.5 m position, it doesn't have much effect to decrease Mn segregation level in area 2-3 being 0.98%, because initial solidification would have been started in that region when it arrived to 3.5 m F-EMS position, so after area 2-3 it is obvious from the Figure 3.32 how the Mn level of segregation decreases until area >6.

If we compare the SEM analysis with porosity analysis, 3491L1 is the billet with lower carbon segregation index along the region of linear F-EMS, and also lower porosity index according to longitudinal and transverse sections.

4 DISCUSSION

It is evident from the results presented in the previous sections that the central soundness in CC billets can be greatly enhanced by applying a final L-EMS beside the mold and strand stirrer, because the final L-EMS is more effective in final stage of solidification of central region of billets. The combination stirring with final L-EMS provides less porosity, significant decrease in V-segregation along the central axis of longitudinal sections, and decreased PDAS in the center comparing to the 3494L4 which is produced without L-EMS. However, PDAS is measured over the sides of the billets' transverse sections, it is visually observed that the billets cast with final L-EMS has solidification in terms of less visible and measurable PDAS comparing to the one fabricated without final L-EMS. It means, the decrease PDAS in the center region of the billets, implies that the solute enriched liquid doesn't have enough time to diffuse into solidification shrinkages formed at the final stage of solidification under the combined stirring. As a result, center defects represented by porosities and solute segregation spots can be more evenly distributed in smaller sizes to minimize the localizing tendency of center defects in preferred center region. According to the porosity indexes and the least number of small and big pores as shown in the histograms of the billet samples' longitudinal and transverse sections, the optimum casting parameters has been chosen at 600 A current intensity, 2.3 m/min casting speed and 2.75 m L-EMS position from the end of strand curve under the name of 3493L1 billet sample. It is better to use the final L-EMS with less current intensity, but not further or closer to the strand curve end.

As the mould and strand stirrer parameters doesn't change, we didn't observe any change in terms columnar dendrite inclination angles and PDAS in the sides of the billets. The increase of the speed from the 2.3 m/min to 2.5 m/min increased significantly white band segregation diameter caused by the strand stirrer and less increase is observed in the white band segregation diameter due to L-EMS.

As represented in the SEM analysis results of section 12, according to the qualitative degree of carbon content, it is observed that as the distance of the final L-EMS from the end of the strand curve increases, its affect to decrease the carbon segregation level in the white band region of the L-EMS getting lower. So, as we observe the negative and positive segregation of L-EMS white band regions for the billets 3490L1 and 3491L1, as we get further in L-EMS position, carbon level gets homogeneity, there is no significant decrease in the carbon level, even if we increase the current intensity as in billet 3494L1 and 3498L1. If we compare the billets with 3494L4 which is produced without L-EMS, we will see the depletion in the carbon segregation level.

SEM analysis microstructural pictures in 1000x magnification (see Appendix A) has been captured beginning from the strand stirrer white band segregation region. Including strand stirrer and final linear stirrer white band segregation, it is observed that both regions has the clear view of pearlite. When the pearlite and black spots due to MnS, P and other inclusions are highly concentrated as shown in the billet 3496L1 (see Appendix A) which has the highest porosity implies that there are high concentrates of segregation because of carbon and other inclusions.

Centerline segregation is known to be the prime source of subsurface cracks and porosity in CC products. So if we choose the optimum F-EMS parameters among the billets in order to decrease the central segregation we will be reducing also the porosity.

5 CONCLUSION

In this study, the effect of using final L-EMS together with mould and strand stirring was investigated through continuous cast high carbon steel billets with the aid of laboratory experiments. Several billet samples were collected from the plant and experimental observations were correlated with the operating parameters of the caster.

Some of the important findings of the study are summarized below:

- Macrostructural examination of the billet samples, in terms of porosity, revealed that the proper positioning of the final L-EMS from the straightener determined to be 2.75 m with 2.3 m/min casting speed at 600 A current intensity.
- As the current intensity increases at constant L-EMS positions the diameter of the final L-EMS white band decreases.
- An increase in casting speed gives rise to the diameter of white band of the strand stirrer.
- As a result, the optimum configuration of 600 A current intensity at 2 and 2.75 m L-EMS distance at 2.3 m/min casting speed has been selected according to carbon segregation index decrease and less porosity at the same time.
- Billet 3491L1 produced with 600 A, 2 m F-EMS position at 2.3 m/min casting speed possess the least segregation of nonmetallic elements in which it coincides with the least porous billet among the SEM analyzed billets.

Appendix A

a)

b)

Billet a) 3490L1 and b) 3491L1

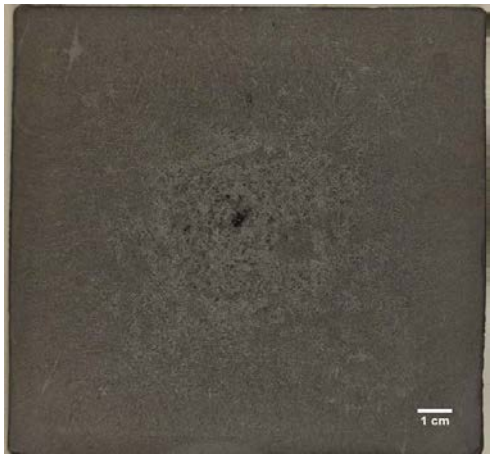

a)

b)

Billet a) 3492L1 and b) 3493L1

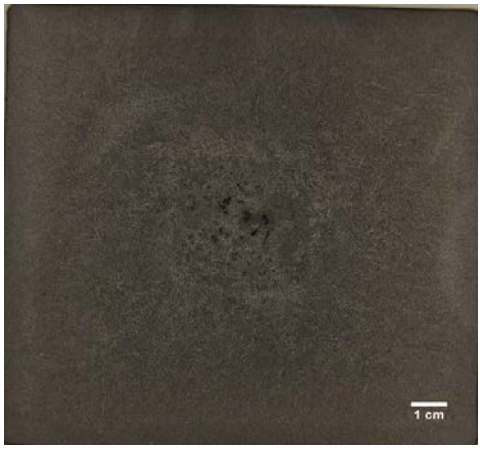

a)

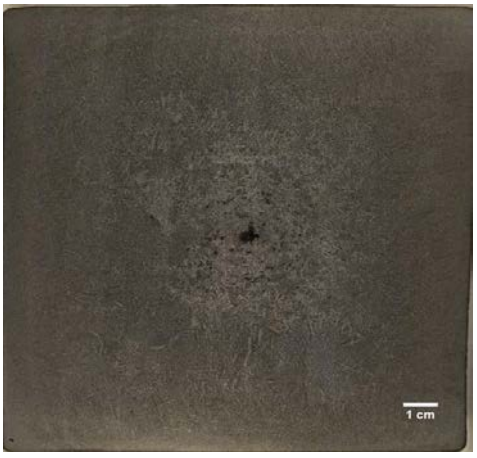

b)

Billet a) 3494L1 and b) 3495L1

a)

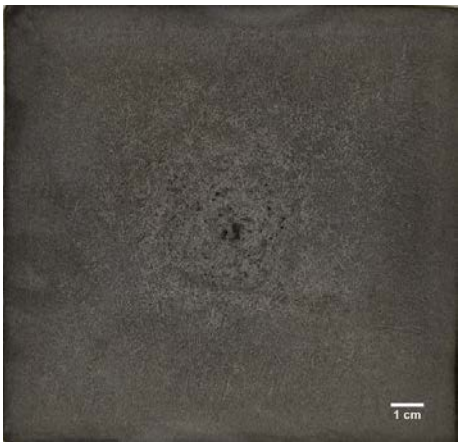

b)

Billet a) 3496L1 and b)3497L1

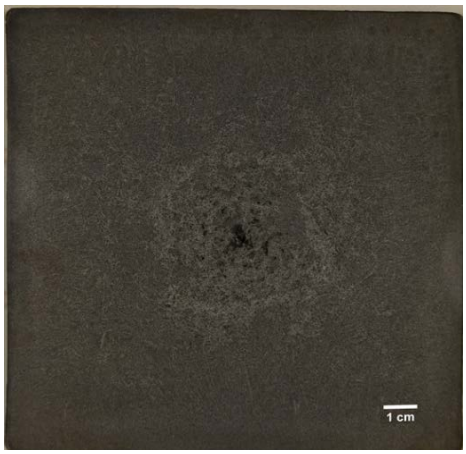

a)

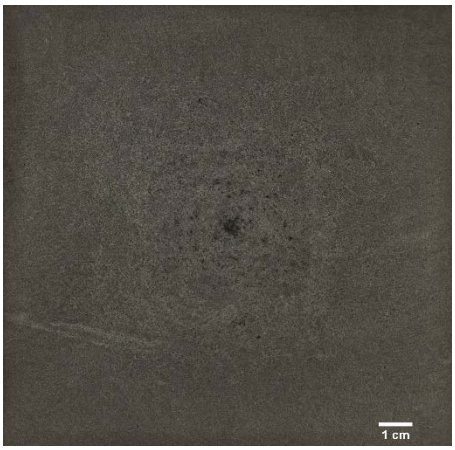

b)

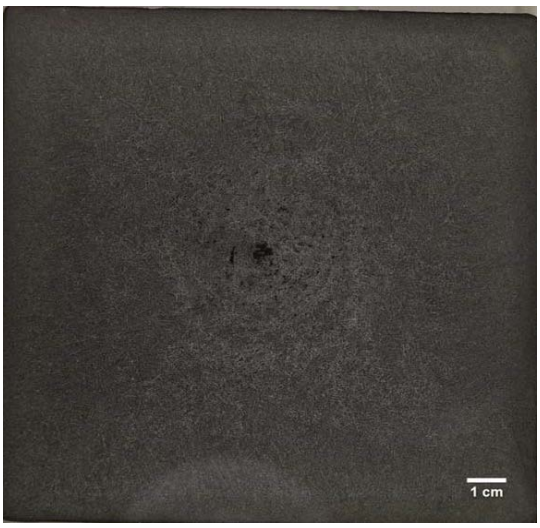

c)

Billet a) 3498L1 b) 3499L1 and c) 3494L4 no final EMS

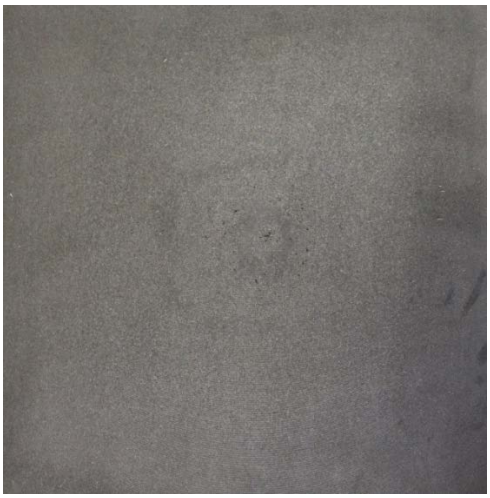

a) b)

Billet 3491 L1 transverse and longitudinal sections

a) b)

Billet 3490L1 transverse and longitudinal sections

a) b)

Billet 3492L1 transverse and longitudinal sections

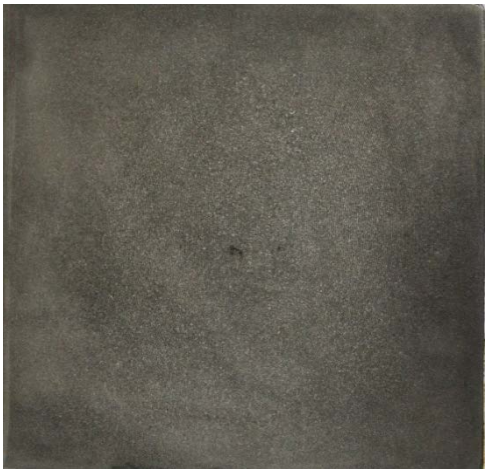

b)

b)

Billet 3493L1 transverse and longitudinal sections

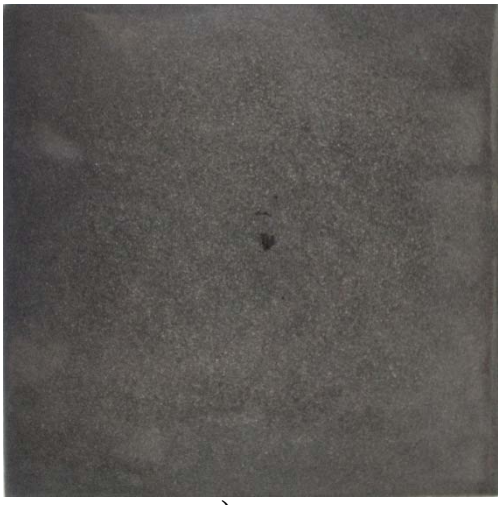

a)

b)

Billet 3494L1 a) transverse and b) longitudinal sections

a)

b)

Billet 3495L1 a) Transverse and b) longitudinal sections

a) b)

Billet 3495L1 a) transverse and b) longitudinal sections

a) b)

Billet 3496L1 a) transverse and b) longitudinal sections

a) b)

Billet 3497L1 transverse and longitudinal sections

a) b)

Billet 3498L1 transverse and longitudinal sections

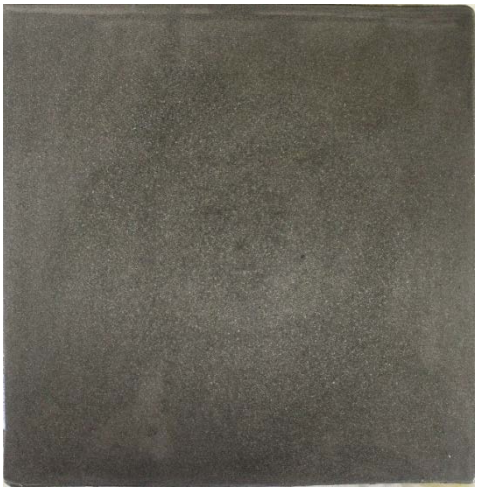

a) b)

Billet 3499L1 transverse and longitudinal sections

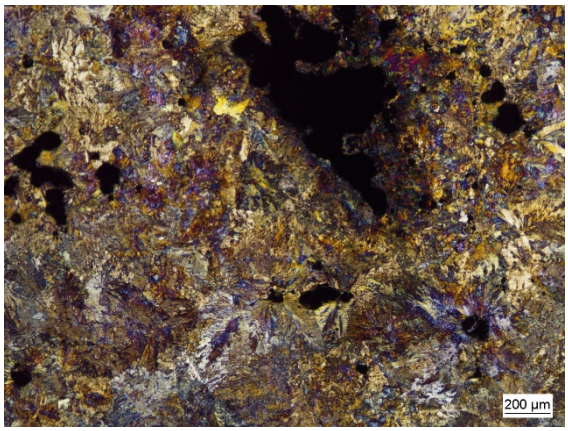

a) Area <1

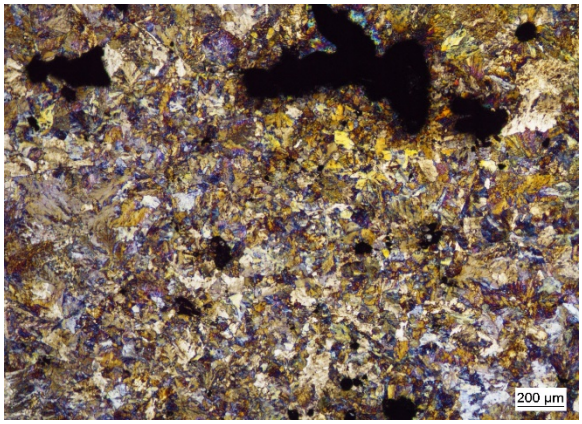

b) Area 1-2

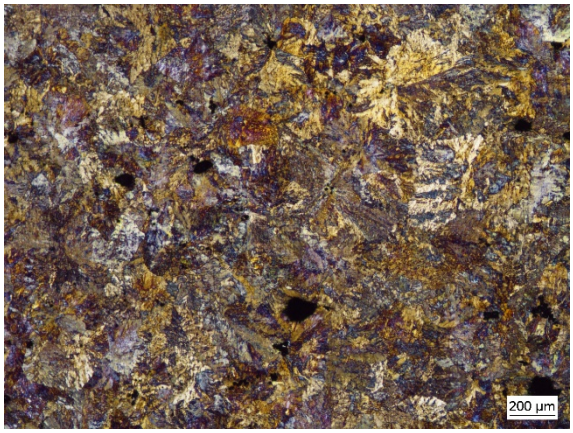

b) Area 2-3

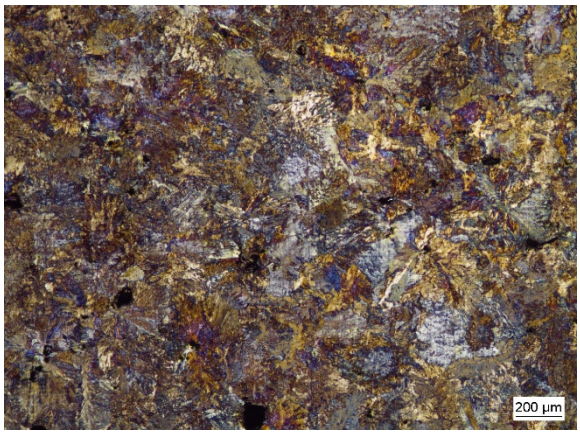

c) Area 3-4

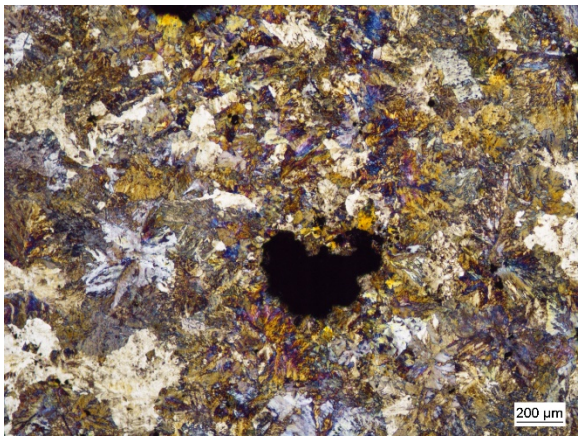

d) Area 4-5

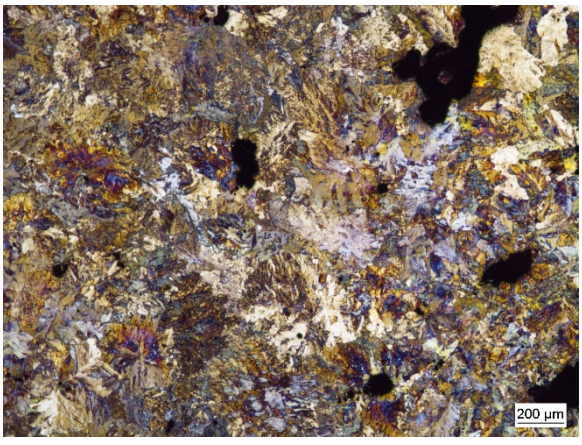

e) Area 5<

3490L1 SEM analysis pictures according to regions

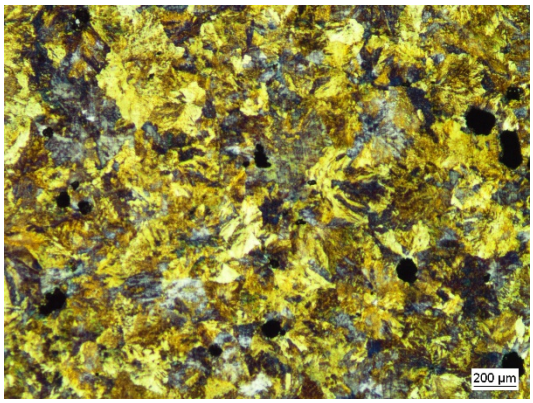

a)

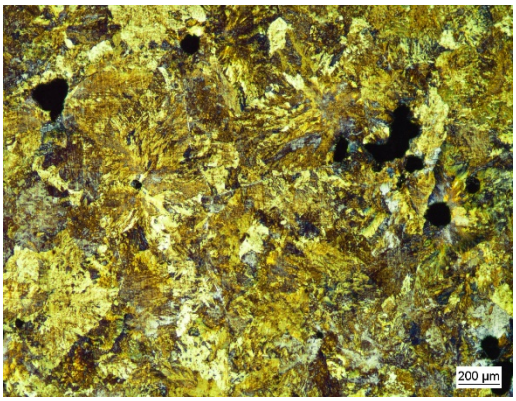

b)

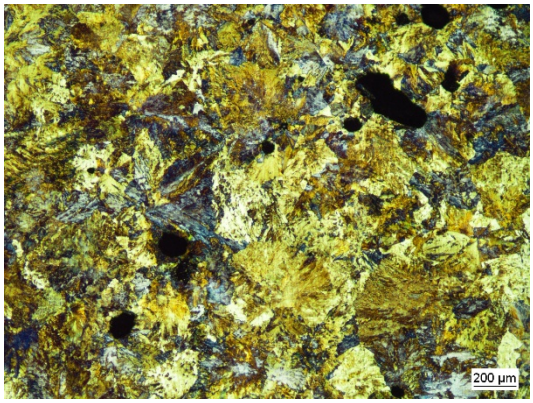

c)

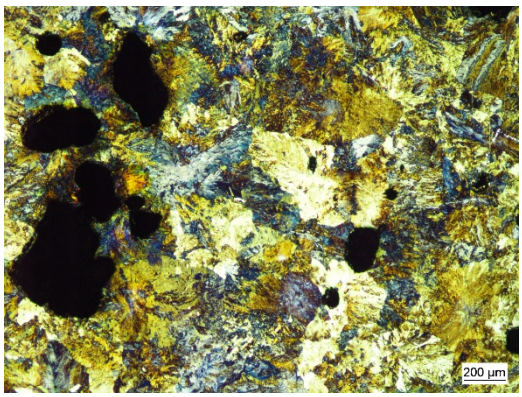

d)

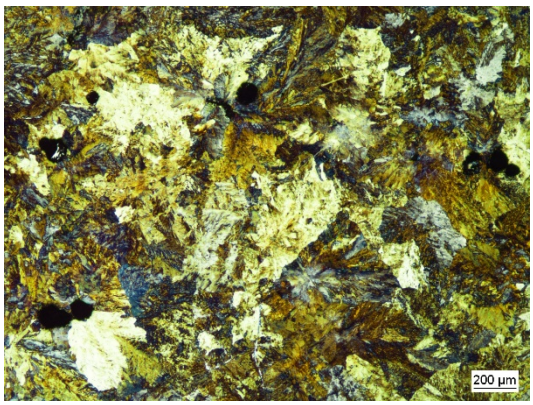

e)

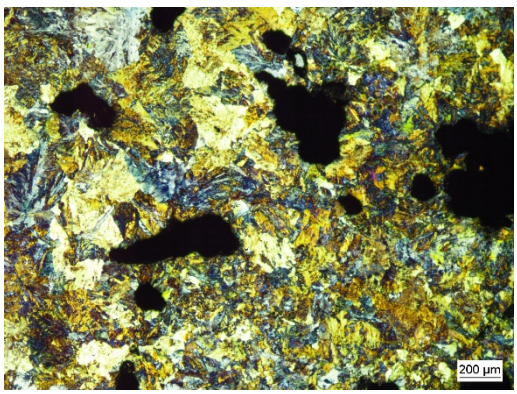

f)

3491L1 SEM analysis pictures according to areas.

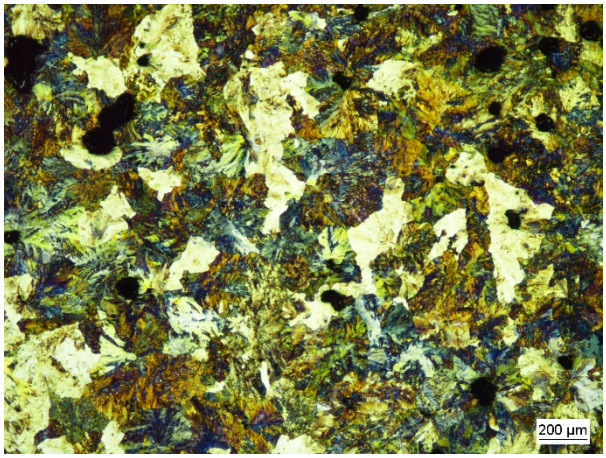

a) Area <1

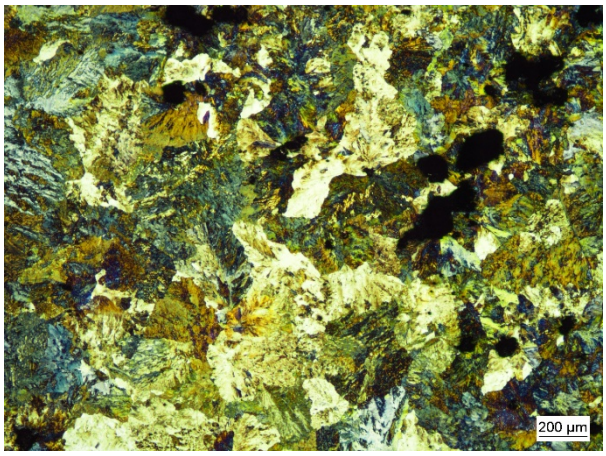

b) Area 1-2

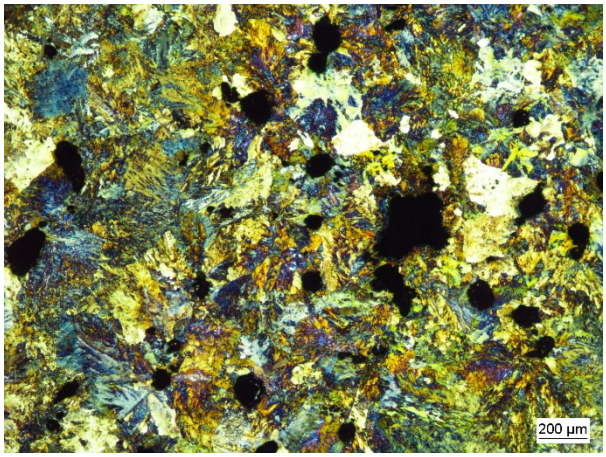

c) Area 2-3

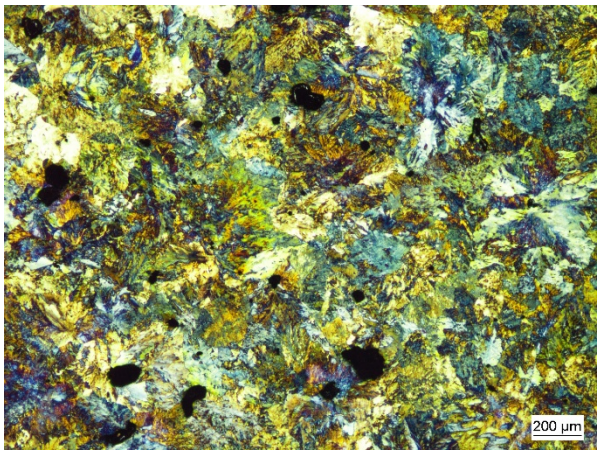

d) Area 3-4

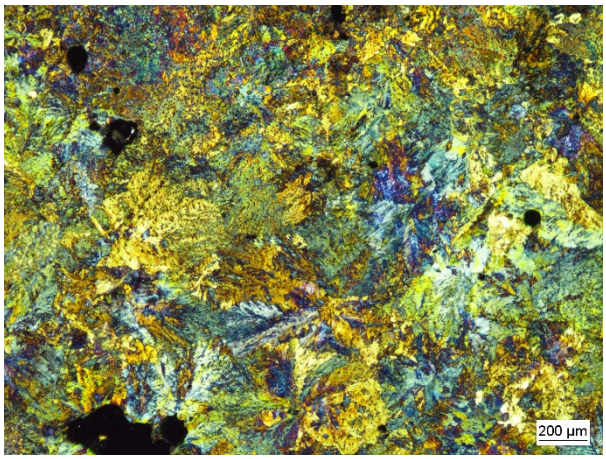

e) Area 4-5

3492L1 SEM analysis pictures according to areas

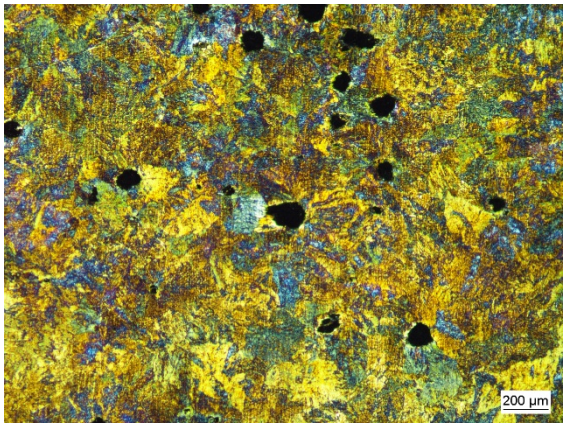

a) Area <1

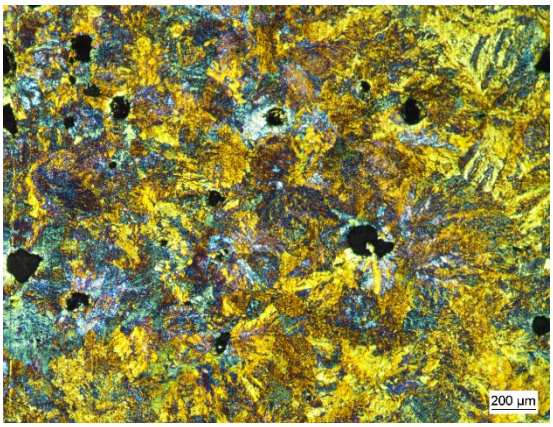

b) Area 1-2

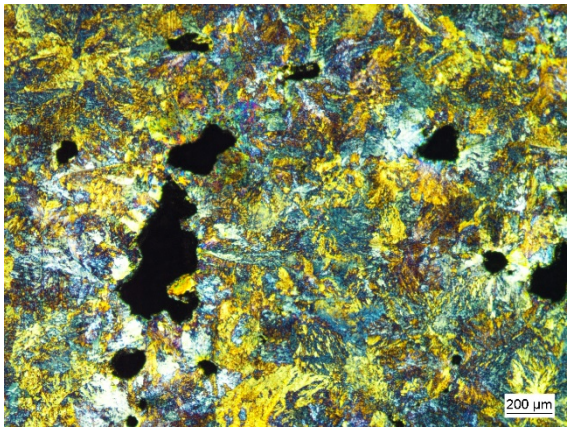

c) Area 2-3

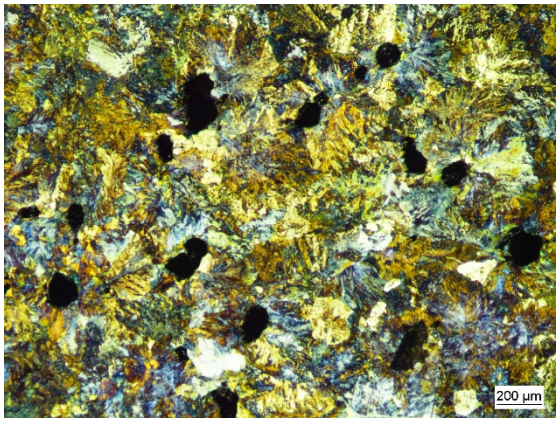

d) Area 3-4

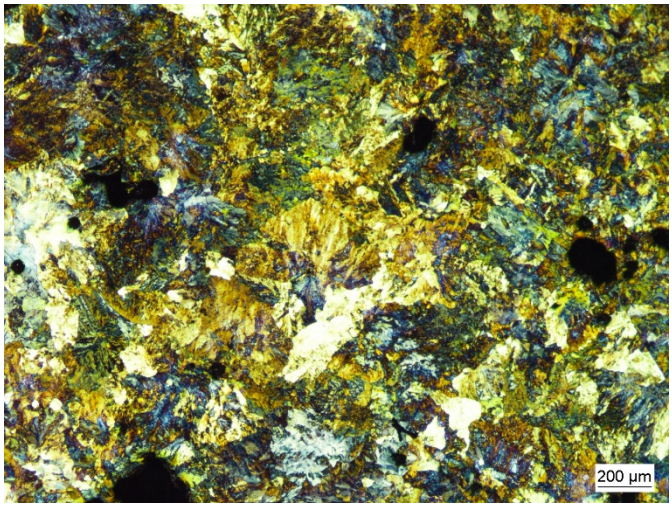

e) Area 4-5

3494L1 SEM analysis pictures according to areas

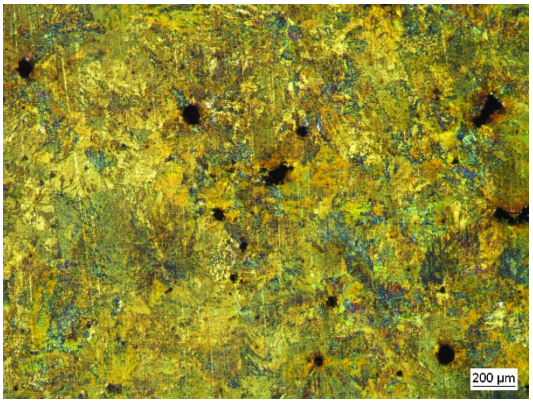

a)

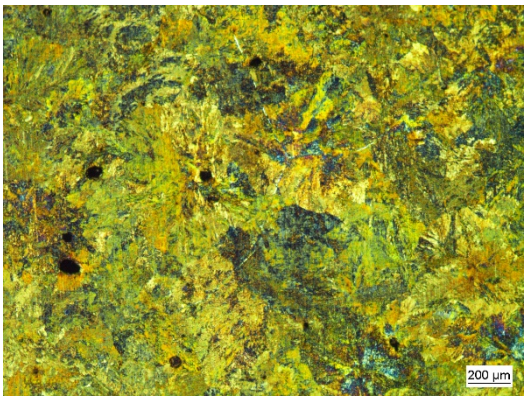

b)

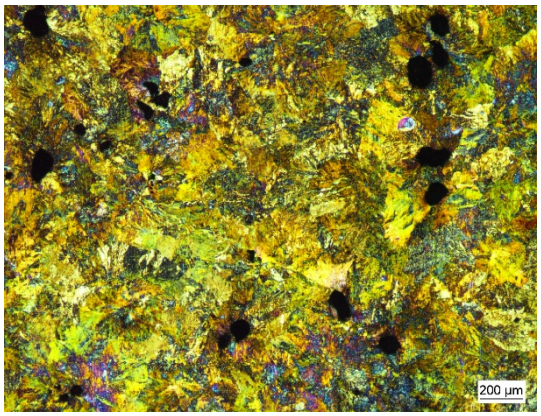

c)

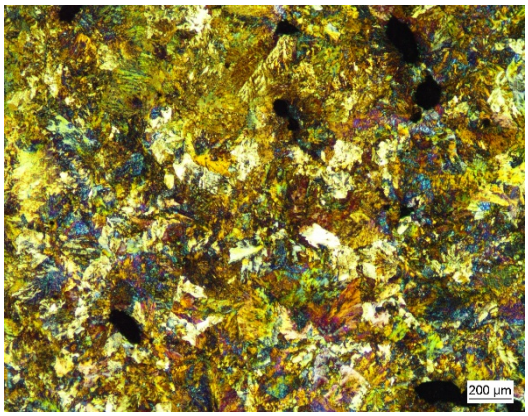

d)

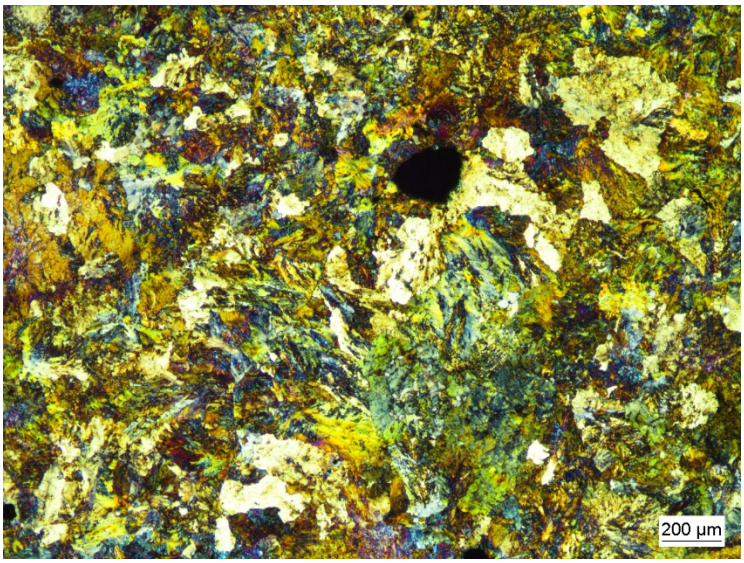

e)

3498L1 SEM analysis pictures according to areas.

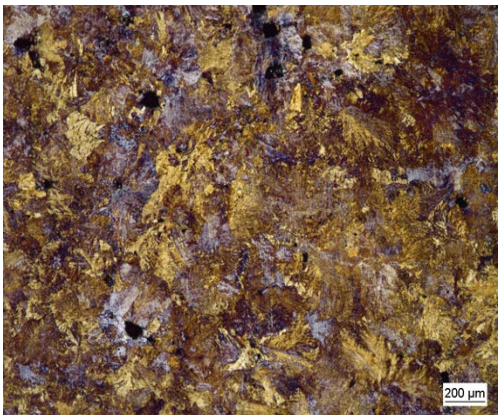

a) **Area <1**

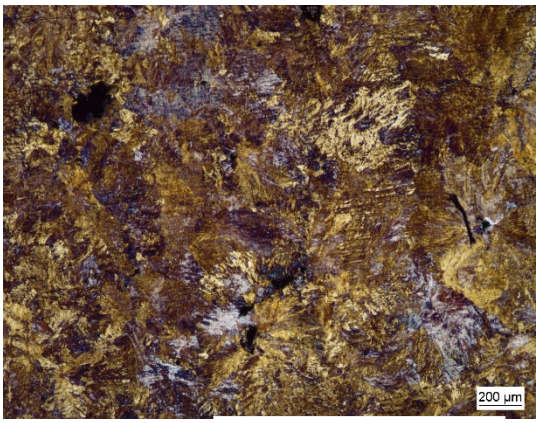

b) Area 1-2

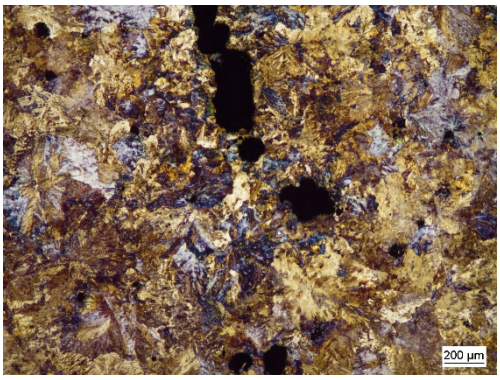

c)Area 2-3

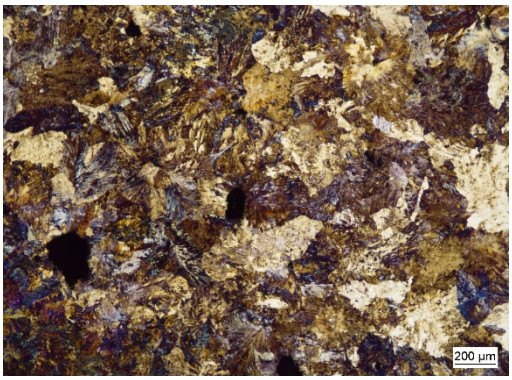

d) Area 3-4

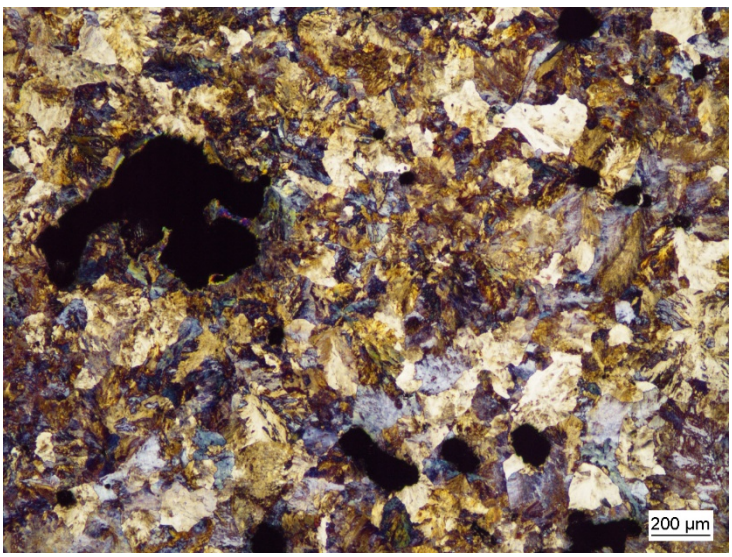

e) Area 4-5

3494L4 SEM analysis pictures according to areas

Billet 3490L1

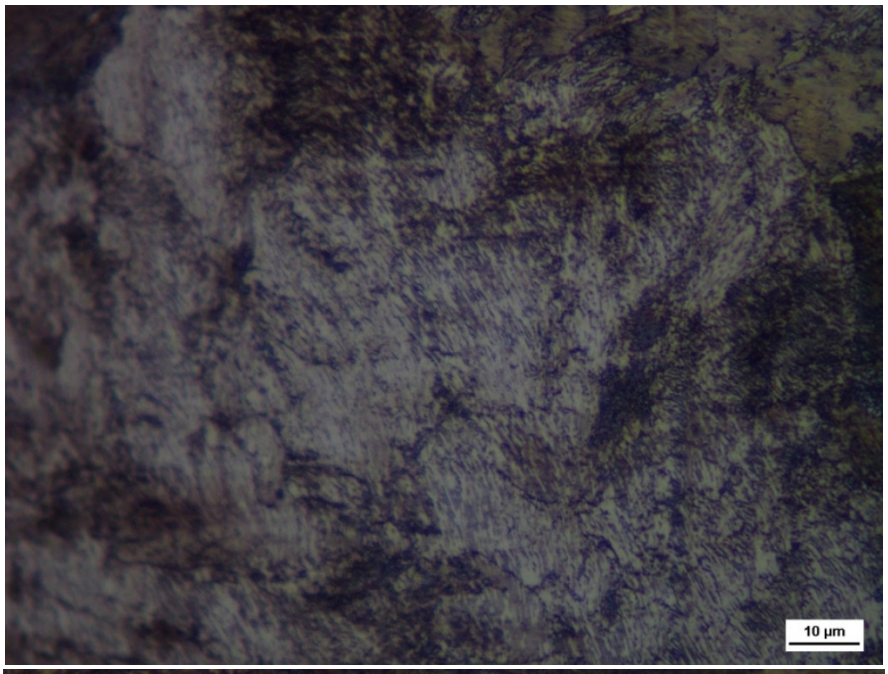

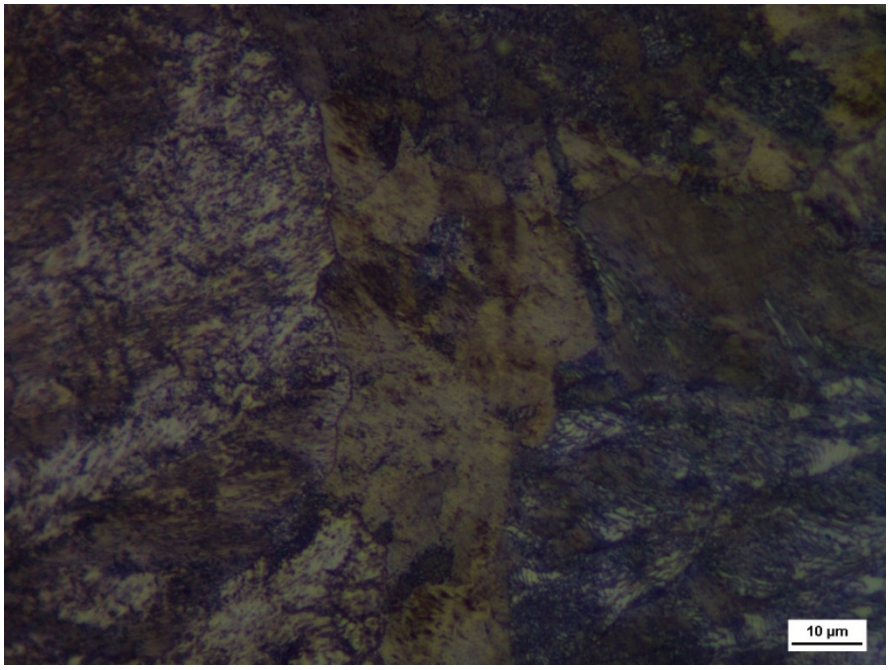

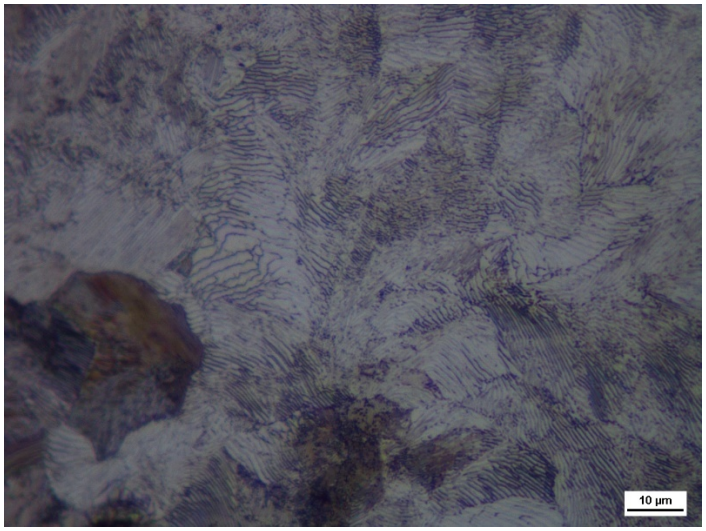
10 µm

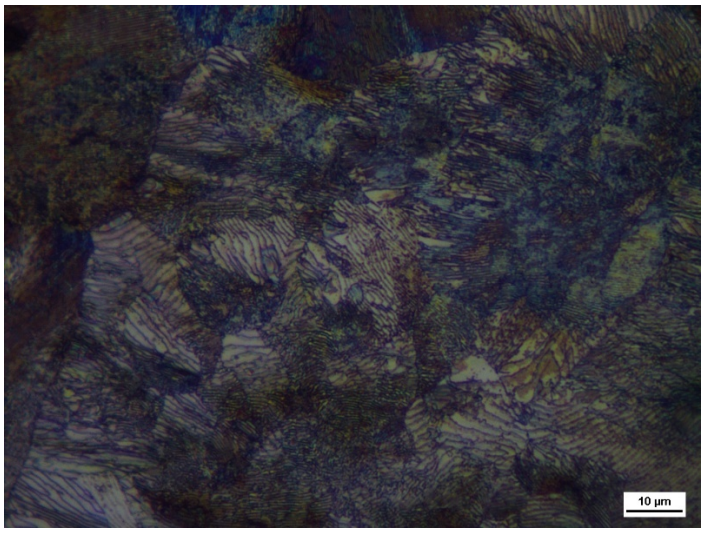
10 µm

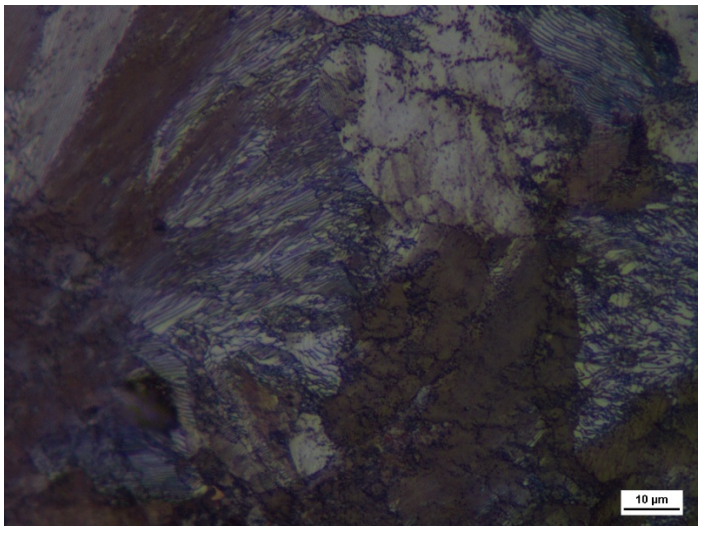
10 µm

Billet 3491L1

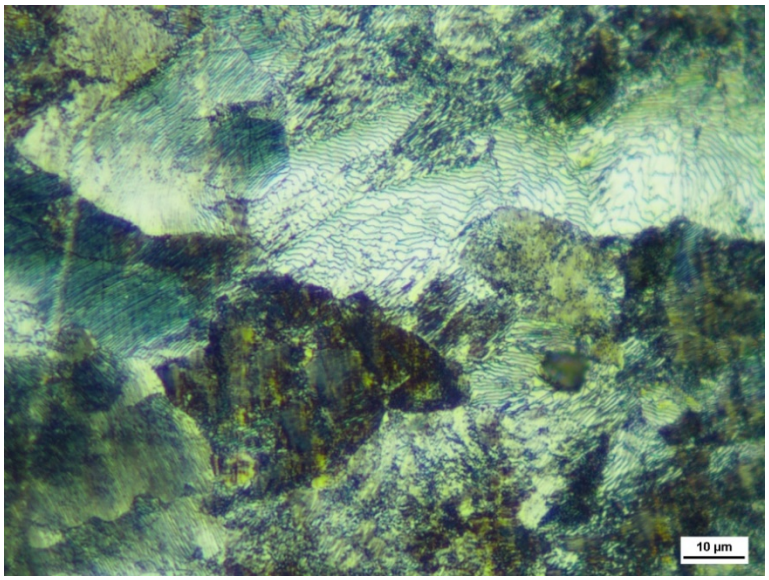

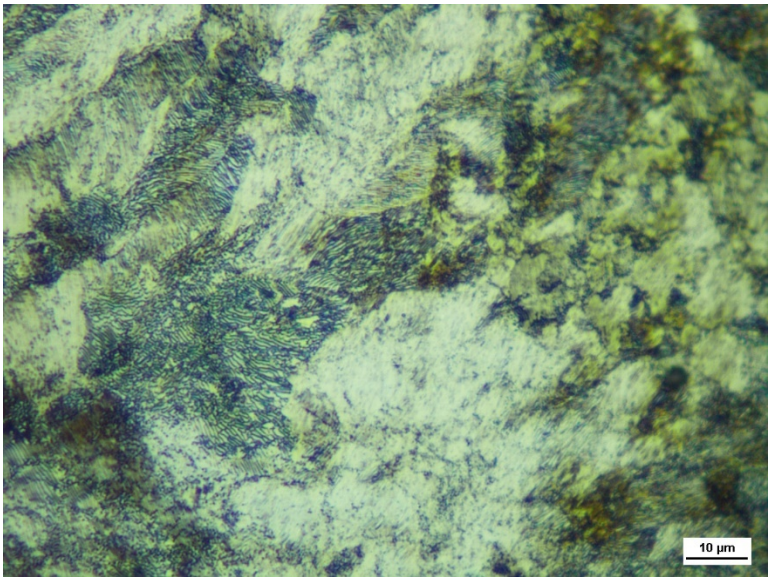

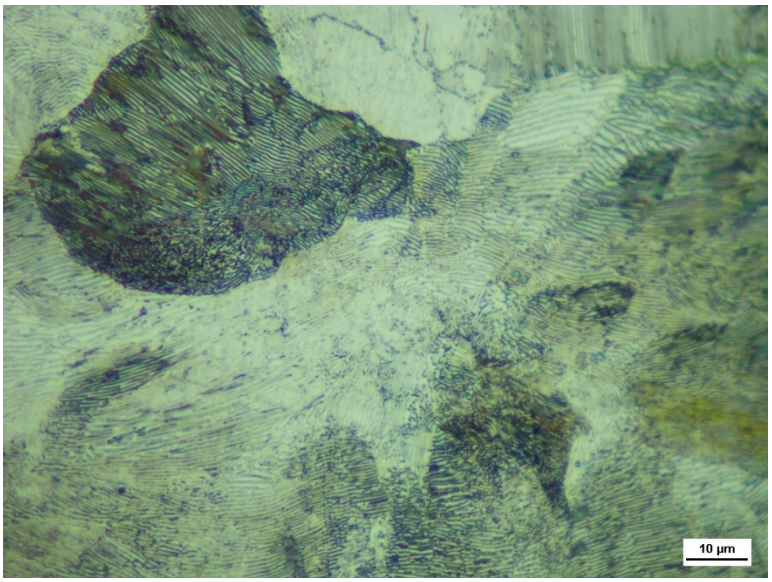

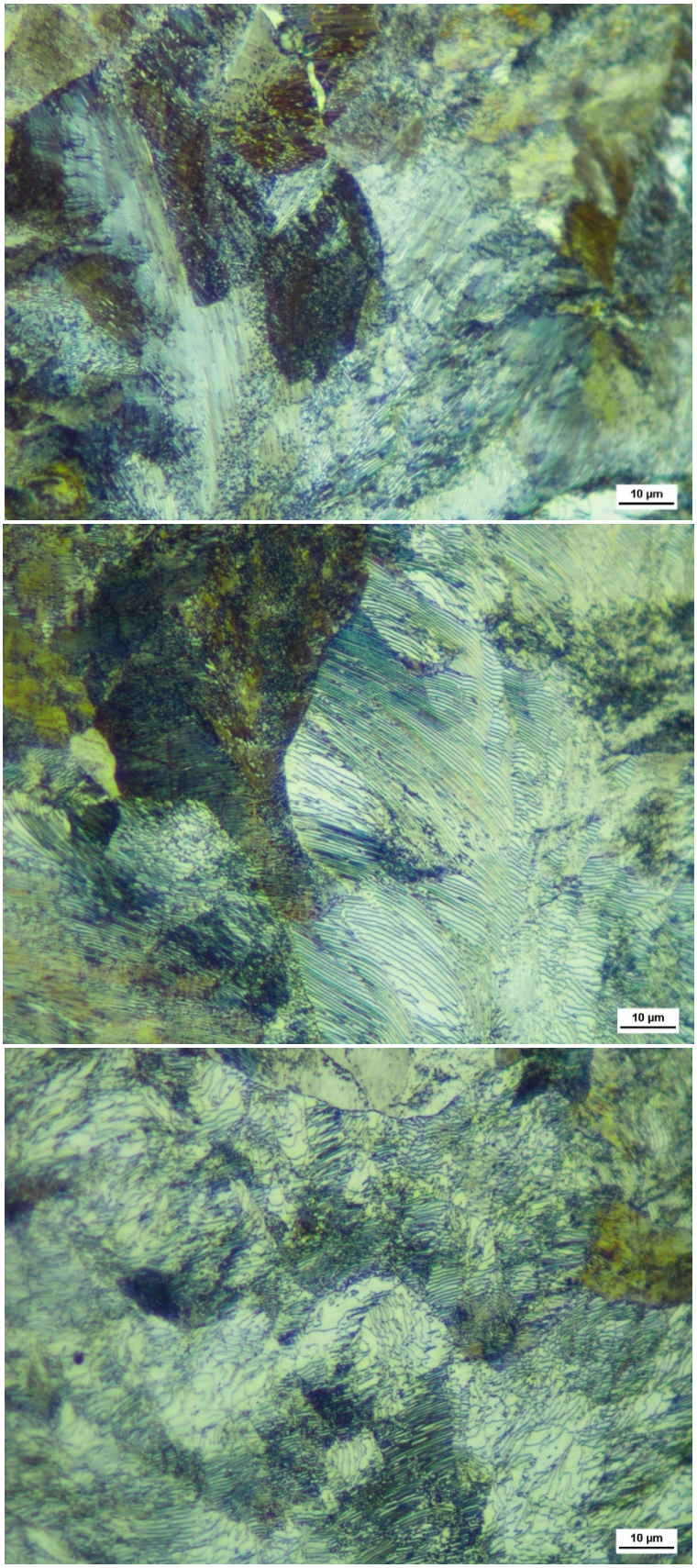
10 µm
10 µm
10 µm

Billet 3492L1

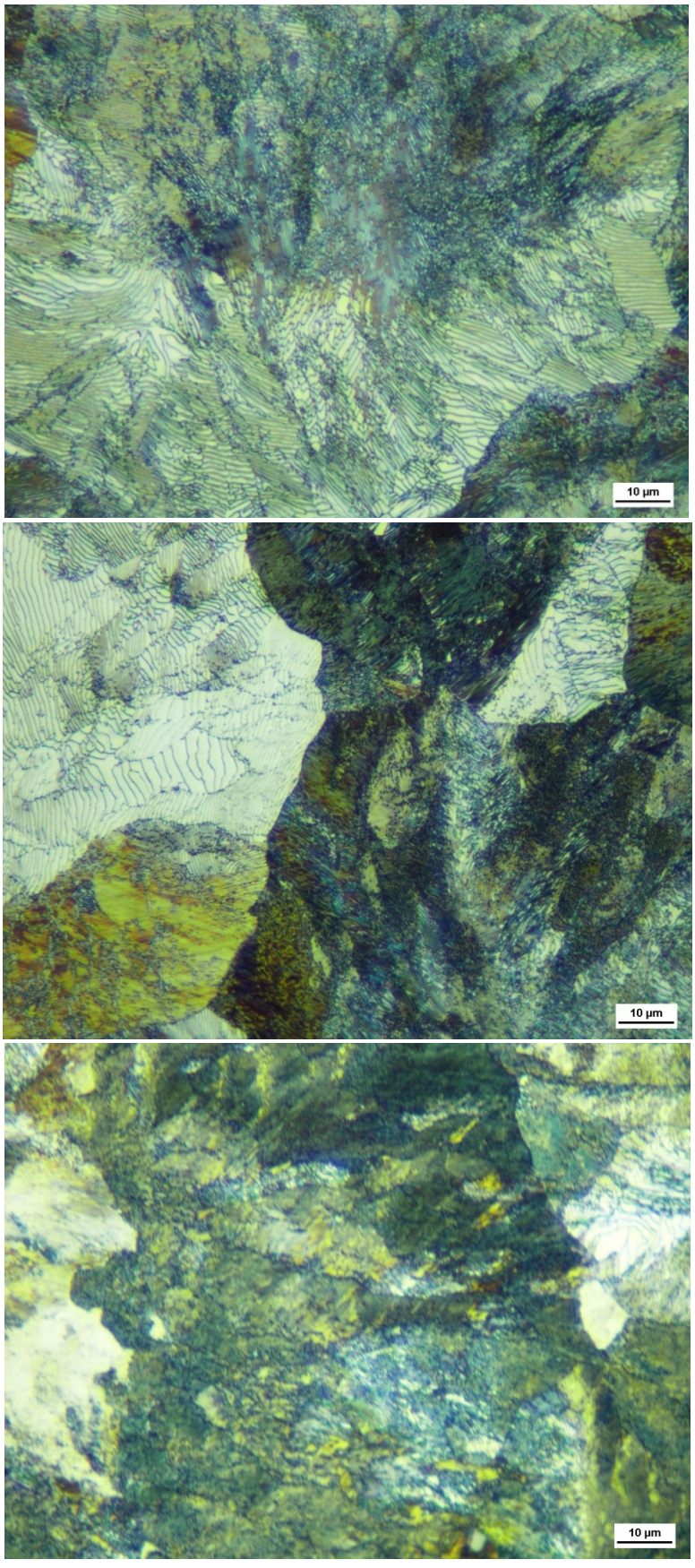

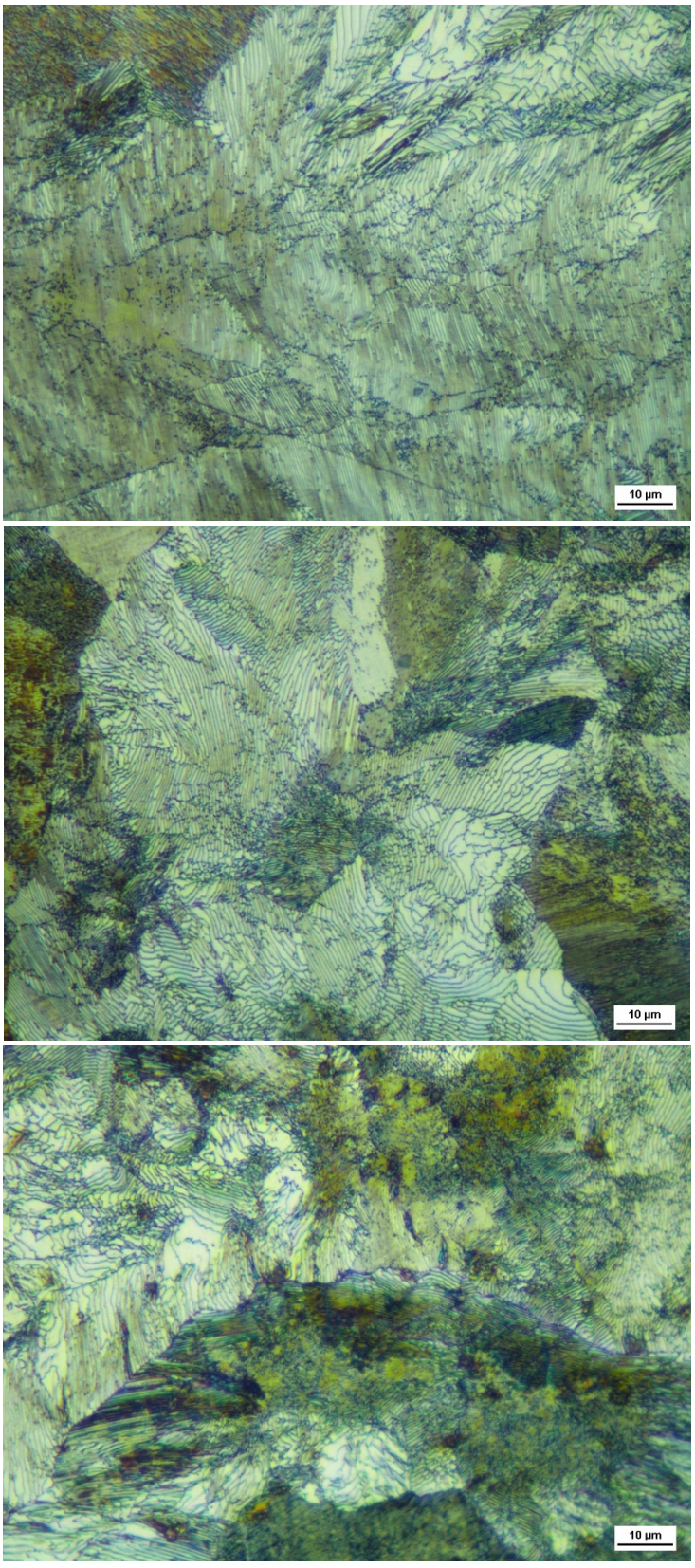
10 µm
10 µm
10 µm

Billet 3493L1

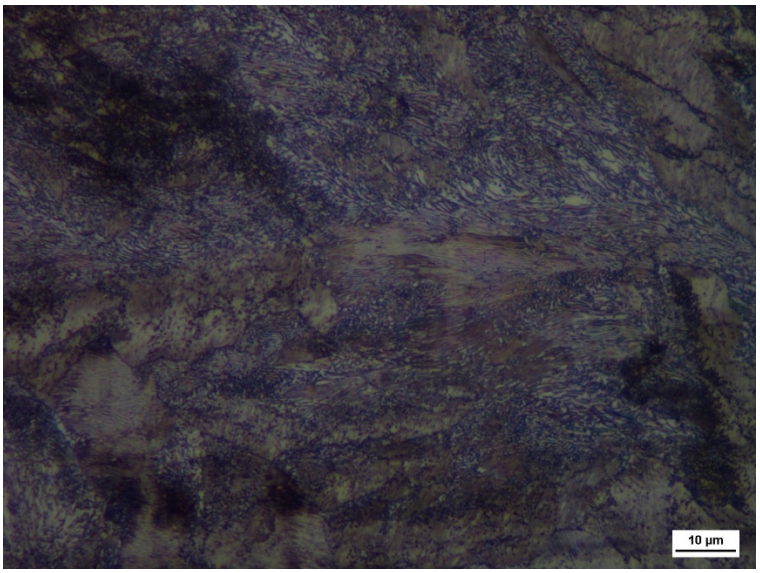

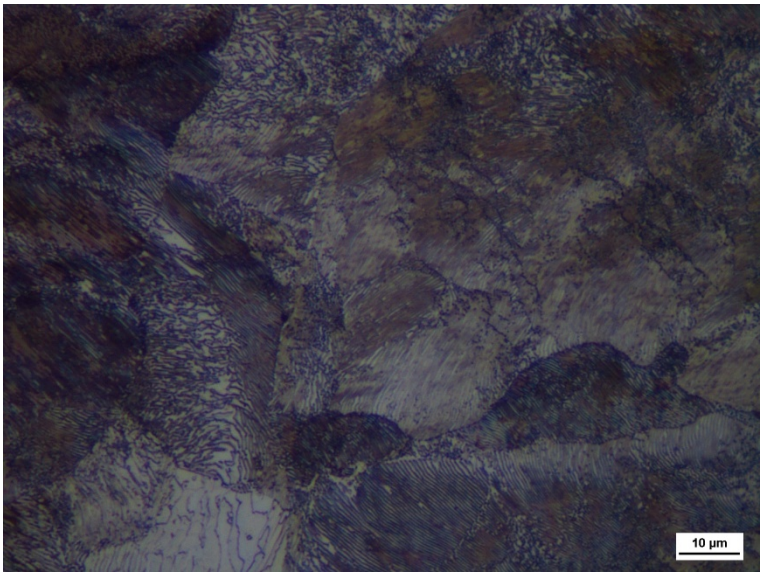

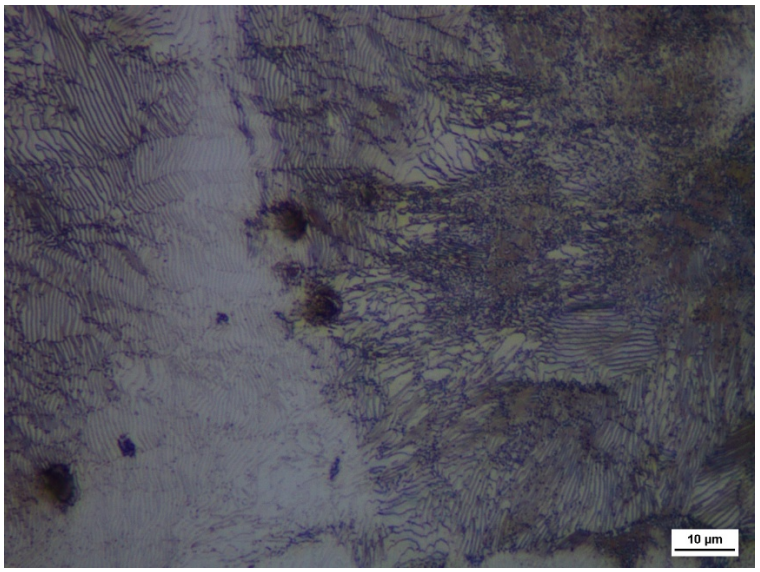

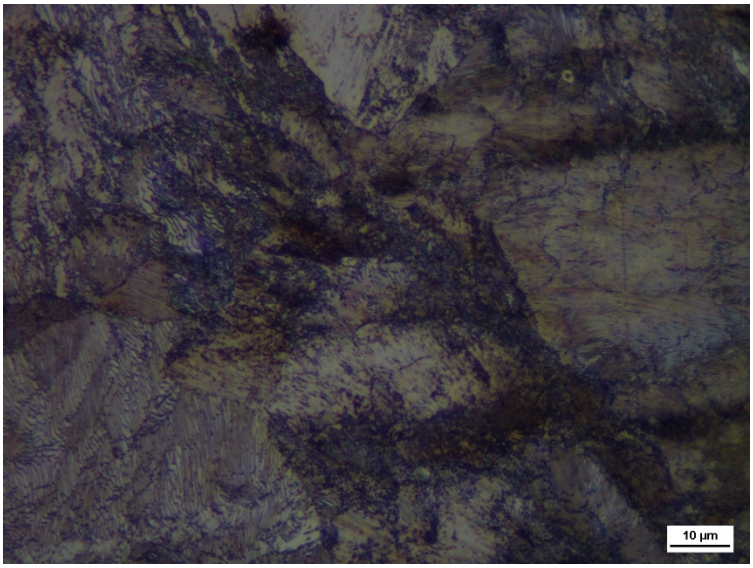
10 µm

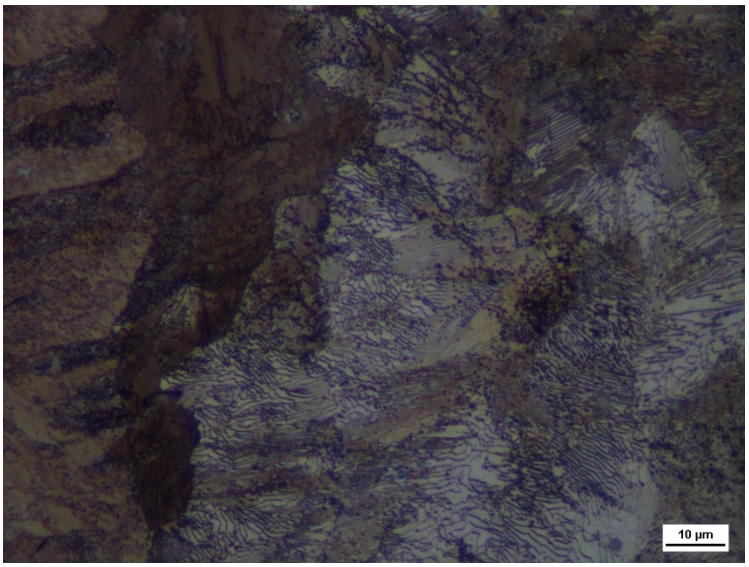
10 µm

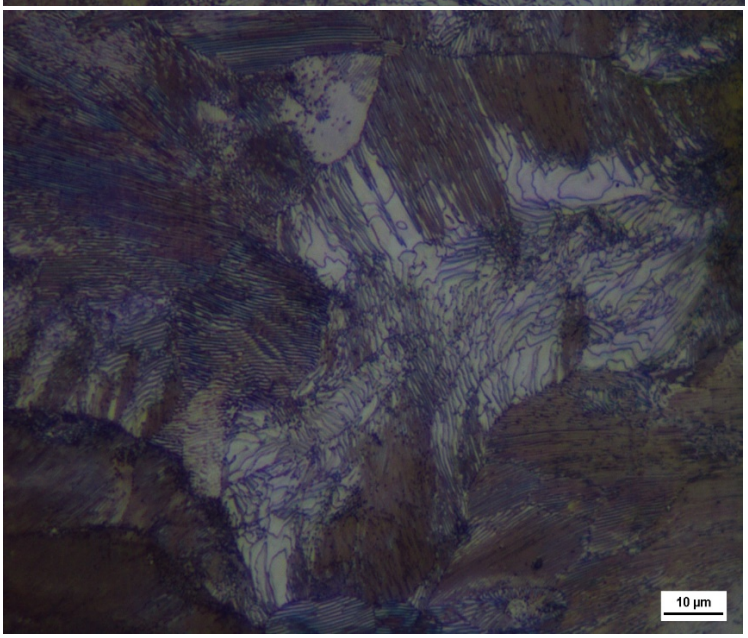
10 µm

Billet 3494L1

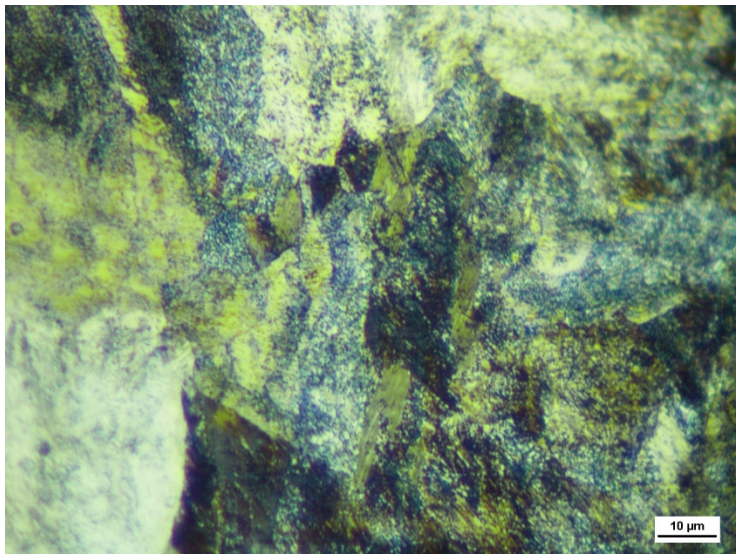

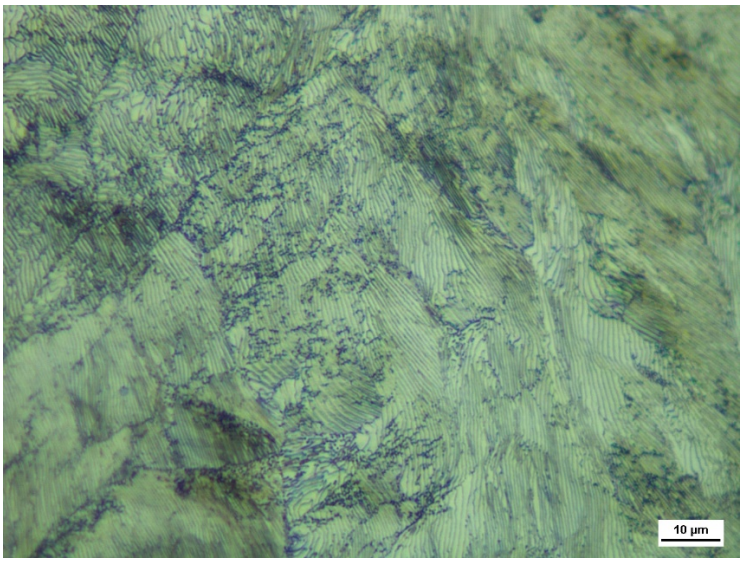

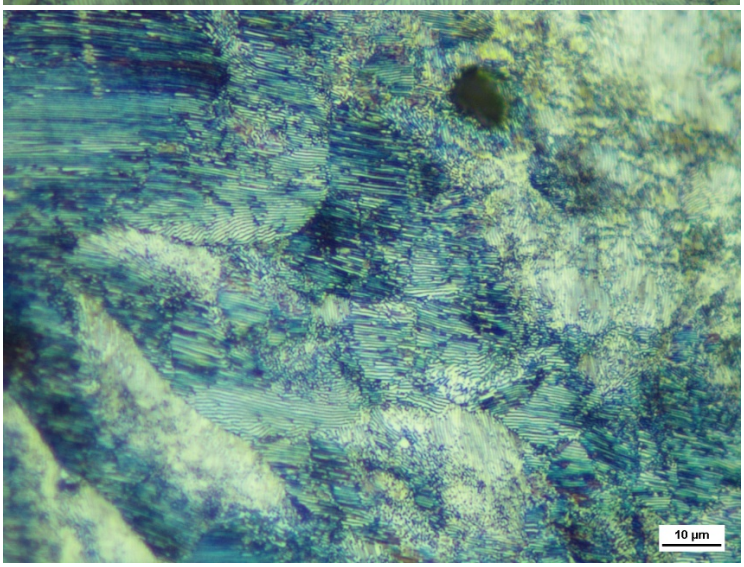

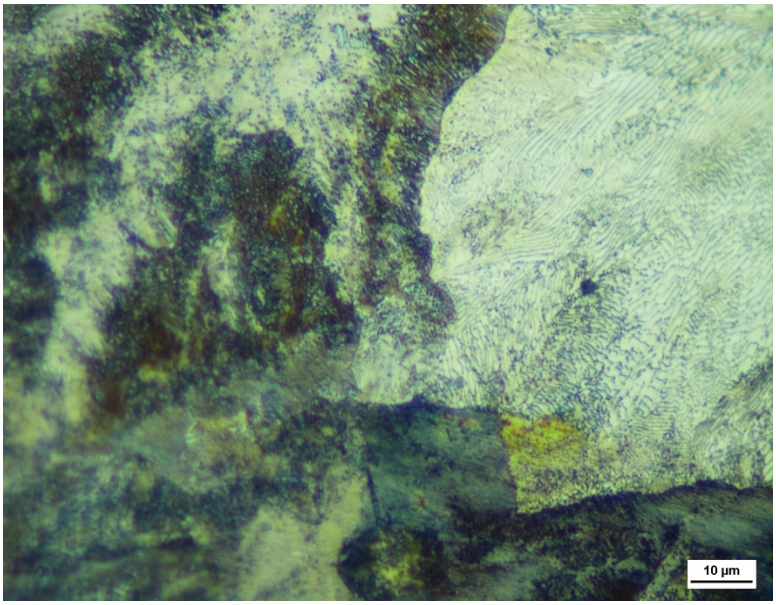
10 µm

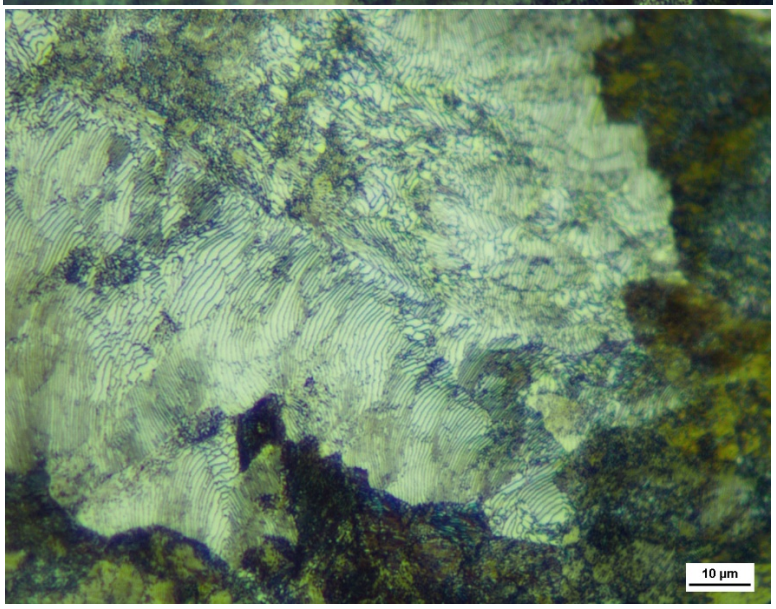
10 µm

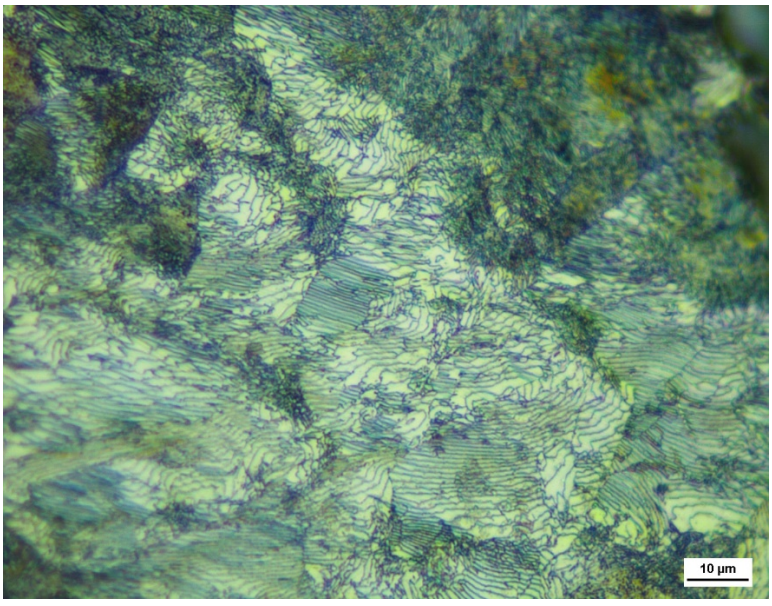
10 µm

Billet 3495L1

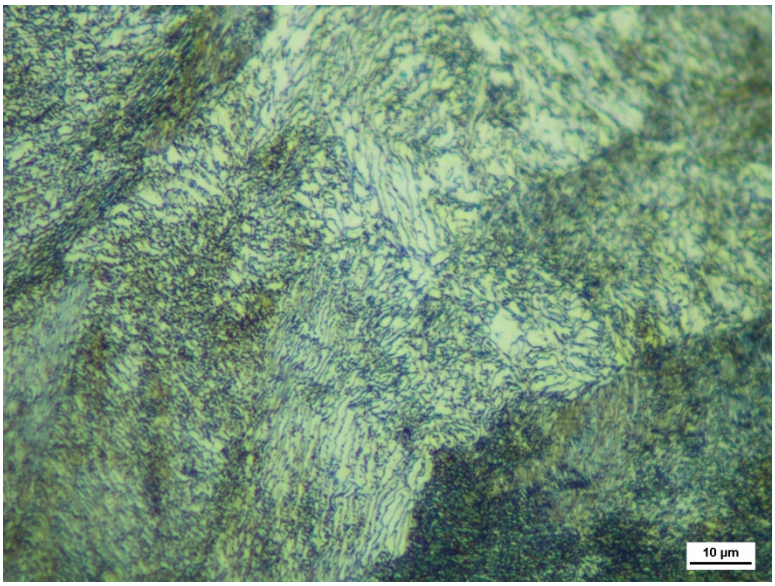

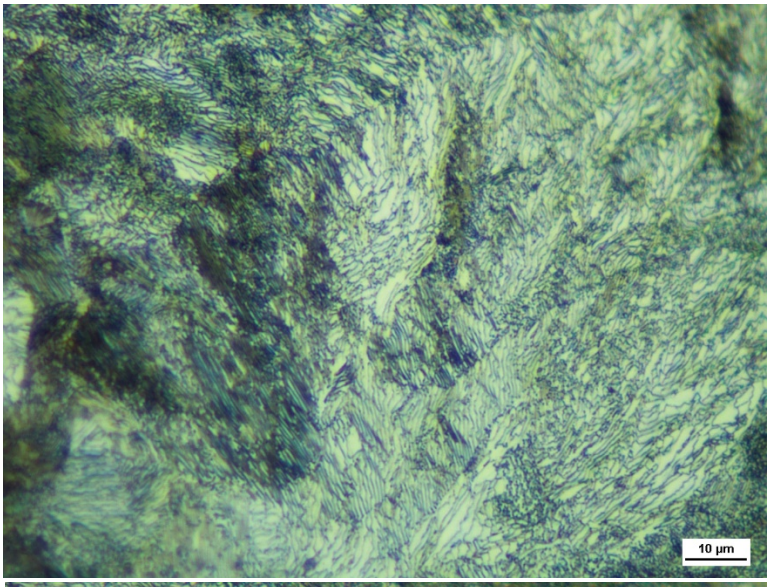

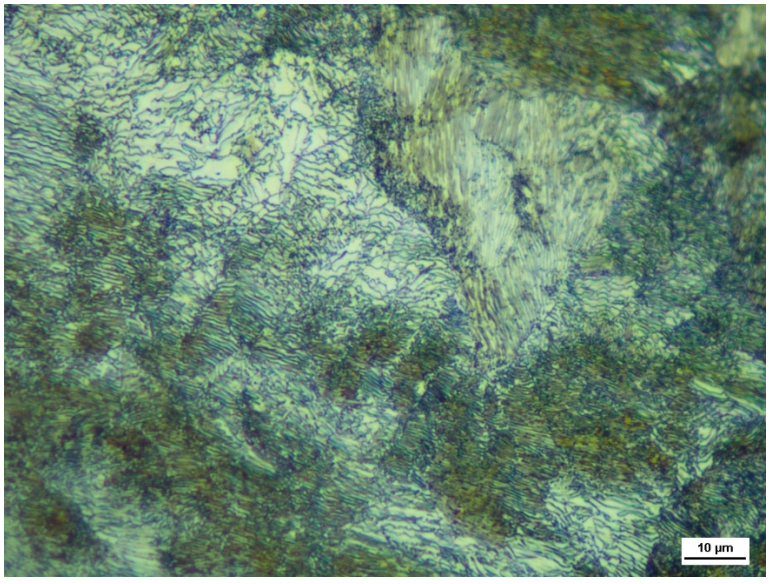

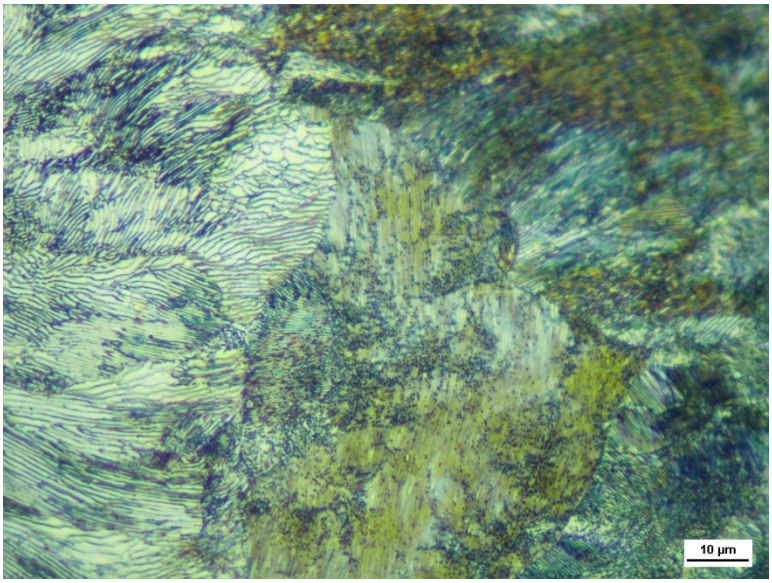
10 µm

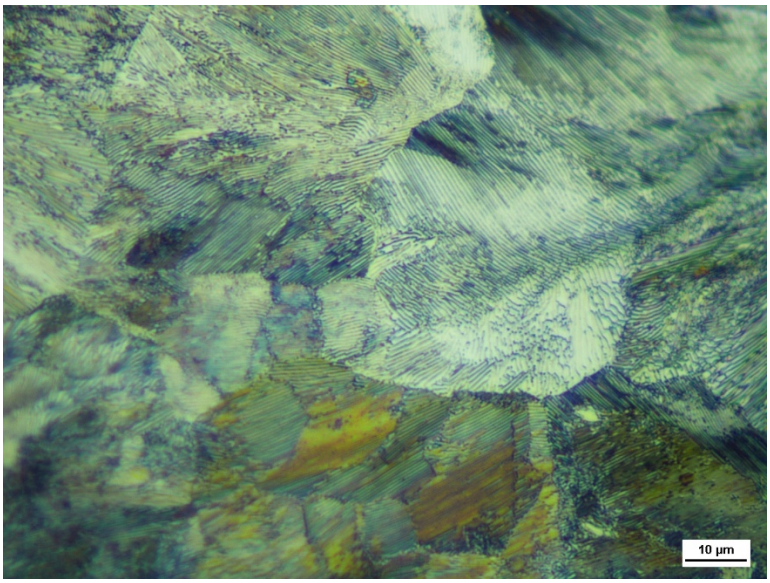
10 µm

Billet 3496L1

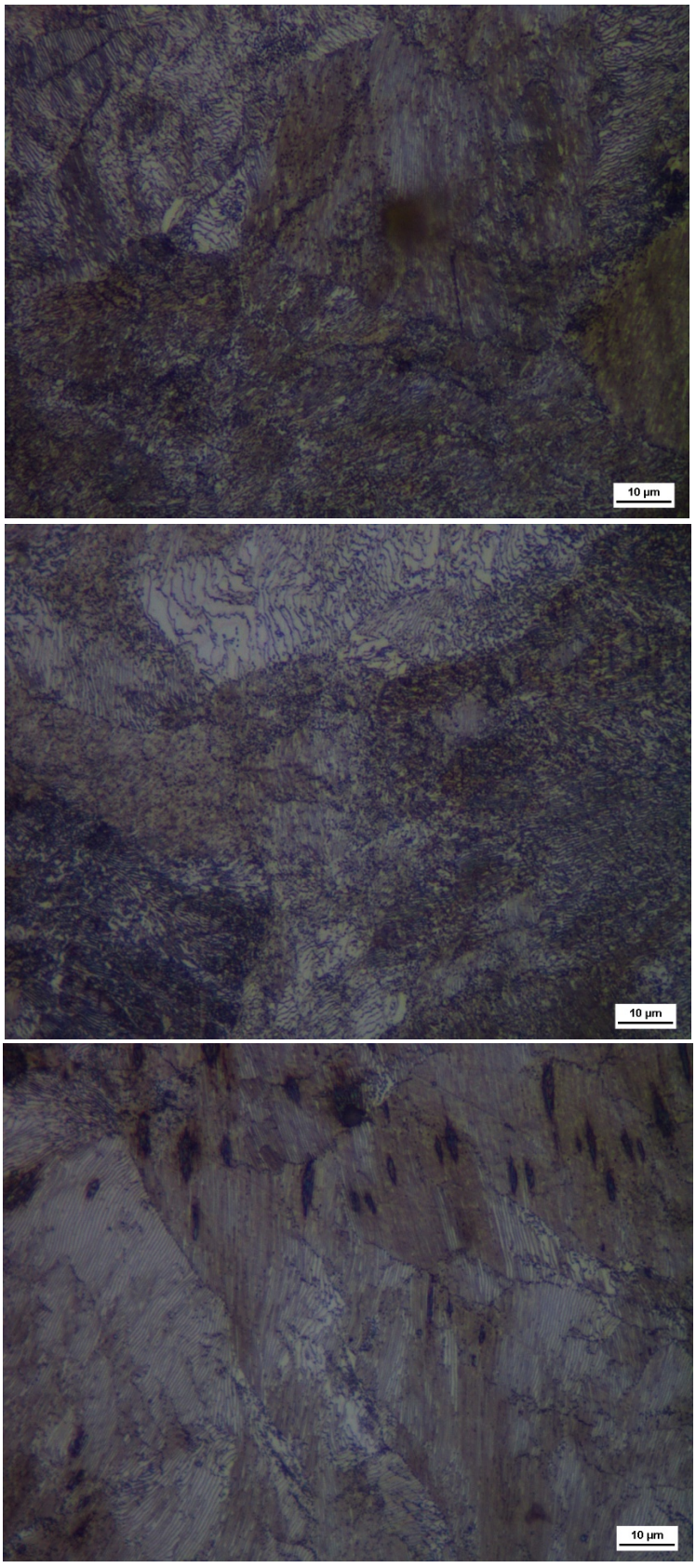

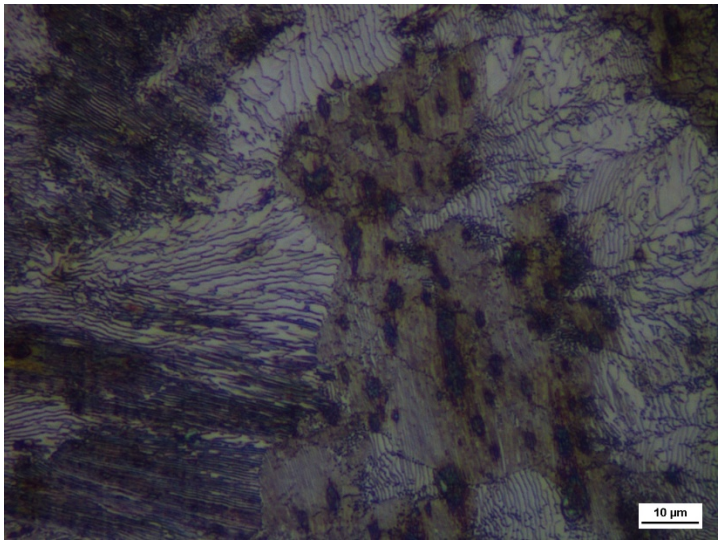
10 µm

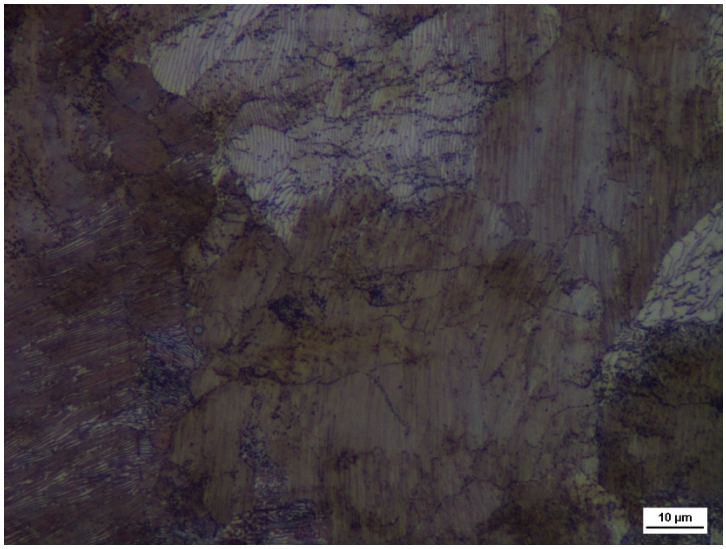
10 µm

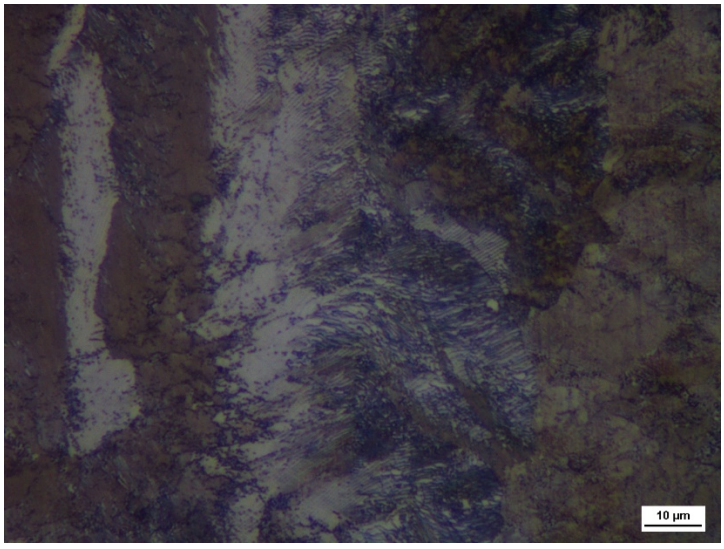
10 µm

Billet 3497L1

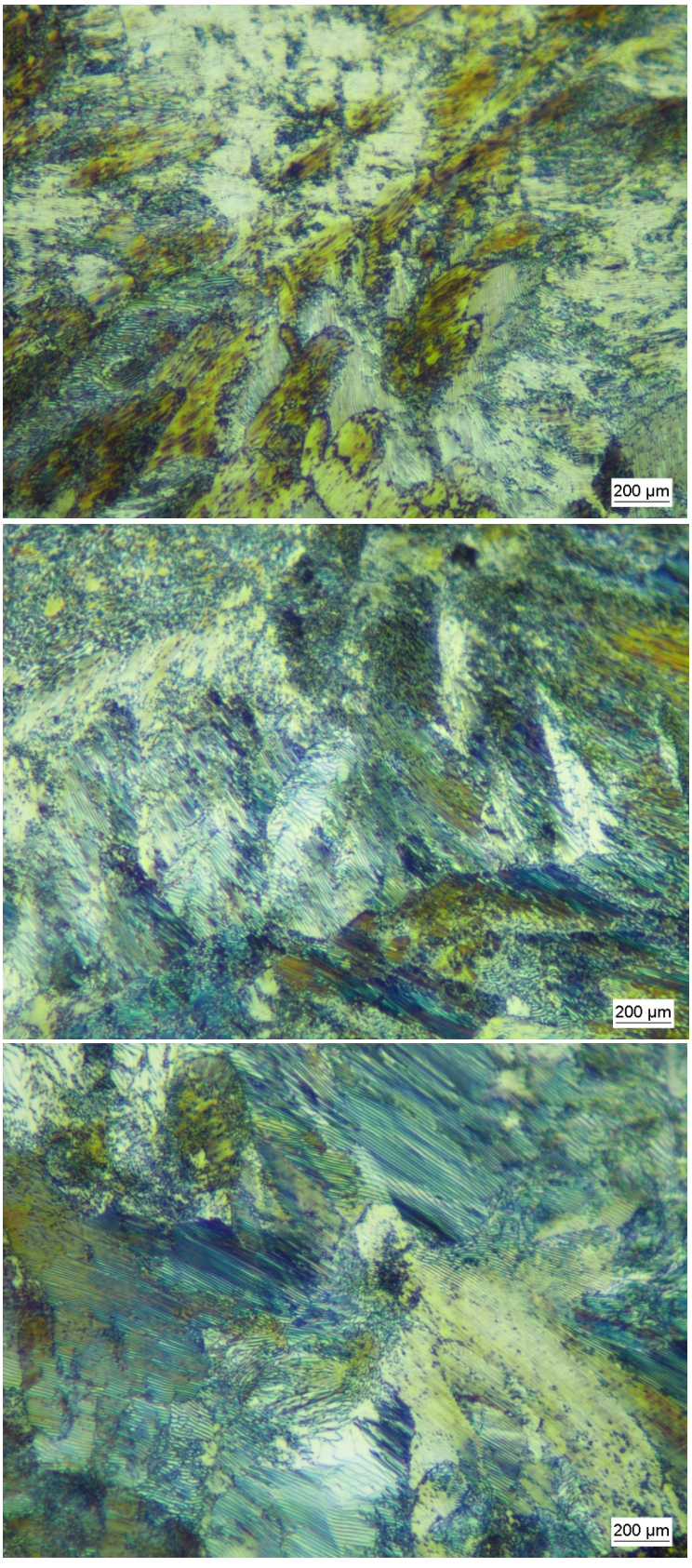

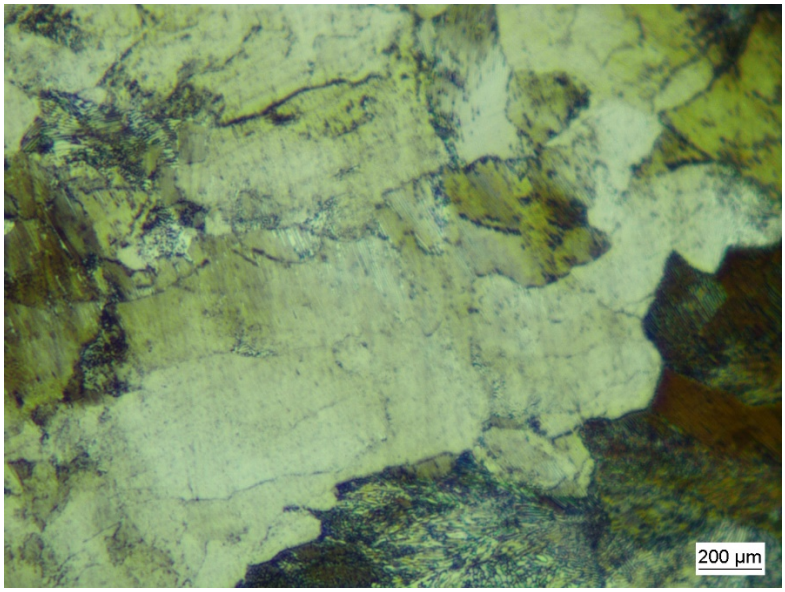
200 µm

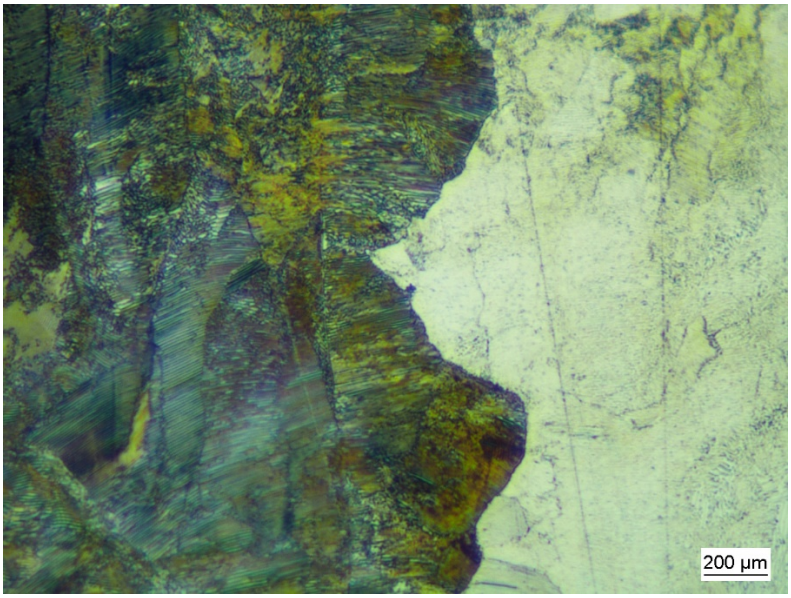
200 µm

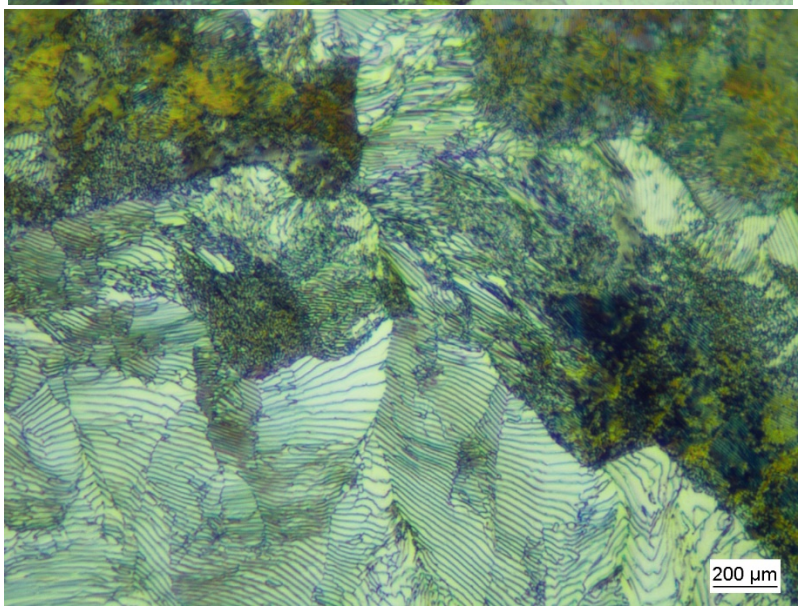
200 µm

Billet 3498L1

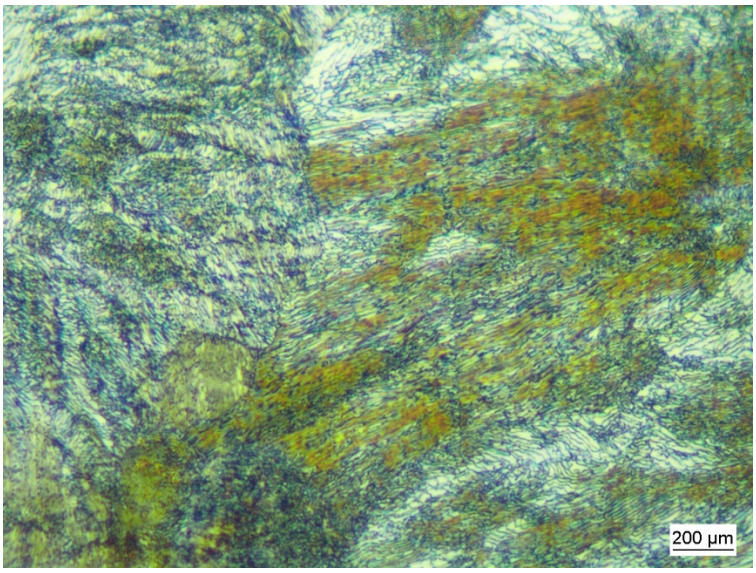

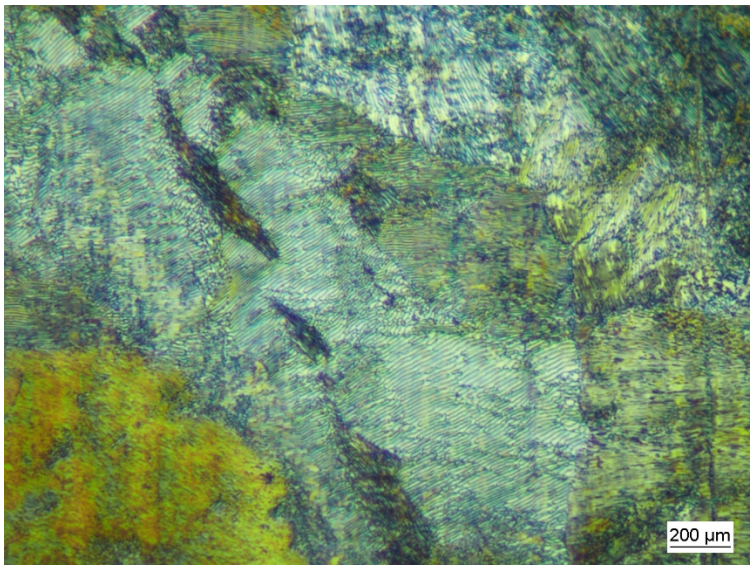

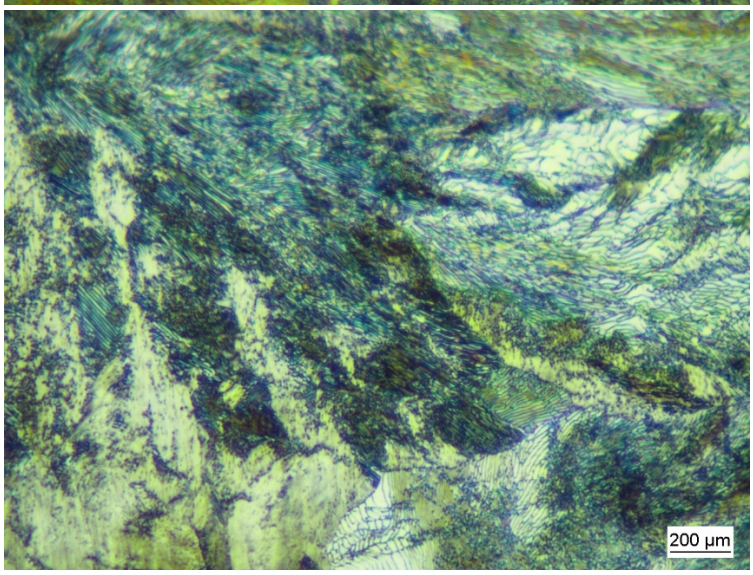

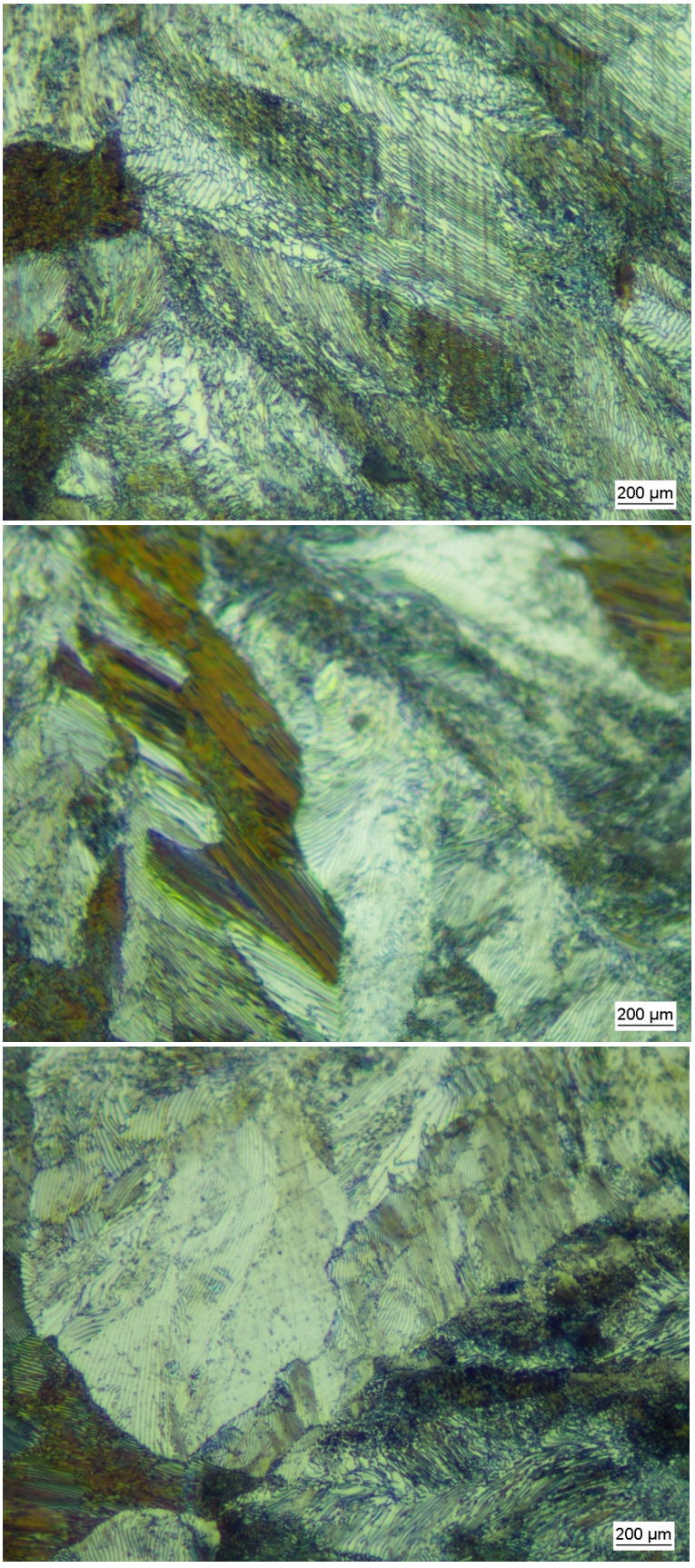
200 µm
200 µm
200 µm

Billet 3499L1

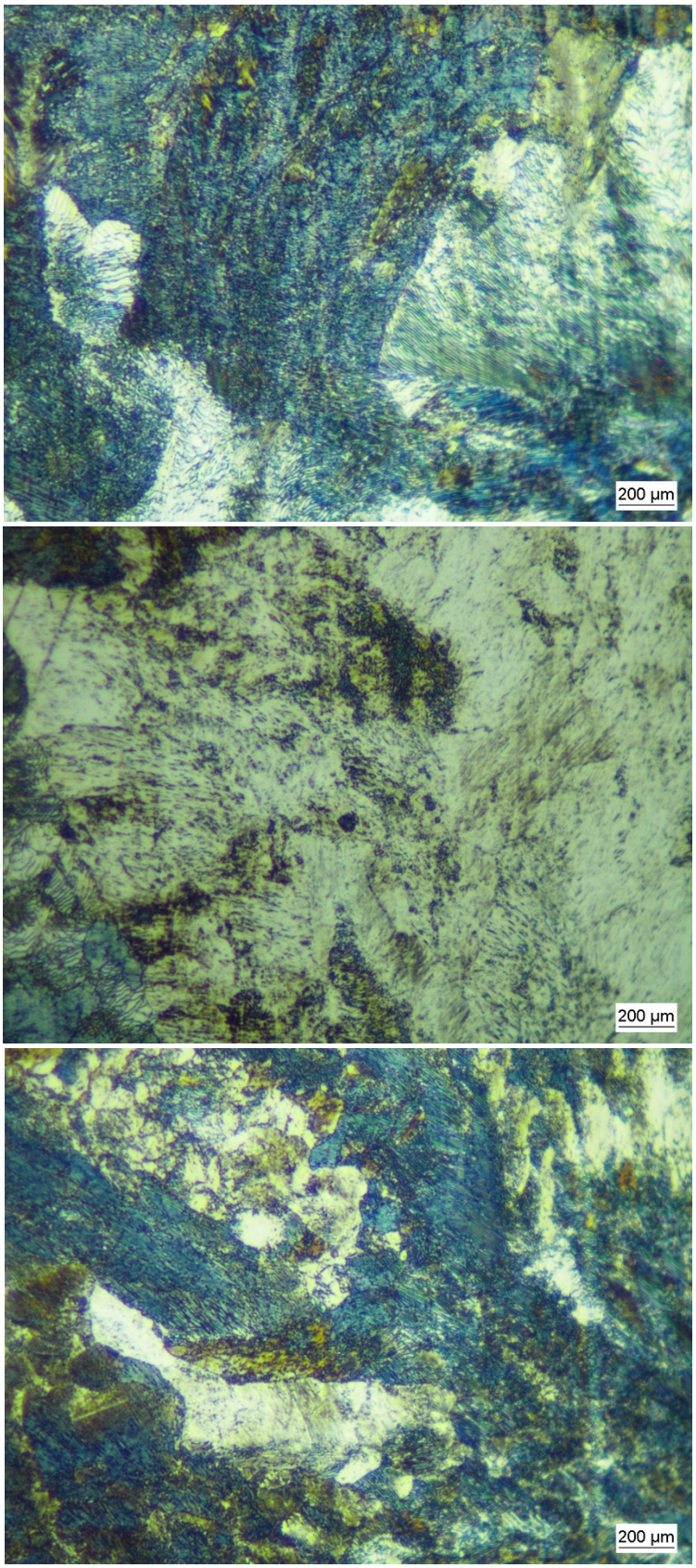

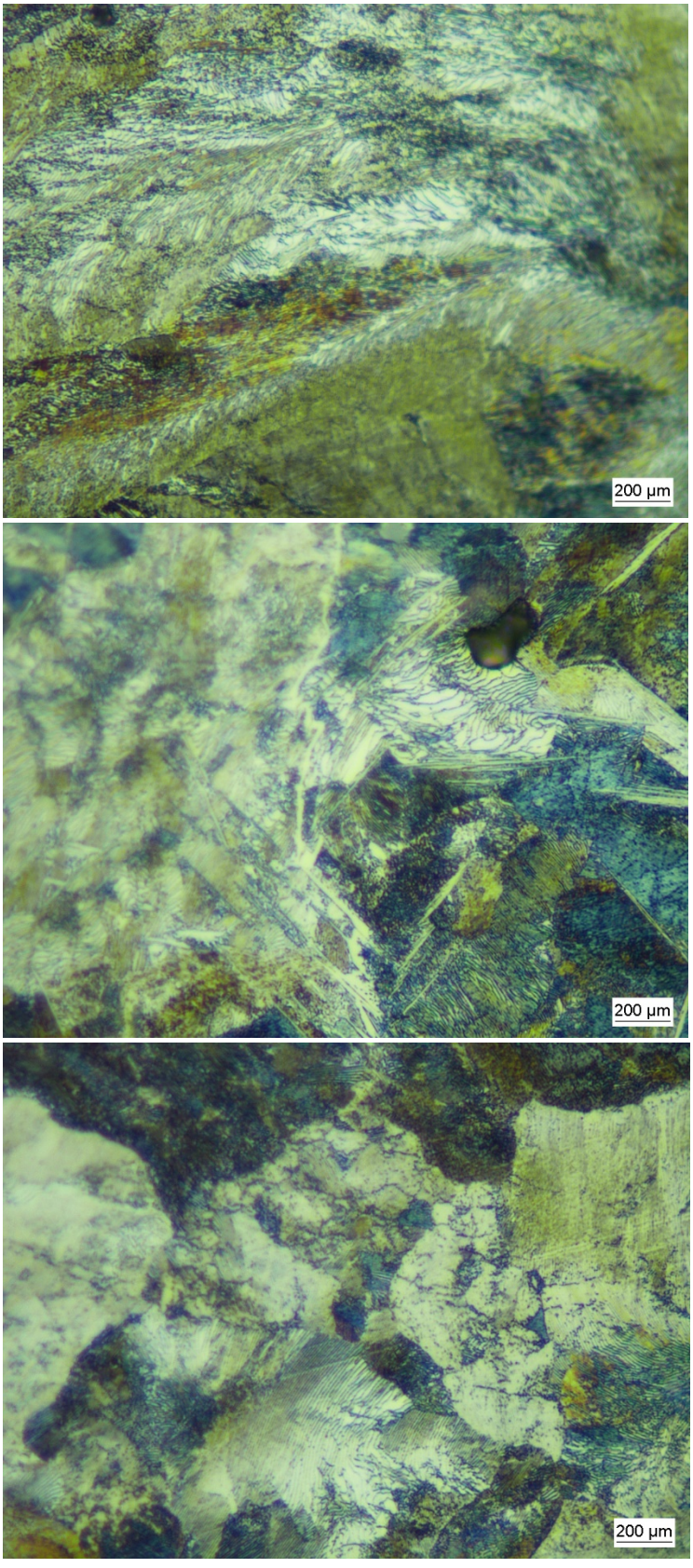
200 µm
200 µm
200 µm

Billet 3494L4 without L-EMS

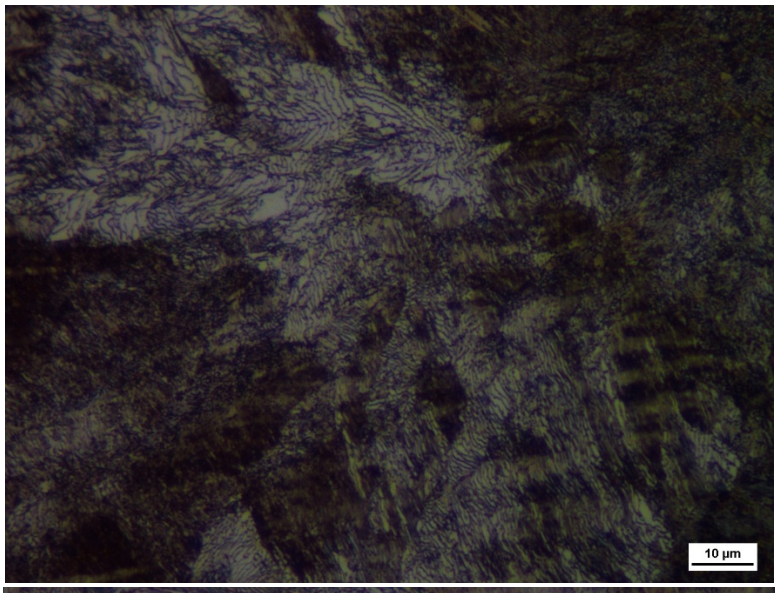

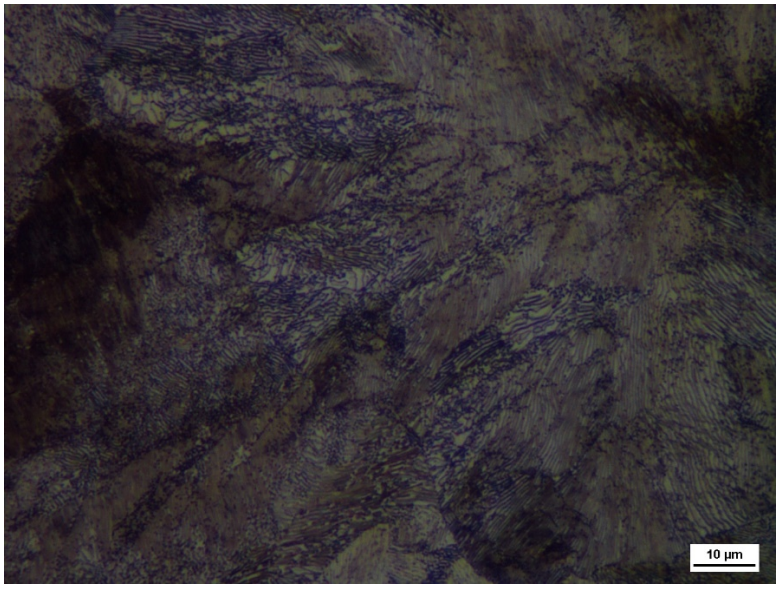

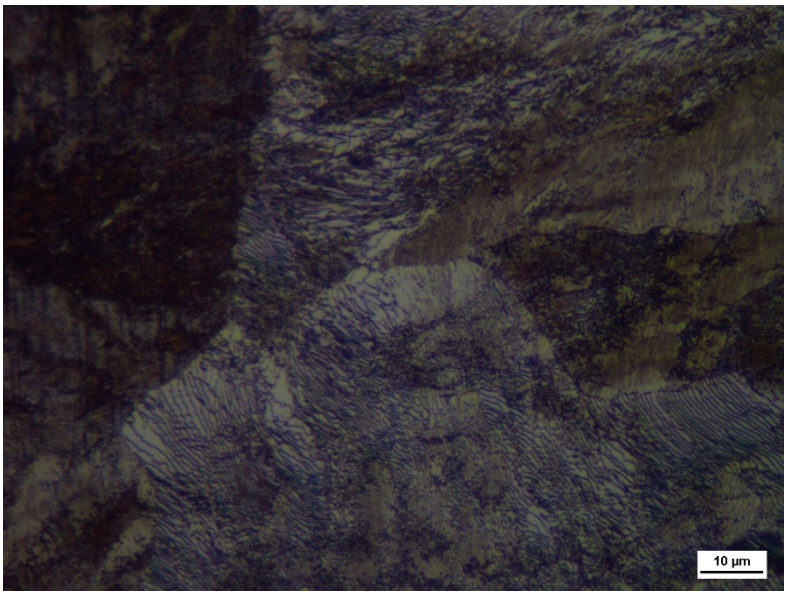

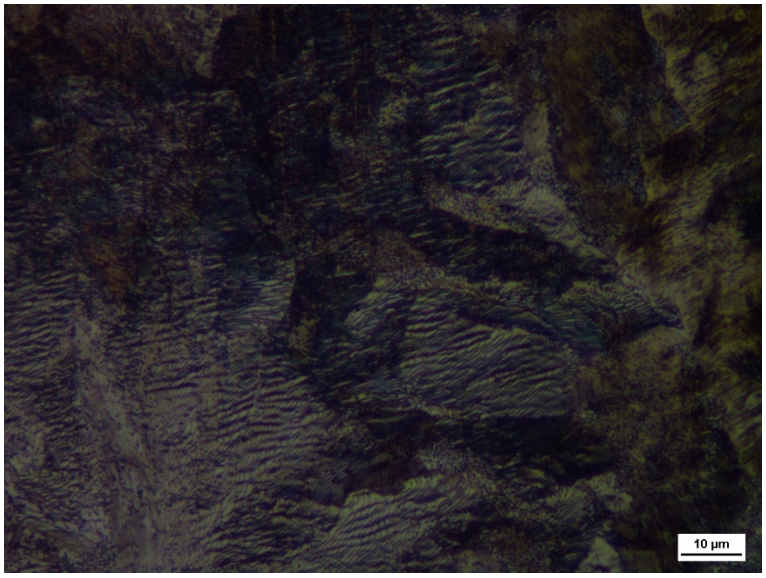
10 µm

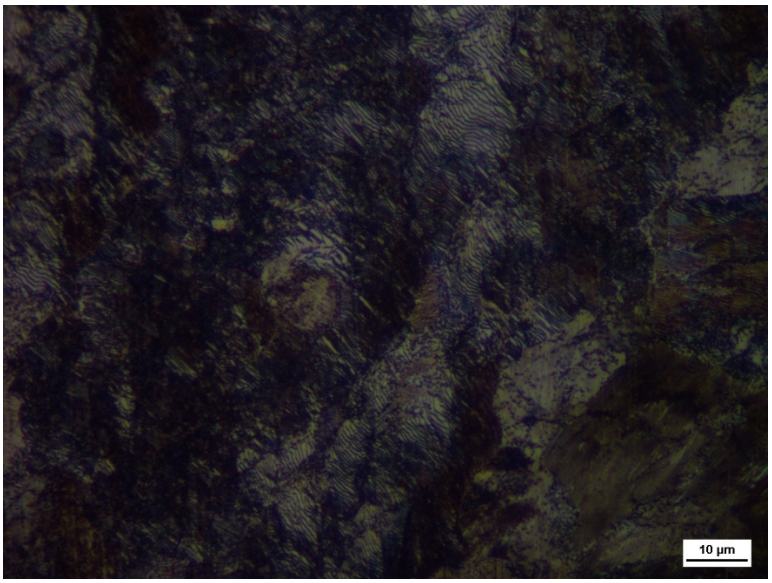
10 µm

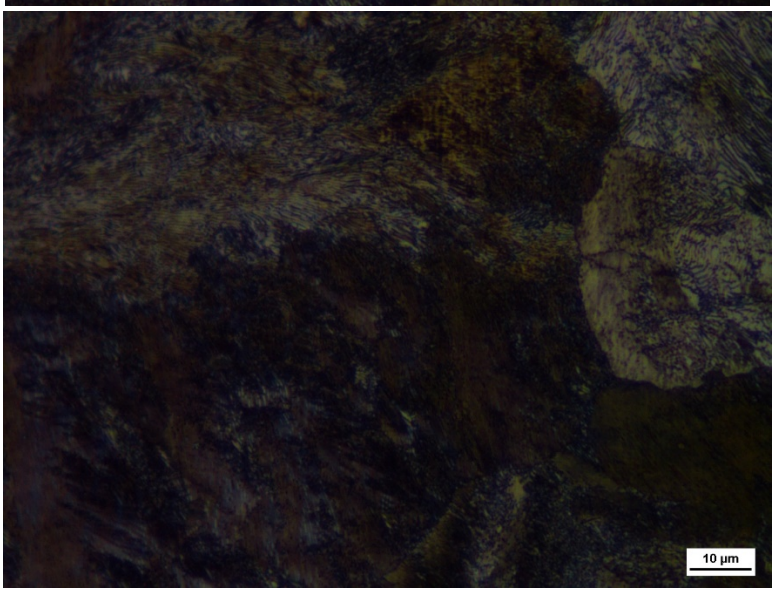
10 µm

BIBLIOGRAPHY

1. Thomas, B.G., “Continuous Casting,” The Encyclopedia of Materials: Science and Technology, K.H. J. Buschow, R. Cahn, M. Flemings, B. Ilschner, E. J. Kramer, S. Mahajan, (D. Apelian, subject ed.) Elsevier Science Ltd., Oxford, UK, Vol. 2, 2001, pp. 1595-1599

2. Continuous Casting Consortium, Illinois, USA

3. M.M. Wolf, "History of Continuous Casting," in Steelmaking Conference Proceedings, 75, (Iron & Steel Society, Warrendale, PA, 1992), 83-137

4. http://masters.donntu.org/2008/mech/trifonov/library/s1.htm

5. H.F. Schrewe, Continuous Casting of Steel, Fundamental Principles and Practice, (Stahl und Eisen, Dusseldorf, Germany, 1991.

6. http://ispatguru.com/basics-of-continuous-casting-of-steel/

7. Solidification control in continuous casting of steel, S Mazumdar and S K Ray

8. Formation of mini-ingot in continuous casting (Moore 1984).

9. Sinfonia Technology Co., Ltd. Japan https://www.sinfo-t.jp/eng/stirrer/principle.htm

10. Fundamentals of Solidifications W.Kurtz D.J Fisher, Thomas Tech Publications 1984

11. Refined Model Development and Performance Assessment of a Linear Induction-Type Electromagnetic Stirrer Cheng-Tsung Liu

12. https://www.google.com/Modelling Temperature profile for the continuous casting billet with a linear final electromagnetic stirrer

13. Metallurgy of Continuous Casting Technology, Dr.T.R.Vijayaram PhD Professor in Mechanical Engineering School of Mechanical and Building Sciences SMBS VIT University

14. https://www.j-magnetics.com/product/sort/en/EMS-Electromagnetic-Stirrer.html

15. Electromagnetic Stirrer for continuous casting machines M.A.N Industries | Andheri East, Mumbai , https://www.indiamart.com/proddetail

16. Continuous Casting of Steel W. R. IRVING FInstP, MIM, CEng

17. Crack Formation in the Continuous Casting of Steel ,J. K. BRIMACOMBE AND K. SORIMACHI, VOLUME 8B, SEPTEMBER 1977, pages 489-505

18. Evaluation of the Effect of Electro-Magnetic Stirring on Soundness of Continuously Cast Billets Using Ultrasonic Technique, Manish Raj and J.C. Pandey, Proc. National Seminar on Non-Destructive Evaluation Dec. 7 - 9, 2006, Hyderabad.

19. M.C. Flemings: Solidification Processing, McGraw-Hill, New York, 1974, p328 W.Kurz, P.R.Sahm: Gerichtet erstarrte eutektische Werkstoffe, Springer, Berlin, 1975

20. G.F. Bolling in Solidification, American Society for Metals, Metals Park, Ohio, 1971, p 341. J.F.Burke, M.C.Flemings, A.E.Gorum: Solidification Technology, Brook Hill, 1974

21. Prediction of dendrite arm spacing for low alloy steel casting processes, Metallurgical and Materials Transactions B August 1996, Volume 27, Issue 4, pp 689–693

22. Flemings, M.C. Our understanding of macrosegregation: Past and present. ISIJ Int. 2000, 40,833–841.

23. Krauss, G. Solidification, segregation, and banding in carbon and alloy steels. Metall. Mater. Trans. B 2003, 34, 781–792.

24. A.A. Tzavaras and H.D. Brody "Electromagnetic Stirring and Continuous Casting – Achievements, problems and goals" Journal of metals ,1984

25. S. W. L. Z. S. S. A. C. a. X. L. XINCHENG WANG, "Analysis on the Deflection Angle of Columnar Dendrites of Continuous Casting Steel Billets Under the Influence of Mold Electromagnetic Stirring," *METALLURGICAL AND MATERIALS TRANSACTIONS A*, vol. 47A, 2016.

26. S. K. C. a. S. GANGULY, "Morphology and Segregation in Continuously Cast High carbon Steel Billets," *ISIJ*, vol. 47, 2007.

27. ASM hand book volume 9

28. Solidification, Segregation, and Banding in Carbon and Alloy Steels The 2003 Howe Memorial Lecture Published with permission of the Iron & Steel Society

29. Optimisation of Electromagnetic Stirring in Steel Billet Caster by Using Image Processing Technique for Improvement in Billet Quality, Preeti Prakash SAHOO, Ankur KUMAR, Jayanta HALDER and Manish RAJ, ISIJ International, Vol. 49 (2009), No. 4, pp. 521–528

30. THE ANALYSIS OF DEFECTS ON CONTINUOUS CAST BILLETS, I. MAMUZIĆ, M.LONGAUEROVA, A.STRKALJ, ISSN 0543-5846 METABK 44 (3) 201-207 (2005)

31. Macrosegregation Behaviour in Continuously Cast High Carbon Steel Blooms and Billets at the Final Stage of Solidification in Combination Stirring, Kyung Shik OH and Young Won CHANG, ISIJ International. Vol, 35 (1995), No. 7, pp. 866-875

32. Structural Effects and Band Segregate Formation during the Electromagnetic Stirring of Strand-Cast Steel, M.R. BRIDGE and G. D. ROGERS, METALLURGICAL TRANSACTIONS B VOLUME 15B, SEPTEMBER 1984, page 581-589

33. Center Segregation with Final Electromagnetic Stirring in Billet Continuous Casting Process, Metallurgical and Materials Transactions B, 2017, Volume 48, Number 1, Page 444 Dongbin Jiang, Miaoyong Zhu

34. https://library.e.abb.com/public/9c5813ad058643fac125764f002fc039/PA%20Paper_1704%20FEMS.pdf
A novel FEMS system for continuous casting of steel billets and blooms
Value Paper Authors: Len S. Beitelman, Douglas Lavers, Göte Tallbäck, Christopher Curran

35. Solidification Structure of Continuous Casting Large Round Billets under Mold Electromagnetic Stirring, TaoSUN FengYUE Hua-jieWU ChunGUO YingLI Zhong-cunM

36. Optimisation of Electromagnetic Stirring in Steel Billet Caster by Using Image Processing Technique for Improvement in Billet Quality, Preeti Prakash SAHOO, Ankur KUMAR, Jayanta HALDER and Manish RAJ, Research & Development, Tata Steel, Jamshedpur-831001, India. E-mail: ppsahoo@gmail.com

37. Effect of Final Electromagnetic Stirring Parameters on Central Cross-Sectional Carbon Concentration Distribution of High-Carbon Square Billet, Yong Wan, Menghua Li, Liangjun Chen, Yichao Wu, Jie Li, Hongbo Pan and Wei Zhong, 7 June 2019